University of Nevada, Reno

Characterizing Habitat and Densities of the Mojave Desert Tortoise (*Gopherus agassizii*) at Multiple Spatial Scales

A thesis submitted in partial fulfillment
of the requirements for the degree of
Master of Science in Geography

by

Justice R. Best

Dr. Kenneth E. Nussear

Thesis Advisor

August 2023

THE GRADUATE SCHOOL

We recommend that the thesis
prepared under our supervision by

JUSTICE R. BEST

entitled

Characterizing Habitat and Densities of the Mojave Desert Tortoise (Gopherus agassizii) at Multiple Spatial Scales

be accepted in partial fulfillment of the
requirements for the degree of

MASTER OF SCIENCE

Kenneth E. Nussear, Ph.D
Advisor

Todd C. Esque, Ph.D
Committee Member

Kevin T. Shoemaker, Ph.D
Graduate School Representative

Markus Kemmelmeier, Ph.D., Dean
Graduate School

August, 2023

Abstract

Determining what environmental and anthropogenic factors have the greatest influence on the distribution of the Mojave desert tortoise (*Gopherus agassizii*) is key to improving population estimates and better understanding how this species uses their habitat around them. The Mojave Desert tortoise is a federally listed threated species and a key component to their delisting is ensuring that they are well distributed throughout their range. Currently range wide surveys of desert tortoises are conducted over large regions of suitable habitat with little consideration of the patchy nature of their distribution. Models were constructed to evaluate influences on desert tortoise densities across their range and are capable of informing conservation managers on where to conduct surveys in the future as well as what habitat to allocate for protection based on desert tortoise habitat preferences. At the range wide scale satellite data is readily available for input into models; however, when evaluating tortoise densities at smaller scales satellite derived remote sensing imagery proves to be too coarse for analyses at these scales. Remote sensing imagery derived from unmanned aerial vehicles (UAV) has recently become a viable option for obtaining data at these scales for various types of analyses. With high resolution imagery obtained with UAVs density models were constructed to evaluate influences on tortoise densities at local scales and with this I was also able to evaluate if tortoise habitat preferences differ amongst scales and regions. Detailed plant and soil data are collected at these small scales through field methods such as the Assessment Inventory and Monitoring (AIM) protocol but do not

have the ability to capture the heterogeneity across the landscape; thus, UAV derived imagery has the potential to bridge the gap between satellite derived imagery and field collected data. Here I've shown that UAVs can capture a more accurate representation of shrub cover than field methods such as the AIM protocol. Shrub cover is important to Mojave desert tortoise habitat as it provides protection from high temperatures and predators. Though the UAV imagery proved useful for obtaining shrub cover, data collected through field methods will still be necessary for obtaining specific plant and soil data as well as for calibration with remotely sensed imagery. The density models constructed at both the range wide and local scales revealed that desert tortoises do show preferences in habitat selection and these preferences vary from region to region and amongst scales. On the other hand, more work is needed to improve the types of data available for collection with UAVs. These results demonstrate the importance of evaluating Mojave desert tortoise densities at different scales and with data collected through various different means.

Acknowledgments

This work would not have been made possible without the help and guidance of many inspiring people. First and foremost, I must express my immense gratitude to my thesis advisor Ken Nussear who has been the epitome of an excellent mentor. Ken Nussear leads by example, setting the tone for hard work and never asking anything of his students that he would not also take the time to do. In addition, he has always had faith that I could accomplish more than even I thought possible. His unwavering belief in my capabilities gave me the confidence as well as the tools to complete my thesis. His expert opinions and knowledge were crucial contributions to this work. I'd also like to thank the rest of my committee, Kevin Shoemaker and Todd Esque. Kevin's expert knowledge in statistics and ecology was key to helping me understand and improve my work. Having studied desert tortoises for many years I was extremely thankful to have Todd's constructive feedback in and out of the field. Many collaborators were involved in this work from the U.S. geological survey, U.S. fish and wildlife service, and the Bureau of Land Management. I'd like to specifically thank Kristina Drake who helped me in obtaining much of the data for this project.

I would also not have been as successful in my endeavors if not for the guidance and assistance of all my geography lab mates. Many thanks go to Anjana Parandhaman, Lauren Phillips, Cas Carroll, Steve Hromada, Kirsten Dutcher and Tom Albright who all took the time to review my writing and presentations and give me their qualified opinions. A special thank you goes out to my lab mate Jackie Dougherty who not only evaluated my writing and presentations but also assisted me in the field for a great majority of my field work despite my thesis work being separate from her own. Jackie's mentorship and positive attitude were instrumental in my success throughout the completion of this thesis.

I am extremely thankful to my father Jeff Best. There aren't quite enough words to describe my gratitude towards my father for helping me get to the point of beginning a master's degree as well as helping me to finish this degree all together. In times of stress and doubtfulness throughout my life and throughout my graduate career my father has consistently been present to keep me grounded and focused. I would simply not be the person I am today without my father's love and guidance and his mentorship has been a pivotal part of the completion of my graduate degree. I'd also like to thank my sister Jamie Best, my mother Angela Best, and my stepmother Tess Best. I'm extremely thankful to have such strong and inspiring women in my life who all kept me going through the toughest parts of this journey and who were there to celebrate the victories when perseverance paid off. Finally, my sincere thanks go to my partner Matt Johnson. I am extremely grateful for his love and patience throughout this process. He has been there through the long nights of writing and coding and early morning send offs to field work. Matt has never doubted my abilities and has always been there to push me when I needed it, I will forever be grateful for his support.

Justice Best

August 2023

DEDICATION

In loving memory of Brennan Kern

11.05.1994 – 05.27.2020

Table of Contents

List of Tables

List of Figures

Introduction

Determining the components of an ecosystem that influence the distribution of a species is a complex task that requires an understanding of the species' habitat requirements and selection of a suitable modeling approach that represents the leverage of these components on the species' distribution. It is common to see spatial variation in animal abundance due to differences in habitat suitability (Mackenzie 2006). For instance, Williams and Middleton (2007) found that rainfall seasonality was the primary driver explaining spatial variation of bird abundance in an Australian tropical rainforest. These authors proposed that seasonal variation in rainfall, likely due to climate change, is causing declines in bird abundance, and is further exacerbated by habitat fragmentation. Understanding how environmental variation influences the densities of a species may aid in future estimates of abundance and distributions. Apps et al. (2016) applied a principal components analysis to derive factors influencing environmental variation of grizzly bear habitat in British Columbia, Canada at several spatial scales, with the best landscape model being a combination of all scales. Using a linear regression of estimated grizzly bear population density per survey area, while considering the mean landscape probability of grizzly bear detection, they found support for extrapolating grizzly bear density estimates among surveyed areas based on landscape variation in detection probability. Boer et al. (2013) performed a continent-wide analysis of both present-day and historical distribution and densities of African elephants in relation to both ecological and human factors, and tested predictor variables of elephant density in a generalized linear model (GLM). They found historic distributions to be significantly correlated with mean annual rainfall, while present-day densities of African elephants were primarily correlated with human factors. Each of these studies demonstrate a necessity for understanding the drivers of species densities for various conservation and management actions. It is not only important to understand what factors shape the distribution of species, but how variation in these factors correlate with the variation in densities across the landscape. It's important to note that higher densities of species may not always be associated with higher habitat quality (Van Horne 1983) and assumptions such as these may vary with scale. At range wide scales it can be assumed that some species exist in regions simply due to encroachment by humans; however, for the purpose of the analyses in this paper I do propose that higher Mojave desert tortoise densities are, in general, consistent with higher habitat quality.

Due to reductions in population sizes and loss and degradation of habitat, the Mojave desert tortoise was listed as threatened under the United States Endangered Species Act in 1990 (U.S. Fish and Wildlife Service [USFWS]1990). Studies addressing the habitat preferences and life history characteristics of Mojave desert tortoises begin as early as the 1940's (Woodbury and Hardy 1948), and much information is available in the pool of literature that exists today. The current recovery plan (USFWS 2011) designates five recovery units, within which there are seventeen tortoise conservation areas (Allison & McLuckie 2018). Threats to the desert tortoise include urbanization, large-scale renewable energy projects, drought, disease, and predation (USFWS 2011).

Range wide monitoring of the Mojave desert tortoise to assess their status and trends is often summarized over large conservation areas with little consideration of the patchy nature of their distribution (Allison & McLuckie 2018). Data from range wide monitoring indicates that tortoises are irregularly distributed across the landscape - even in areas considered to be suitable habitat. Understanding the nature of desert tortoise distributions may aid in the interpretation of monitoring outcomes as well as the allocation of protected habitat. A better understanding of the potential influences on what defines these patches could aid researchers and managers in predicting tortoise population numbers and the suitability of habitat in general. The realization of these patchy density distributions has given rise to questions such as whether these patches are the result of demographic stochasticity or of finer scale habitat preferences that have not yet been fully explored.

There are several methods available for investigating the patchiness of a species. Some of these methods involve evaluating significant clusters of animals in regions using kernel density analyses (Hengl et al. 2009). Other methods include modeling the influence of environmental and anthropogenic variables on species distributions using generalized linear or non-linear models (Buzas 1971). In addition to the methods available for evaluating the patchiness of a species there are also various scales at which species distributions can be assessed. These spatial scales are species dependent, as the scale at which a species is distributed is often largely based on their responses to landscape characteristics, which also vary by scale. Factors influencing habitat suitability at the scale of one kilometer (e.g. habitat attributes such as local topography or resource arrangement) may differ from factors that influence habitat suitability at the scale of several hundred kilometers (e.g. extreme temperatures), and different data might be important to aid in analyzing the pattern of patches at these different scales. At large scales, satellite derived imagery is often available and allows for spatial analysis with multiple environmental variables such as temperature, precipitation, vegetation, elevation, and soil composition (e.g., Nussear et al. 2009). However, the use of satellite imagery is limited as it is difficult in arid environments to corroborate field-based vegetation measurements, such as plant species composition, due to the low vegetative prevalence in even a 30 m pixel (Nagendra et al. 2008). At smaller scales there are many field-based methods to measure vegetation composition and abundance, and the BLM has implemented the Assessment Inventory and Monitoring (AIM) protocol, typically used in rangeland ecosystems, for this purpose. Data collected through programs such as AIM are limited, as they cannot accurately depict the heterogeneity of vegetation across the landscape with the same sampling intensity as remotely sensed data, because the data are obtained at only a few point locations (Gillan 2020). Additionally, because AIM data are obtained along points on 25-50 meter long transects, it also may be difficult to transform the data to be used in spatial analyses, as the “point” samples span larger areas than a single remotely sensed pixel. However – remotely sensed data cannot accurately capture the level of detail taken on transects and suffer from translating pixel-based data to practical field measurements without calibration. Recently, advances in near remote sensing using unmanned aerial vehicles (UAVs) have become a viable option for obtaining environmental data at finer scales (Gillan 2020). Imagery obtained with UAVs has the potential to bridge the gap between on the ground field methods and large-scale satellite imagery (Gillan 2020).

Expanding our understanding of the patterns in desert tortoise densities is key to determining influential factors on their distribution and future conservation decisions. In addition, exploring new technologies and their applications, such as UAVs and remotely sensed imagery, will aid in efforts to characterize suitable habitat at multiple spatial scales of species and distribution analyses. The aim of Chapter 1 of this thesis is to characterize the patchy distribution of tortoises through exploring the potential drivers of differential tortoise densities across their range, analyzed by exploring several environmental covariates hypothesized to influence their distribution. In Chapter 2 I use UAV remotely sensed imagery to characterize vegetation measures likely associated with finer scale desert tortoise habitat suitability, to evaluate tortoise densities, and corroborate AIM derived field data such as shrub cover. Finally, in Chapter 3, I compare the ability of models using UAV data and/or Satellite data to predict densities of tortoises at local scales and evaluate local tortoise habitat preferences.

Study Area

This study focused on the range of the Mojave desert tortoise including areas north and west of the Colorado River in California, Nevada, Arizona, and Utah (Figure 1). Mojave Desert tortoise habitat occurs in sandy flats to rocky foothills, and consists of alluvial fans, washes and canyons (USFWS 2021). Part of the methods in this study focused on targeted locations of tortoise habitat located around the Las Vegas, Nevada region where AIM plots have been conducted. These locations have been studied for detailed habitat use, health evaluations, and population numbers of resident tortoise populations such as in the McCullough Range, Nevada and Sheep Mountain Summit, Nevada (Figure 2).

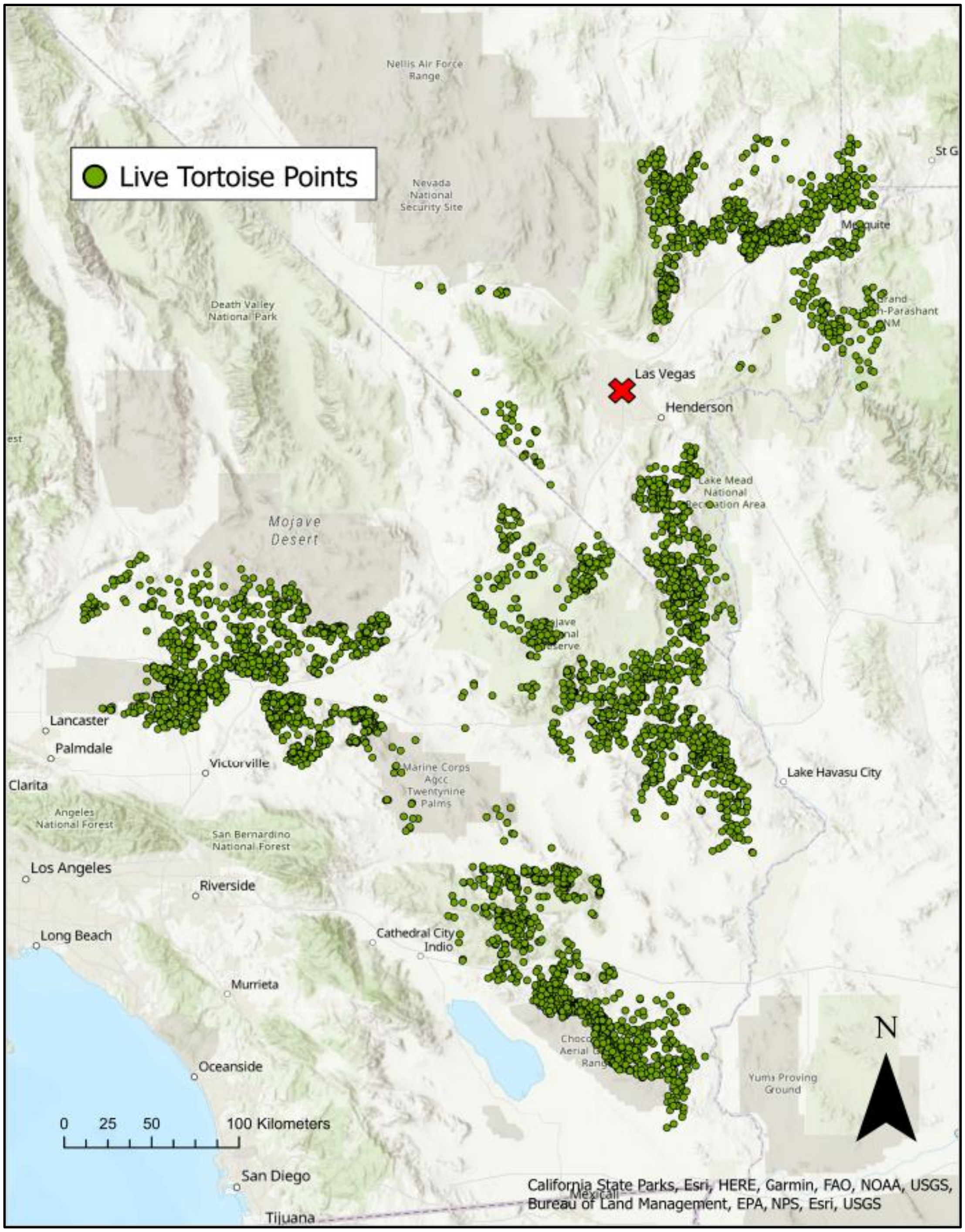

FIGURE 1: MOJAVE DESERT TORTOISE RANGE SHOWING TORTOISE LOCATIONS WITHIN DESERT WILDLIFE MANAGEMENT AREAS MONITORED BY THE USFWS DURING SPRING SURVEYS FROM 1999 TO 2018

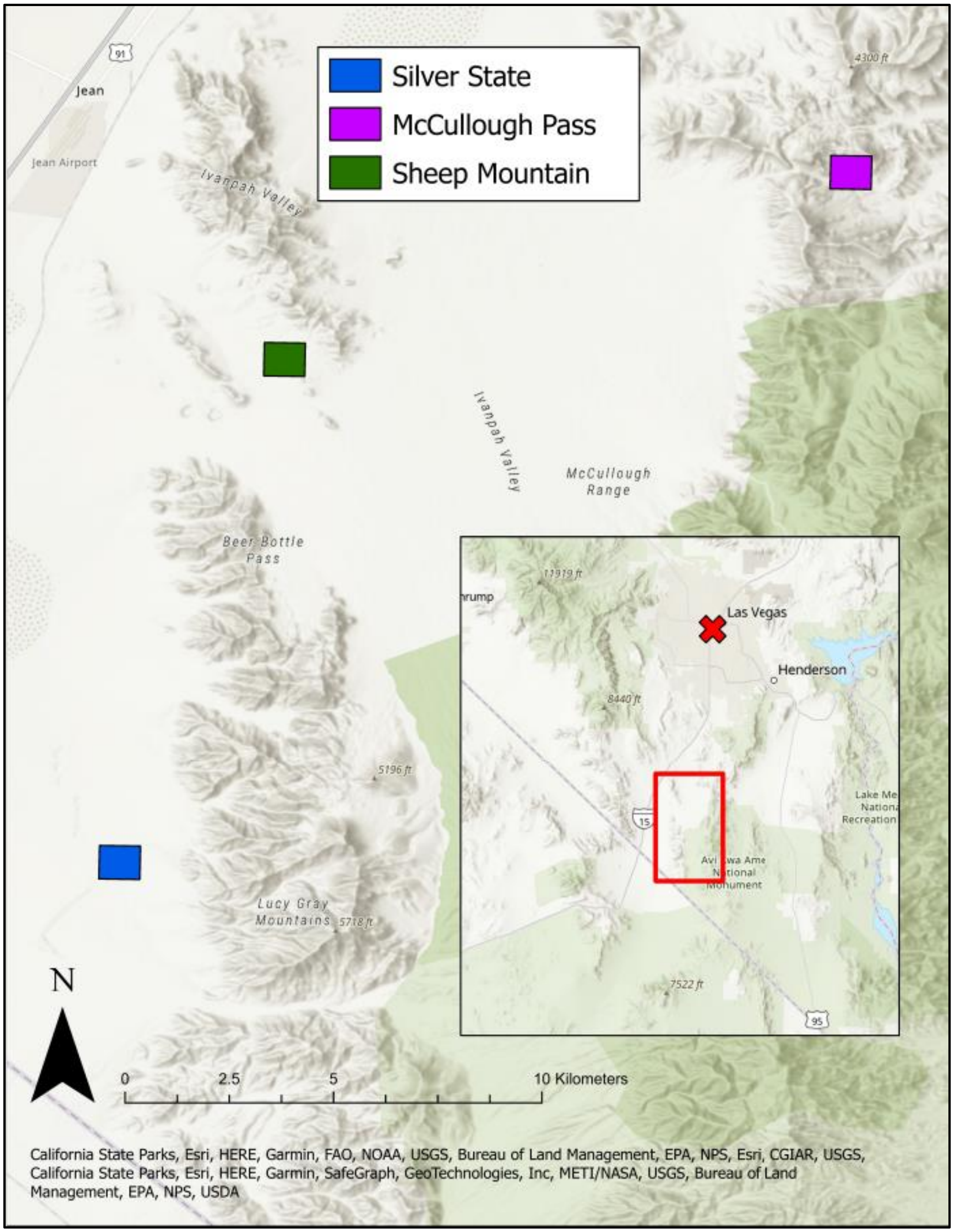

FIGURE 2: MOJAVE DESERT BLM ASSESSMENT INVENTORY AND MONITORING LOCATIONS AT SILVER STATE, SHEEP MOUNTAIN, AND MCCULLOUGH PASS

Chapter 1: Factors influencing desert tortoise density and patchiness modeled at a landscape scale

Species are rarely distributed uniformly in space, and often the factors influencing species density patterns vary both spatially and temporally (Anderson 1982). Desert tortoises are known to have several attributes that may be associated with their distribution that could be important toward understanding the differences in relative densities among habitat areas (Germano 1994). For example, desert tortoises spend most of their lives underground within burrows, therefore soil structure is likely a key factor in the species habitat preference, and soils vary widely across the Mojave Desert, and even within the confines of smaller survey areas, such as the 1 km capture recapture plots used to study tortoise density (Mitchell et al. 2021). Moreover, desert tortoises are highly incompatible with human presence and disturbance. In a study published in 1994 Corn found a decline of large tortoises in the western Mojave Desert in part due to human disturbance. This study also found a decline in juvenile tortoises due to a reduction in average precipitation of 4.93 cm in 1979 to 2.73 cm in 1985. Both of these findings along with similar studies (e.g. Carter et al. 2020) present the importance of both human disturbance and precipitation to the distribution and densities of tortoises. Understanding the associations of key habitat attributes with density distributions of desert tortoises will aid in future surveys and estimates of population numbers that can be used to inform conservation management decisions (Apps et al. 2016).

There have been many methods used to model tortoise densities on the landscape, and if I analyze the data differently these could be used to aid in our understanding of tortoise distributions. For example, as a part of the range-wide monitoring program conducted by the US Fish and Wildlife Service, transects are surveyed throughout Designated Critical Habitat Units. Encounter rates on these transects are on average 0.12 tortoises per linear kilometer surveyed but this varies by transect (Nussear and Tracy 2007). The nature of calculating densities using distance sampling requires a substantial number of encounters (Nussear and Tracy 2007) and these numbers are rarely achieved for areas smaller than a single critical habitat unit (approximately 1000 km^2 in area). However, it is evident that some survey locations result in almost no tortoise sightings despite being conducted in what is considered suitable habitat (Allison & McLuckie 2018). Thus, this method may be missing important drivers of local tortoise densities. Similarly, tortoise densities have been monitored using capture-recapture methods on smaller plot areas. These plots comprise much smaller land area, and thus provide point estimates of density for a given location (Tracy et al. 2005), however even within a $1mi^2$ or $1km^2$ plot I can see differential densities on the plots that are not well accounted for using capture recapture methods. Thus, a method of estimating density that allows for the inclusion of covariates expressed at a scale like the survey unit could be helpful toward our understanding of tortoise's use of habitat, and toward a more accurate assessment and prediction of tortoise densities at multiple scales.

Various methods exist for evaluating point densities generally (Table 1). For instance, clustering can reveal whether points are random, clustered, or over dispersed, and identify potentially important clusters; however, simply clustering points together will not explain the reasoning for their distribution. Kernels on the other hand create a continuous surface representing a model of the result of the point process; however, just as with clustering this method is not informed by covariates to describe why the points may be more or less dense in certain areas. From clusters or kernels I could obtain point samples of the density function and then run generalized linear models (GLM) or generalized additive models (GAM) to include covariates to model their potential influences. Density surface models are another potential method. These models use distance sampling data, and segment transects down to smaller units that can associate local encounter rates with covariates (e.g. see the prey model in Wiens et al. 2015). While these can produce finer scale spatially explicit estimates of density, they require substantial GIS processing, and still rely on detection estimates that are evaluated at the scale of the larger survey areas and are limited to data collected using distance transect methods. Another method, point process models (PPMs), model the intensity (or point density) across the landscape and thus allow for evaluation of covariates similar to GLM or GAM models.

Generalized additive models can be manipulated to behave like a PPM to model the process by which a density distribution occurs and deal with complex situations by accounting for the effects of multiple variables on point densities (Baddeley 2016).

GAMs, not unlike the other modeling methods, depend on sufficient sampling throughout a given area such that the densities are well represented (both in high- and low-density areas). Given the extensive nature of the range wide tortoise surveys, there are sufficient data for this type of analysis, but these methods are also applicable toward plot-based data. This process is to a large degree survey method agnostic, opening the possibility to also be applied to much of the historical tortoise survey data that have been collected to date.

In this analysis I use generalized additive models to analyze tortoise densities at several scales. Models were constructed using Mojave Desert tortoise presence points from previous sampling efforts, and associated environmental covariates derived from satellite remote sensing imagery to determine if variability in occupied habitat can explain differences in densities across the range of the desert tortoise. This analysis contributes insight as to why tortoises display a patchy distribution throughout their range and what variables influence this process.

Previous studies on habitat suitability of the Mojave Desert tortoise have revealed some of the important habitat indicators for the species. In a study published in 2009, Nussear et al. found ten covariates to be significantly correlated with tortoise distributions and implemented them in a MAXENT species distribution model. The covariates chosen were perennial and annual plant cover, mean dry season precipitation, mean wet season precipitation, elevation, average surface roughness, percent smooth, average soil bulk density, depth to bedrock, and average percentage of rocks (Nussear et al. 2009). From a study on Mojave Desert tortoise population trends published in 2018, Allison and McLuckie revealed adult tortoise declines from 2004 to 2014 in 4 of 5 tortoise conservation areas. The change in tortoise densities found through distance surveys conducted throughout the tortoises' range demonstrates the need to reevaluate how habitat suitability varies across the landscape and how this variation influences tortoise distributions.

TABLE 1: METHODS OF QUANTIFYING ABUNDANCE AND DENSITIES OF MOJAVE DESERT TORTOISES AND THE LIMITATIONS OF THESE METHODS

	Contributions	Limitations
Generalized Additive Models	Models non-linear relationships between independent and dependent variables	Computationally complex and has a tendency for overfitting
Point Process Models	Models the pattern of a point process in relation to a set of covariates Fixed effect model	Assumes points are independent and uniformly distributed
Cox and Cluster Processes	Models point patterns influenced by unobserved random processes Random effect model	Assumes points are not independent of one another
Maximum Entropy	Predicts probability of species presences under specific conditions distributed in space	Similar to fitting a PPM with log linear intensity (specific intensity)
Density Surface Models (DSM)	Derives a likelihood function based on density of animals and probability of detection at a specific location	Can only be used on line transect data Methods for fitting general models using likelihood derivations often met with convergence problems (Buckland 2004)
Distance Sampling	Obtains detection curves and density estimates through counts obtained by visual search along a transect	Detectability of animals decreases with distance from line transect Must be conducted over large areas for accurate estimates

Mark-Recapture	Estimates total species abundance from only a subset of the population through a series of capturing, marking, and releasing animals	Assumes: Equal chance of detection among all animals; Animals do not lose marks; Animals classified correctly (marked vs unmarked); Marks do not affect survival; Marking does not significantly affect subsequent behavior (Roff 1973)

Although this analysis focuses on the entire range of the desert tortoise and uses satellite remote sensing imagery, with the introduction of finer scale environmental data it may be possible to apply similar methods at smaller scales. Evaluating patterns in tortoise densities at finer scales may reveal insights into processes not detectable in larger scale evaluations. Through the construction of localized density models not only will we have a better understanding of preferential (or more densely occupied) habitat, but perhaps most crucial to this analysis we will begin to understand drivers of local scale tortoise occurrence and thus be able to conduct management decisions accordingly. There are many factors that influence species densities and distributions including disease and demographic stochasticity; however, environmental variation plays a larger role at landscape scales, but its influence seems to be less well known in relation to these dynamics (Santini 2018).

Research Questions

- What environmental covariates have the greatest influence/are better able to predict patchiness of tortoise distributions on the landscape?

Methods

Live tortoise point locations were obtained from a range wide analysis of population trends in Mojave desert tortoises (Allison & McLuckie 2018). In this study line-distance transects were walked throughout designated tortoise critical habitat between 2001 and 2019. I separated the range wide points into 4 groups - roughly based on critical habitat units - to enhance the ability of our models to predict densities based on our variables of interest while less influenced by the grouping of points caused by the location of survey transects (Figure 3). I created a kernel density raster for each region (Northeast Mojave, Central Mojave, South Mojave, and West Mojave) using the density.ppp function (spatstat.explore, version 3.0-5) in Rstudio (R core team 2022) and then masked each raster to only the area where line-distance transects were placed. I then placed 1000 random sample points in each region to obtain a gradient of densities values for input into the GAMs.

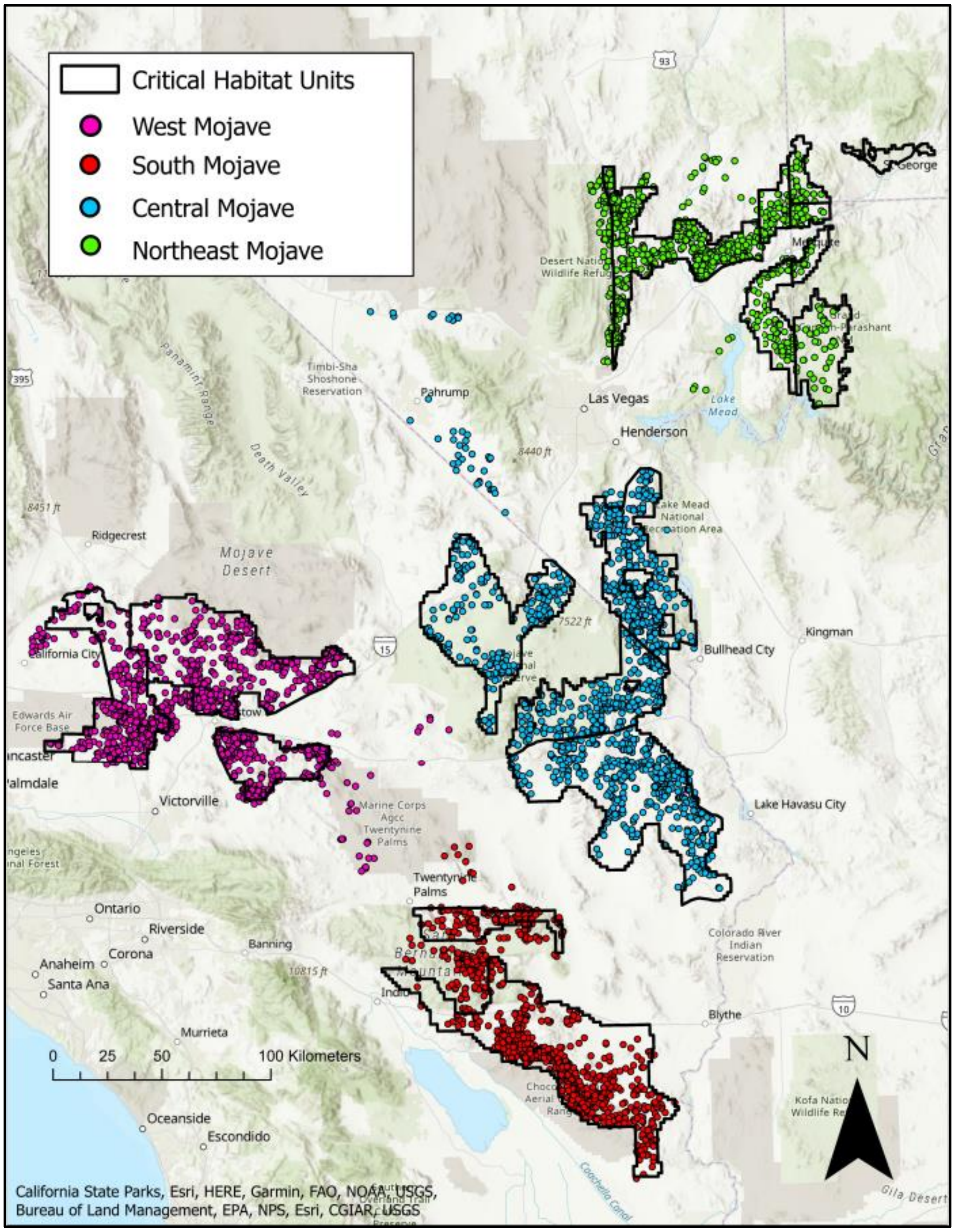

FIGURE 3: MOJAVE DESERT TORTOISE RANGE SHOWING TORTOISE LOCATIONS APPROXIMATELY SEPARATED BY CRITICAL HABITAT UNITS (CHU) MONITORED BY THE USFWS DURING SPRING SURVEYS FROM 1999 TO 2018

Tortoises sustain a generalist diet and rely primarily on winter annuals and perennial grasses for foraging (Germano 1994). Introduced species such as *Bromus rubens* pose threats to the persistence of tortoise's natural forage (Drake et al. 2016).

Precipitation is minimal and variable throughout the Mojave Desert, but in general most rain or snowfall occurs in the fall and winter (Germano 1994). Due to the limiting nature of precipitation in the Mojave Desert, determining the minimum amount of precipitation required to sustain tortoise numbers is crucial for understanding their densities across the landscape. Tortoises are mostly found at elevations between 200 m and 1570 m asl (Germano 1994; Berry and Murphy 2019), which is a pattern likely driven by environmental factors such as temperature and topography. Mojave desert tortoises spend a majority of their lives in burrows or naturally formed dens, thus soil composition and geology are unquestionably important factors influencing the density of tortoises throughout their habitat. Soils must be sturdy enough to construct burrows without the concern for collapsing easily, but also not too rocky otherwise penetration will be impossible (Bury 1982). Because burrows can be up to 3 m or more in depth, the depth to bedrock may also influence whether tortoises occupy certain sites.

Generalized additive models were constructed to evaluate the effects of covariates on tortoise point densities and allowed for the analysis of non-linear effects. GAMs were assessed using multiple diagnostics metrics to examine the fit of each model and relative influence of the covariates. These include percent deviance explained, adjusted R-squared, and p-values for individual variable analysis. These modeled relationships are then predicted across tortoise habitat and compared to existing representations of tortoise densities.

With improvements in remote sensing imagery and data collection methods as well as changes in tortoise densities I re-evaluate the influence of previously suggested drivers as well as test for the influence of newly considered variables which are expected to be important. Based on evidence from the literature and inferences by experts I considered the following variables for analysis: Normalized difference vegetation index (NDVI) obtained from the USGS phenology website (USGS 2019), Soils (coarse fragments, sand on surface) obtained from soilgrids.org (ISRIC 2020), Depth to bedrock obtained from isric.org (ISRIC 2020), Winter precipitation (30-year normal) and Maximum temperature (30-year normal) obtained from PRISM (PRISM 2012), and TDI (terrestrial disturbance index) (Carter et al. 2020). All imagery was scaled using the scale() function in R in order to place all variables on a level playing field and avoid potential effects from high leverage values. I masked all imagery to only the region where line-distance transects were placed. This is so when I evaluated range wide tortoise points in relation to our variables of interest no bias would arise due to density values of zero being generated in the non-surveyed regions. It is in the non-surveyed regions where I am uncertain whether tortoise densities are high or low and the models help to predict this. After scaling and masking the imagery to the appropriate regions I used the same 1000 sample points used to obtain the tortoise density values (from the kernel analyses) to extract values for each environmental variable for input into the GAMs. With this I had 1000 density values for each region and 1000 corresponding values for each variable of interest for each region as well.

Results:

The generalized additive models reveal that individual tortoises do appear to show preferences in habitat selection and some of these preferences vary from region to region, while other preferences appear consistent. The west Mojave displays an increase in densities with an increase in depth to bedrock (Figure 12). The other three regions, northeast, central, and south, have little to no relationship between densities and depth (Figures 6, 9, and 15). In general, densities appear to decrease with increasing percentage of coarse fragments on surface (Figures 6, 9, 12, and 15). In all regions except the northeast there is a steady increase in densities with a peak followed by a drop off with increasing sand on surface (Figures 9, 12, and 15). In the northeast there is a steady increase in densities with an increase in sand on surface with no drop off as seen in the other regions (Figure 6). Regarding climatic variables, in all regions there is a peak in densities as maximum temperature increases with drop offs in densities towards the extreme highs and lows of maximum temperature (Figures 6, 9, 12, and 15). In all regions except the northeast there is a general increase in tortoise densities with an increase in winter precipitation (Figures 9, 12, and 15). Surprisingly, in the northeast there is a very slight increase in densities with an increase in winter precipitation followed by a general downward trend as the precipitation continues upward (which may reflect precipitation seen in the higher elevation areas) (Figure 6). Not surprisingly, in the northeast and south Mojave I see decreases in density with increases in terrestrial disturbance where the data points are concentrated (Figures 6 and 15). In the central and west regions there is little to no trend in relation to TDI (Figures 9 and 12). Finally, in the western and southern regions their densities decrease with an increase in NDVI or “greenness” on the landscape, possibly related to increasing elevation, and associated increased habitat quality on the upper bajadas (Figures 12 and 15). In the northeast region there is a peak in densities with increasing NDVI followed by a threshold response with a decline as greenness continues to increase (Figure 6). The central Mojave displays a slight upward trend in densities with increasing NDVI (Figure 9). It is important to note that the grey error regions on the figures represent uncertainty in the analyses where there were few data points to inform the trends.

Discussion:

These analyses give us insight into tortoise habitat use in relation to changing environmental and anthropogenic conditions and indicate how much variation can occur among regions. Each of the four generalized additive models across the range of the Mojave desert tortoise reveal that tortoises do show preferences in habitat selection. These models also reveal the ability of generalized additive density models to predict the potential densities of tortoises in regions not yet surveyed by producing prediction maps. The dark regions of each predicted density map that do not have tortoise localities may give insight into where we could conduct surveys for tortoises in the future to improve estimates of densities and population numbers (Figures 4, 7, 10, and 13). This is especially crucial given the low detection rates of tortoises due to their cryptic behavior which skews estimates and makes conservation management decisions even more difficult (Nussear and Tracy 2007).

Furthermore, understanding tortoises' preferences for habitat selection in relation to anthropogenic impacts as well as vegetation, climactic, and soil variables will also aid in deciding where tortoise habitat protection should be prioritized across the landscape. For instance, in the northeast region there appears to be a decrease in densities with an increase in NDVI (Figure 6); however, in the central region there appears to be an increase in densities with an increase in NDVI (Figure 9). This discrepancy in density interactions on its own could be indicative of variation in vegetation types in each region. Further investigation could reveal that there may be higher densities of unfavorable invasive species in the northeast region where there are declines in densities with increasing NDVI. For example, invasive grasses fueled wide ranging wildfire in the northeast Mojave in 2005, causing further alterations to habitat (Van Linn et al. 2013, Drake et al. 2016). Although this is just one potential hypothesis for this pattern, further support could be provided for this and other ideas by evaluating plant data revealing specific species from on the ground field methods such as the BLM's AIM protocol.

While the relationship between tortoise densities and coarse soil fragments on the surface was consistent across regions there was once again variation in density patterns across regions in relation to depth to bedrock and sand on surface. Given the need for tortoises to construct burrows it is unsurprising to see an increase in tortoise densities in the west Mojave with an increase in depth to bedrock. A greater depth to bedrock allows tortoises to burrow to their preferred burrow lengths of up to three meters or more (Bury 1982). Contrastingly, there appeared to be a slight decrease in densities with an increase in depth to bedrock in the northeast Mojave. This was only a marginal relationship and could potentially be explained by other interactions. Mojave desert tortoises tend not to occupy steep slopes or very high elevations, thus indicating that variation in topography could explain the discrepancy in densities between the west and northeast regions.

The Mojave desert tortoise range spans over a wide range of habitats, elevations, and topographies. This explains why there are clear differences in the relationship between tortoise densities and some of our variables of interest. For example, all regions except the northeast revealed an increase in densities with increasing precipitation. Given the low prevalence of precipitation in the Mojave it is unsurprising the tortoises would seem to favor regions with higher precipitation. However, in the northeast there was a decrease in densities with increasing precipitation. This difference is possibly explained by the colder temperatures at higher elevations in the most northern region of the desert tortoise's range. It is variations from region to region such as this that reveal why it is crucial to evaluate species densities at different scales. This is so that we do not apply "one size fits all" management solutions across the range of Mojave tortoises that may benefit the animals in certain regions but could be potentially detrimental to the animals in other regions.

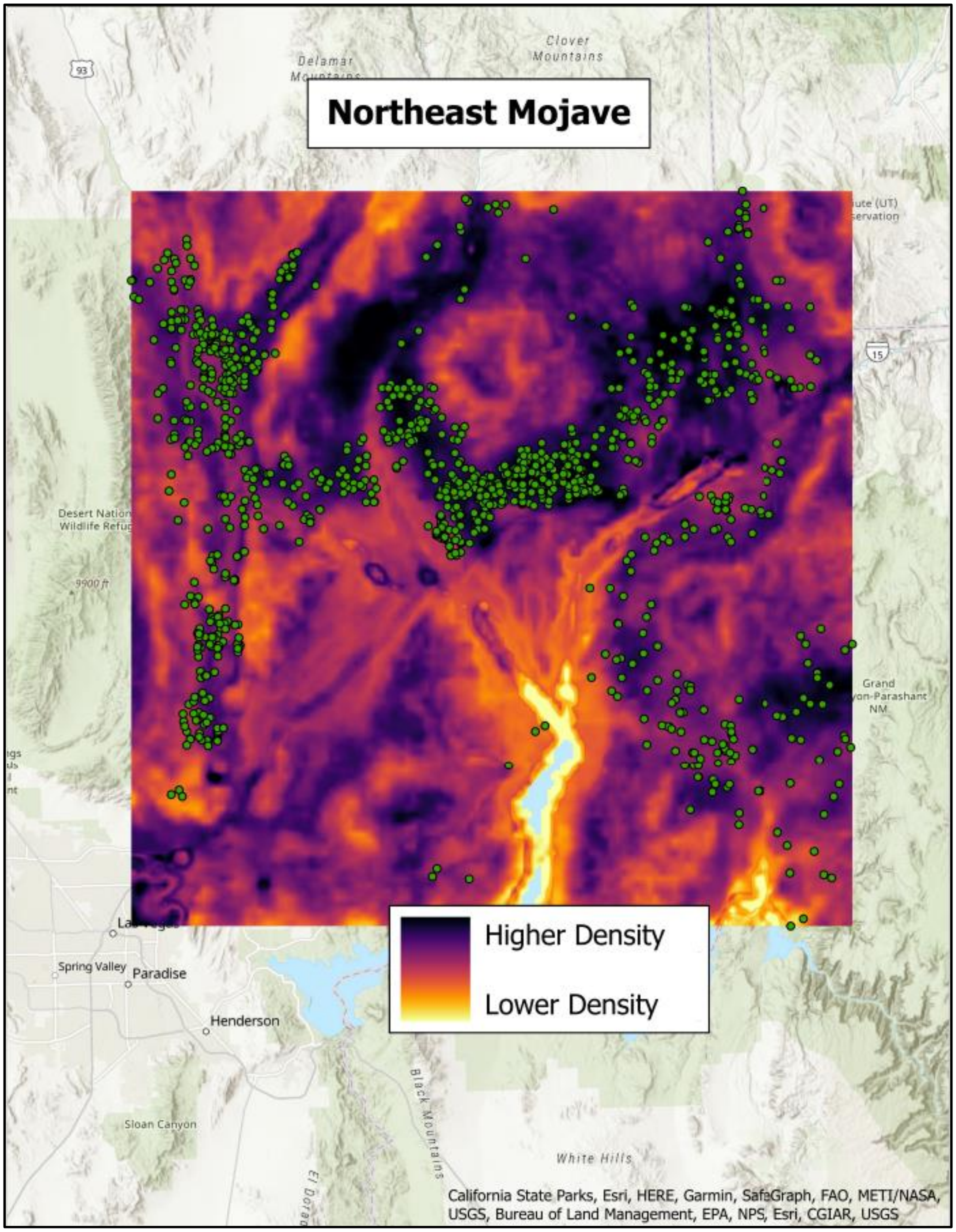

FIGURE 4: NORTHEAST MOJAVE GENERALIZED ADDITIVE MODEL TORTOISE DENSITY MAP AND TRUE TORTOISE POINTS

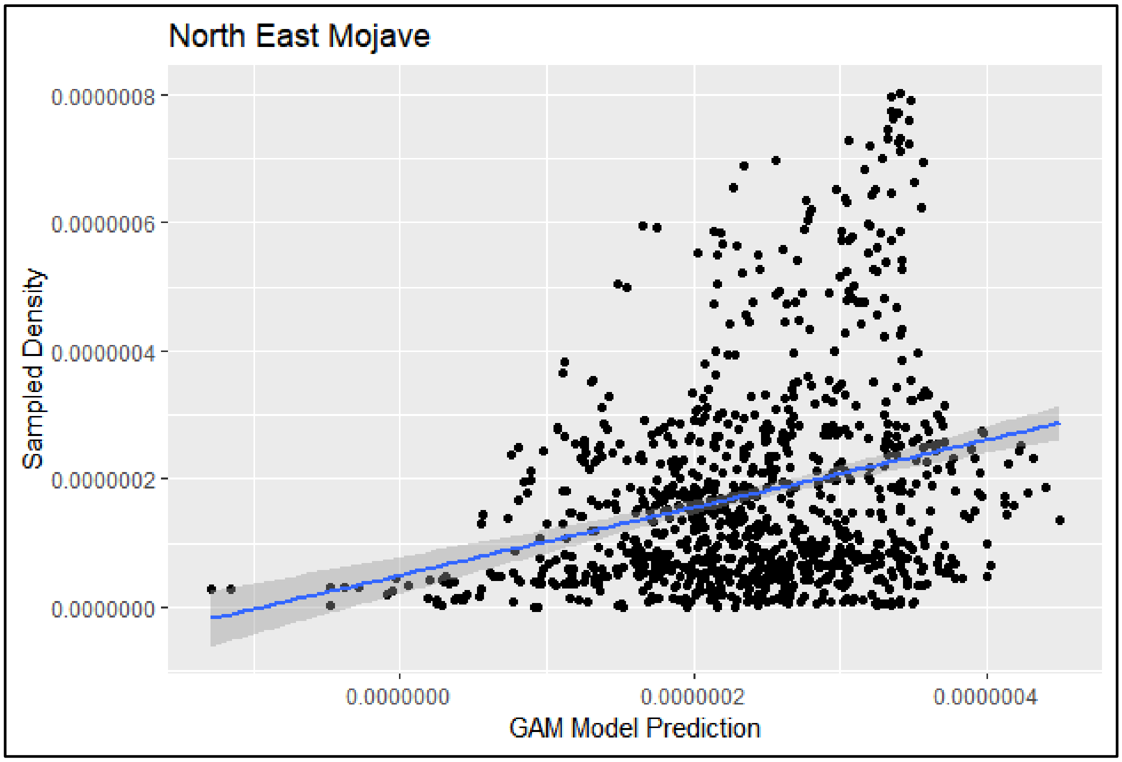

Figure 5: Tortoise true sampled density (y-axis) versus model predicted density (x-axis)

Table 2: Northeast Mojave GAM summary including: estimated degrees of freedom (EDF), reference number of degrees of freedom (Ref.df), F-statistic (F) and p-values.

Terms	edf	Ref.df	F	p-value	
Terrestrial Disturbance Index	5.4463	9	2.322	0.000638	***
Normalized Difference Vegetation Index	6.9590	9	13.910	< 2e-16	***
Depth to Bedrock	0.3575	9	0.016	0.523188	
Sand on Surface	4.6868	9	18.625	< 2e-16	***
Coarse Fragments on Surface	4.8095	9	3.935	1.04E-06	***
Winter Precipitation	3.5502	9	7.980	< 2e-16	***
Maximum Temperature	5.8290	9	17.207	< 2e-16	***
Deviance Explained = 46.7%	**R-squared (adj) = 0.449**				

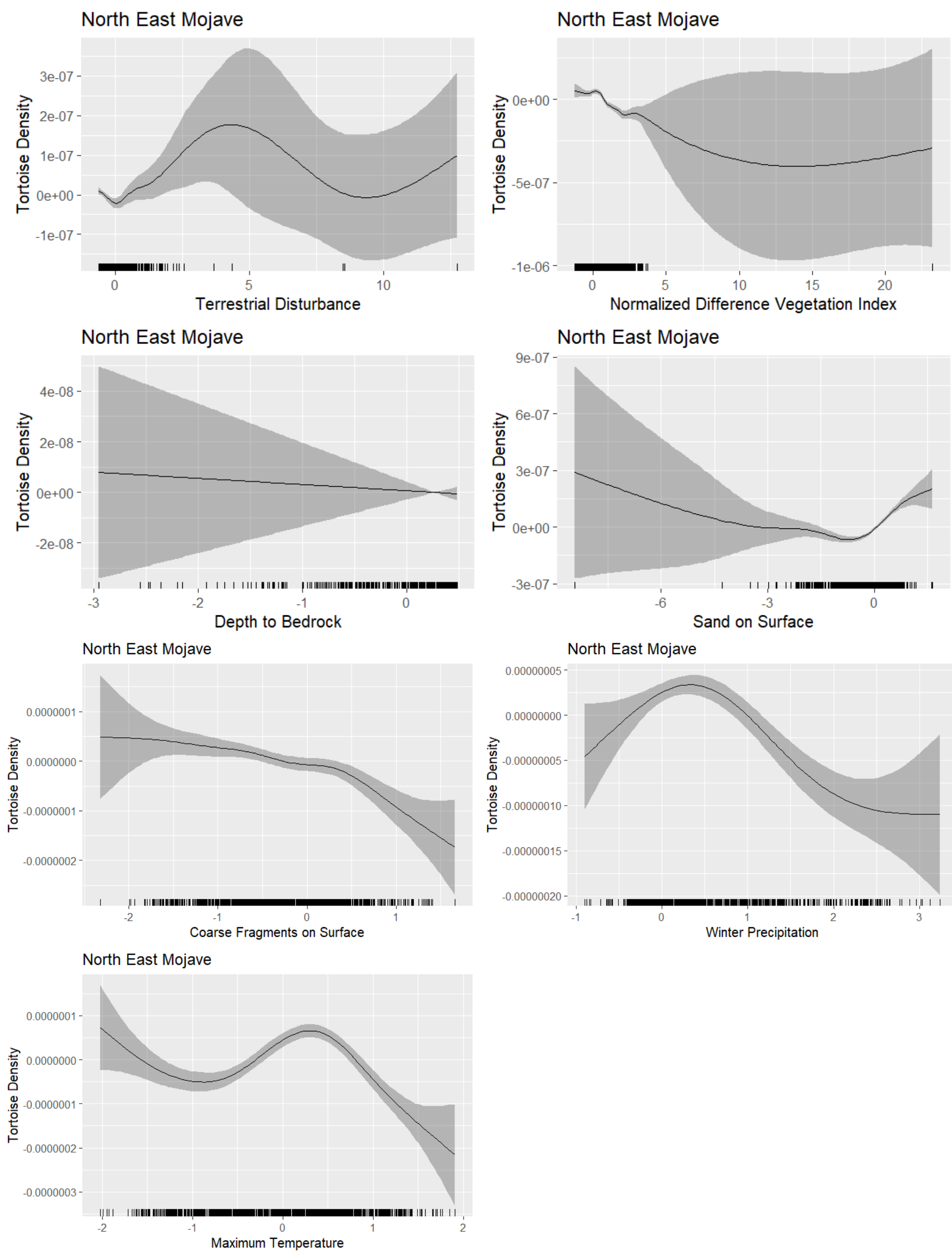

FIGURE 6: NORTHEAST MOJAVE TORTOISE DENSITY INTERACTIONS WITH COVARIATES. GRAY REGIONS REPRESENT UNCERTAINTY DUE TO LACK OF DATA POINTS.

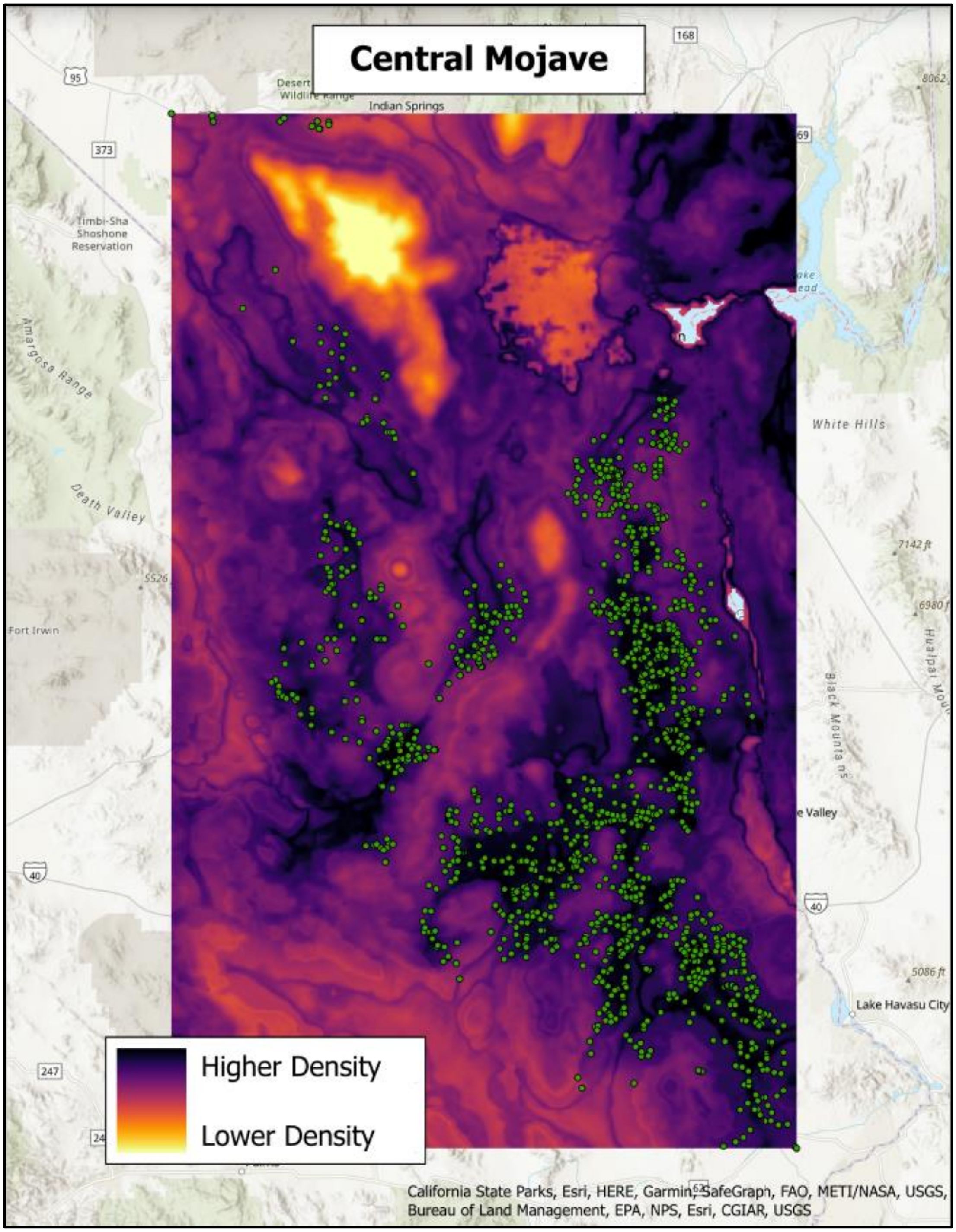

FIGURE 7: CENTRAL MOJAVE GENERALIZED ADDITIVE MODEL TORTOISE DENSITY MAP AND TRUE TORTOISE POINTS

.

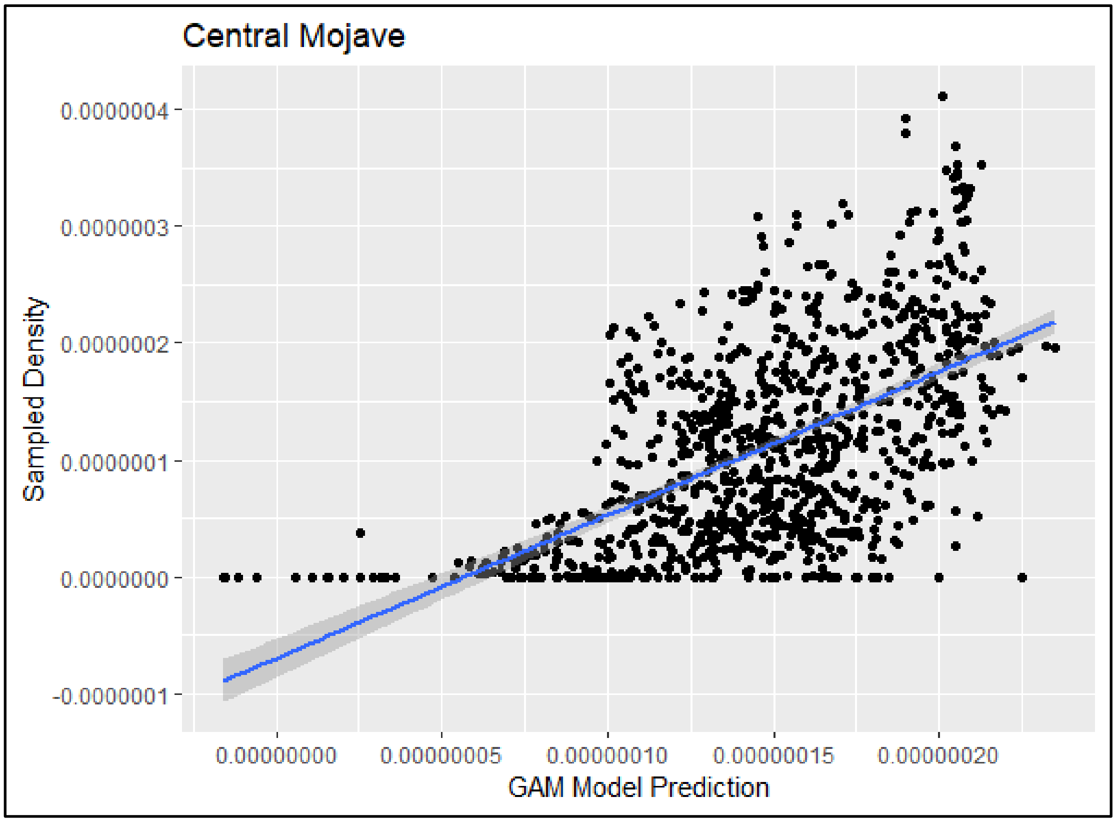

FIGURE 8: TORTOISE TRUE SAMPLED DENSITY (Y-AXIS) VERSUS MODEL PREDICTED DENSITY (X-AXIS)

TABLE 3: CENTRAL MOJAVE GAM SUMMARY INCLUDING: ESTIMATED DEGREES OF FREEDOM (EDF), REFERENCE NUMBER OF DEGREES OF FREEDOM (REF.DF), F-STATISTIC (F) AND P-VALUES.

Terms	**edf**	**Ref.df**	**F**	**p-value**	
Terrestrial Disturbance Index	3.65557	9	0.548	0.2323	
Normalized Difference Vegetation Index	1.39499	9	0.384	0.0654	
Depth to Bedrock	0.00158	9	0.000	0.9740	
Sand on Surface	2.96894	9	2.273	2.72E-05	***
Coarse Fragments on Surface	6.06847	9	15.911	< 2e-16	***
Winter Precipitation	7.39078	9	39.128	< 2e-16	***
Maximum Temperature	4.63104	9	15.822	< 2e-16	***
Deviance Explained = 46.7%	**R-squared (adj) = 0.449**				

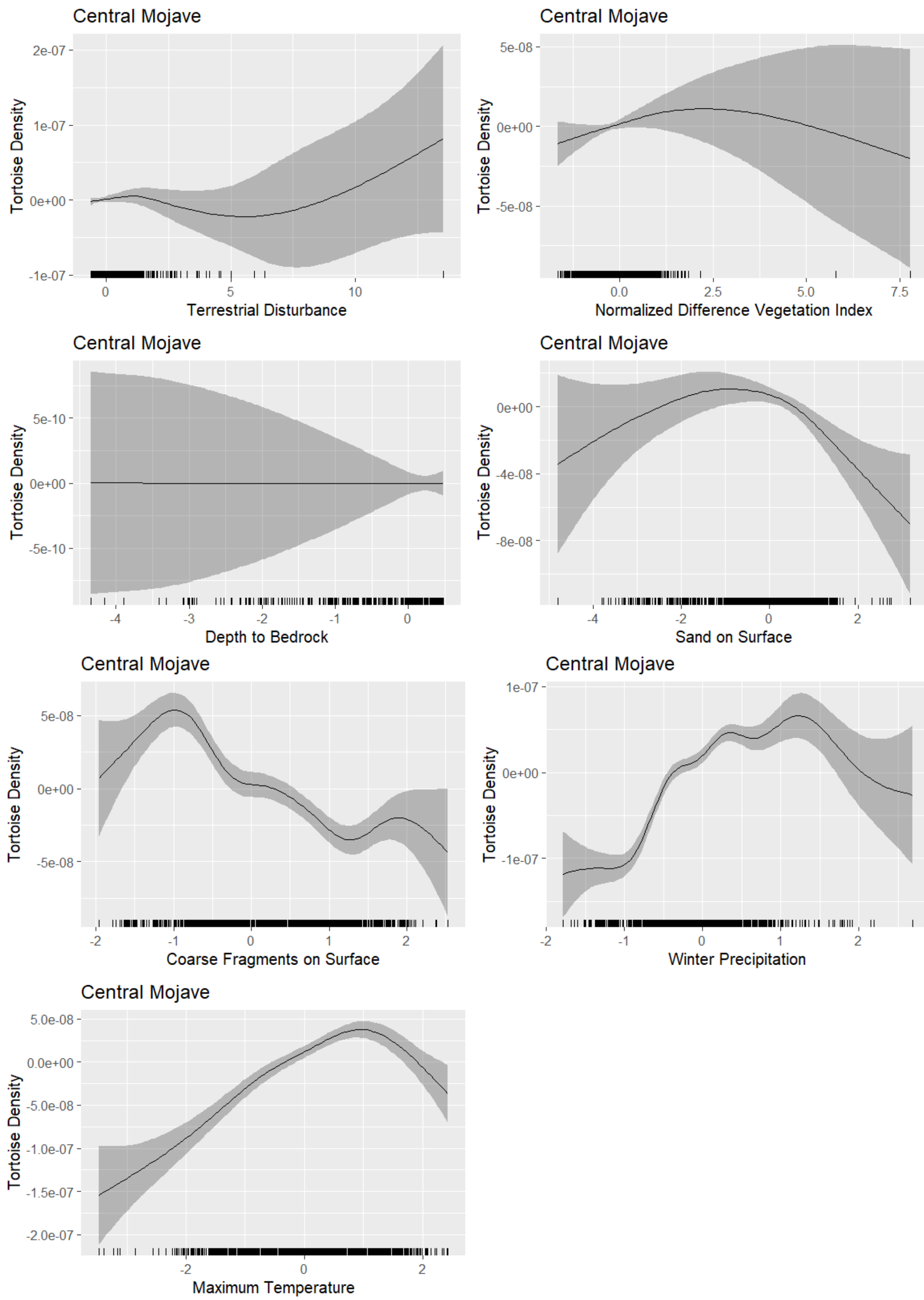

FIGURE 9: CENTRAL MOJAVE TORTOISE DENSITY INTERACTIONS WITH COVARIATES. GRAY REGIONS REPRESENT UNCERTAINTY DUE TO LACK OF DATA POINTS

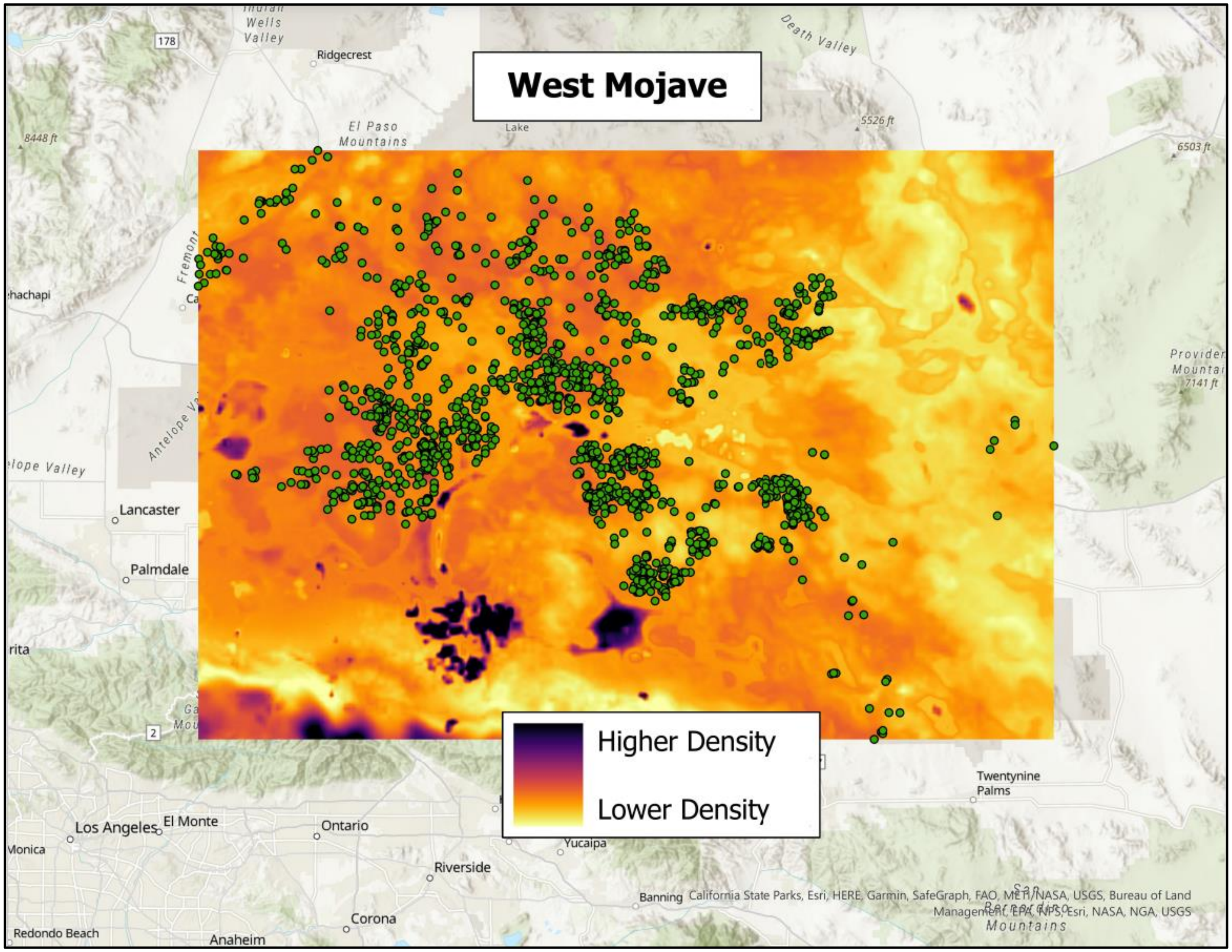

FIGURE 10: WEST MOJAVE GENERALIZED ADDITIVE MODEL TORTOISE DENSITY MAP AND TRUE TORTOISE POINTS

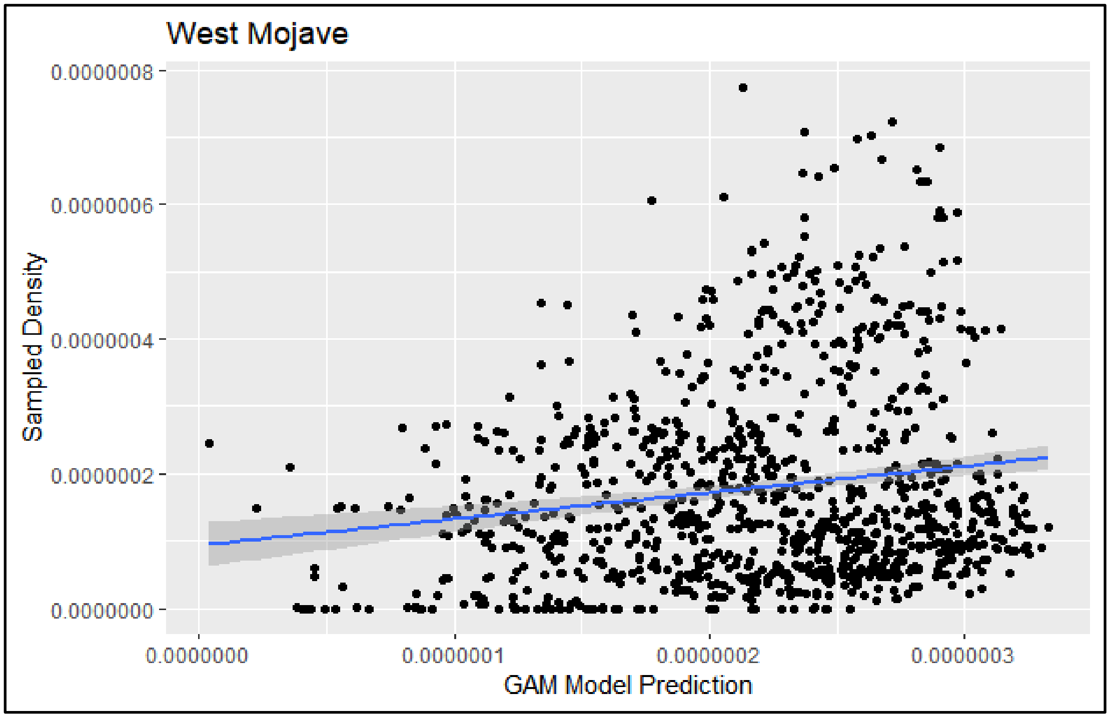

FIGURE 11: TORTOISE TRUE SAMPLED DENSITY (Y-AXIS) VERSUS MODEL PREDICTED DENSITY (X-AXIS)

TABLE 4: WEST MOJAVE GAM SUMMARY INCLUDING: ESTIMATED DEGREES OF FREEDOM (EDF), REFERENCE NUMBER OF DEGREES OF FREEDOM (REF.DF), F-STATISTIC (F) AND P-VALUES.

Terms	**edf**	**Ref.df**	**F**	**p-value**	
Terrestrial Disturbance Index	0.002783	9	0.000	0.901591	
Normalized Difference Vegetation Index	5.015619	9	8.322	< 2e-16	***
Depth to Bedrock	0.631629	9	0.257	0.030780	*
Sand on Surface	8.637385	9	8.392	< 2e-16	***
Coarse Fragments on Surface	2.339846	9	1.760	0.000101	***
Winter Precipitation	8.008219	9	13.069	< 2e-16	***
Maximum Temperature	5.881726	9	8.825	< 2e-16	***
Deviance Explained = 35.1%	**R-squared (adj) = 0.331**				

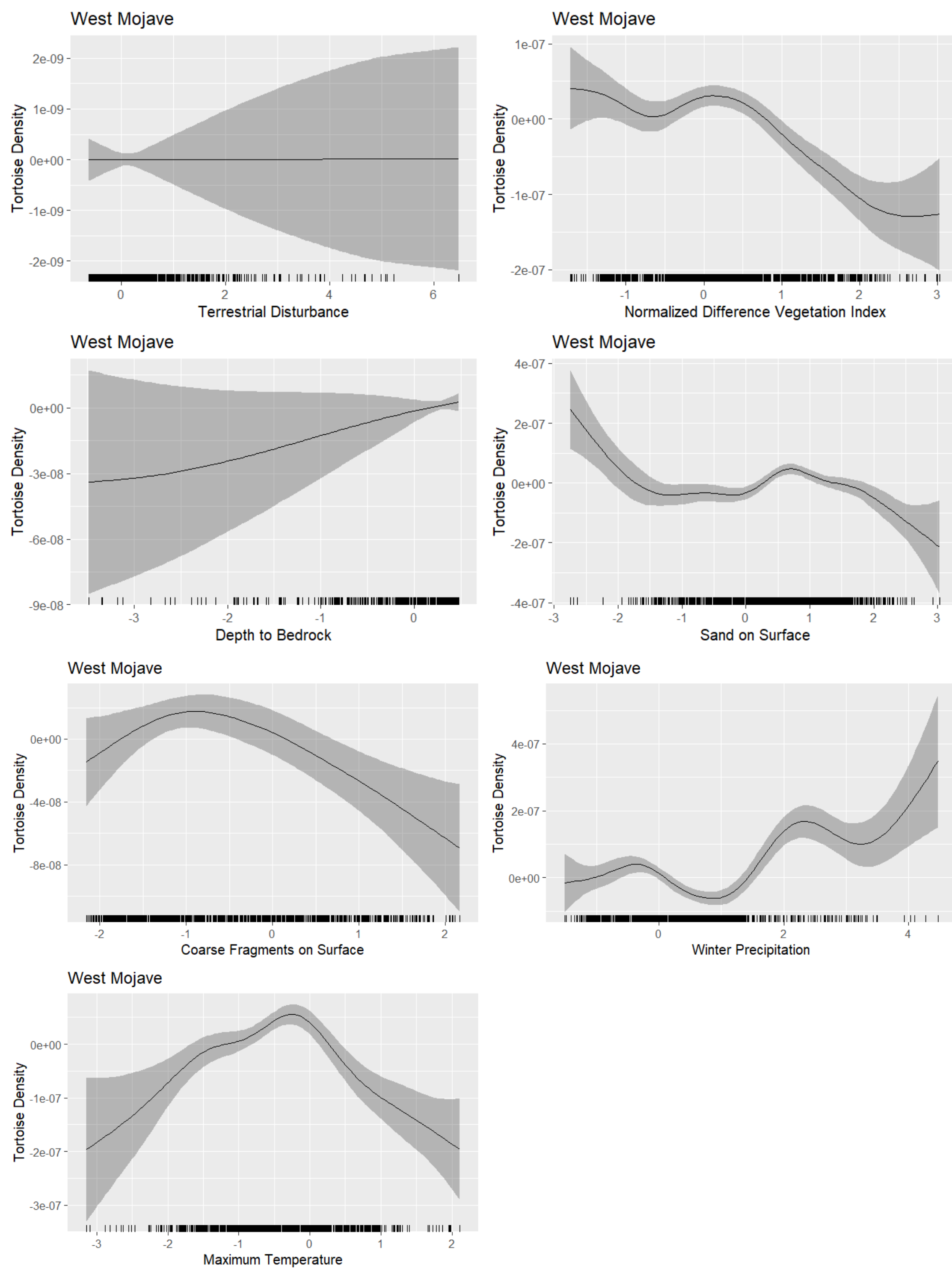

FIGURE 12: WEST MOJAVE TORTOISE DENSITY INTERACTIONS WITH COVARIATES. GRAY REGIONS REPRESENT UNCERTAINTY DUE TO LACK OF DATA POINTS.

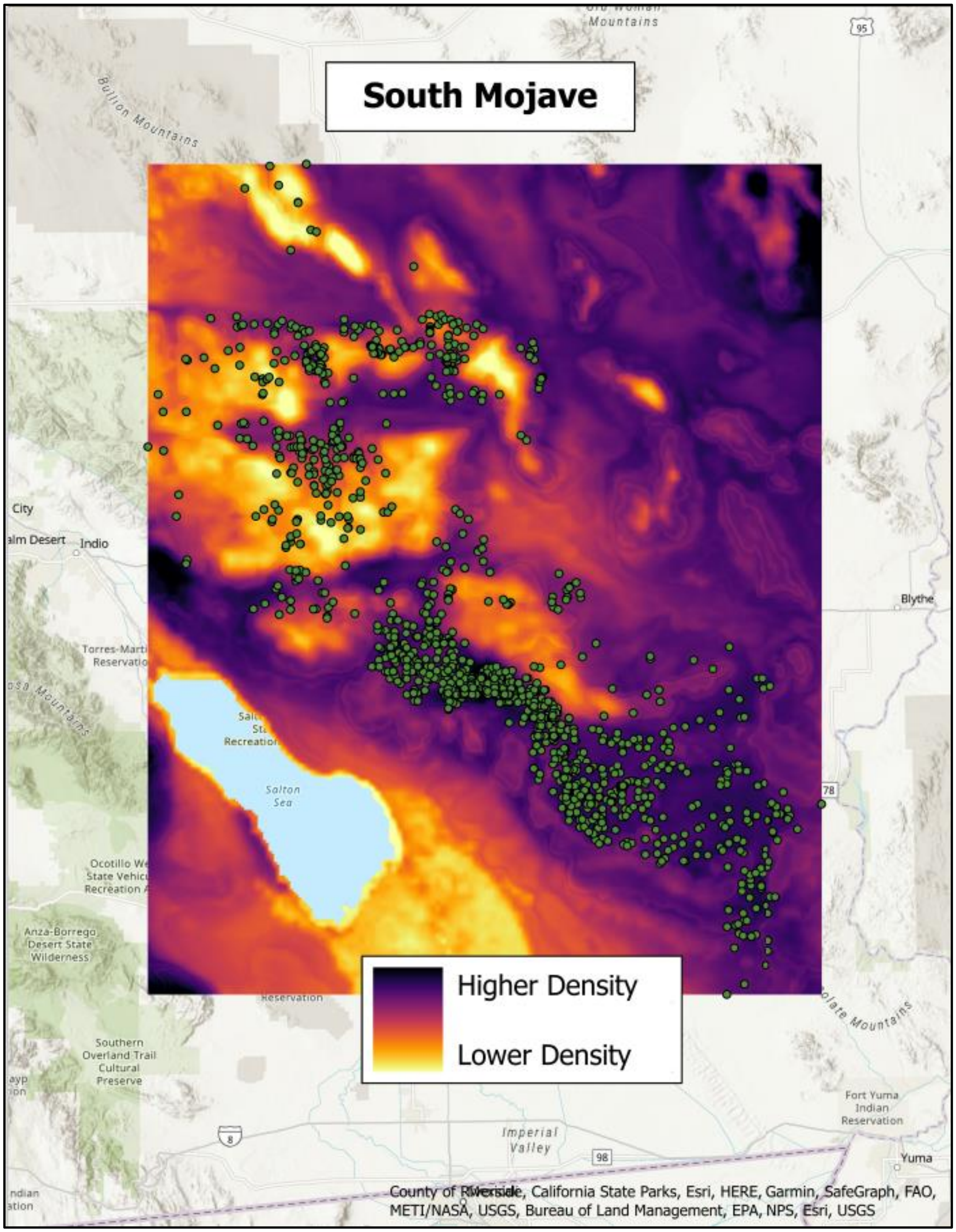

FIGURE 13: SOUTH MOJAVE GENERALIZED ADDITIVE MODEL TORTOISE DENSITY MAP AND TRUE TORTOISE POINTS

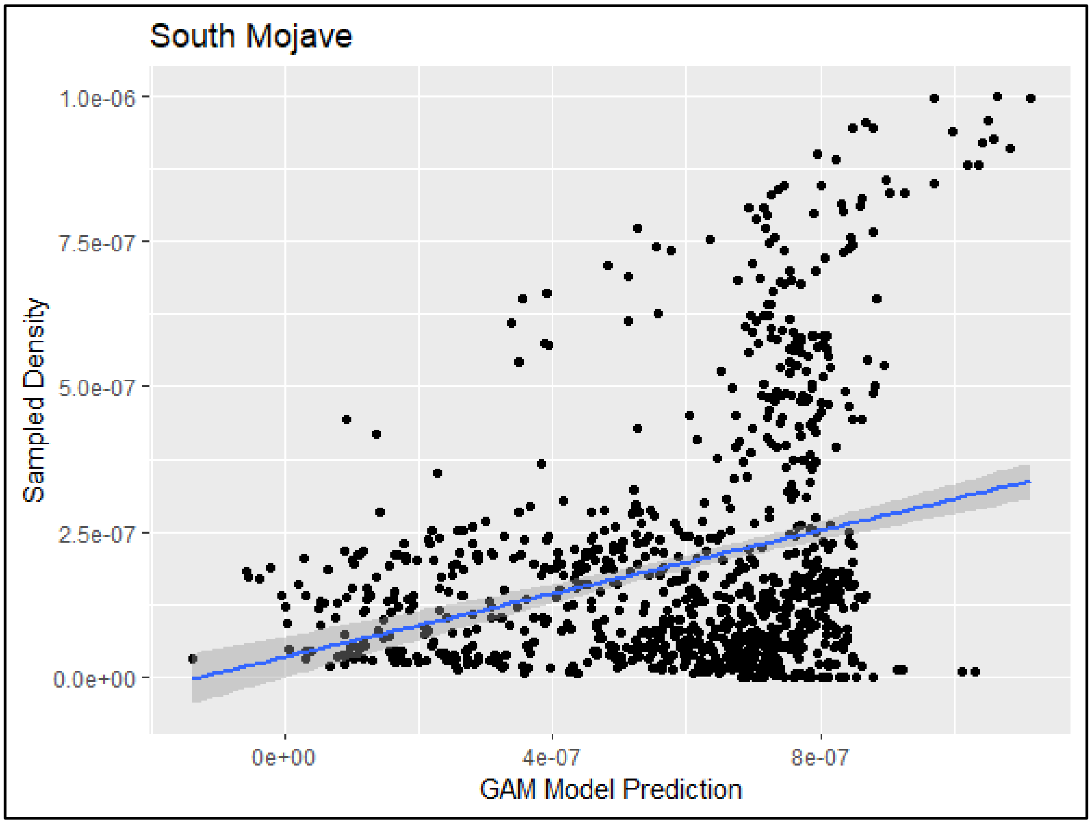

FIGURE 14: TORTOISE TRUE SAMPLED DENSITY (Y-AXIS) VERSUS MODEL PREDICTED DENSITY (X-AXIS)

TABLE 5: SOUTH MOJAVE GAM SUMMARY INCLUDING: ESTIMATED DEGREES OF FREEDOM (EDF), REFERENCE NUMBER OF DEGREES OF FREEDOM (REF.DF), F-STATISTIC (F) AND P-VALUES.

Terms	**edf**	**Ref.df**	**F**	**p-value**	
Terrestrial Disturbance Index	3.113	9	8.211	< 2e-16	***
Normalized Difference Vegetation Index	2.664	9	1.409	0.00148	**
Depth to Bedrock	7.760	9	3.663	4.36E-05	***
Sand on Surface	7.114	9	4.229	2.26E-06	***
Coarse Fragments on Surface	4.815	9	6.971	< 2e-16	***
Winter Precipitation	5.543	9	95.409	< 2e-16	***
Maximum Temperature	7.285	9	83.854	< 2e-16	***
Deviance Explained = 73.2%	**R-squared (adj) = 0.722**				

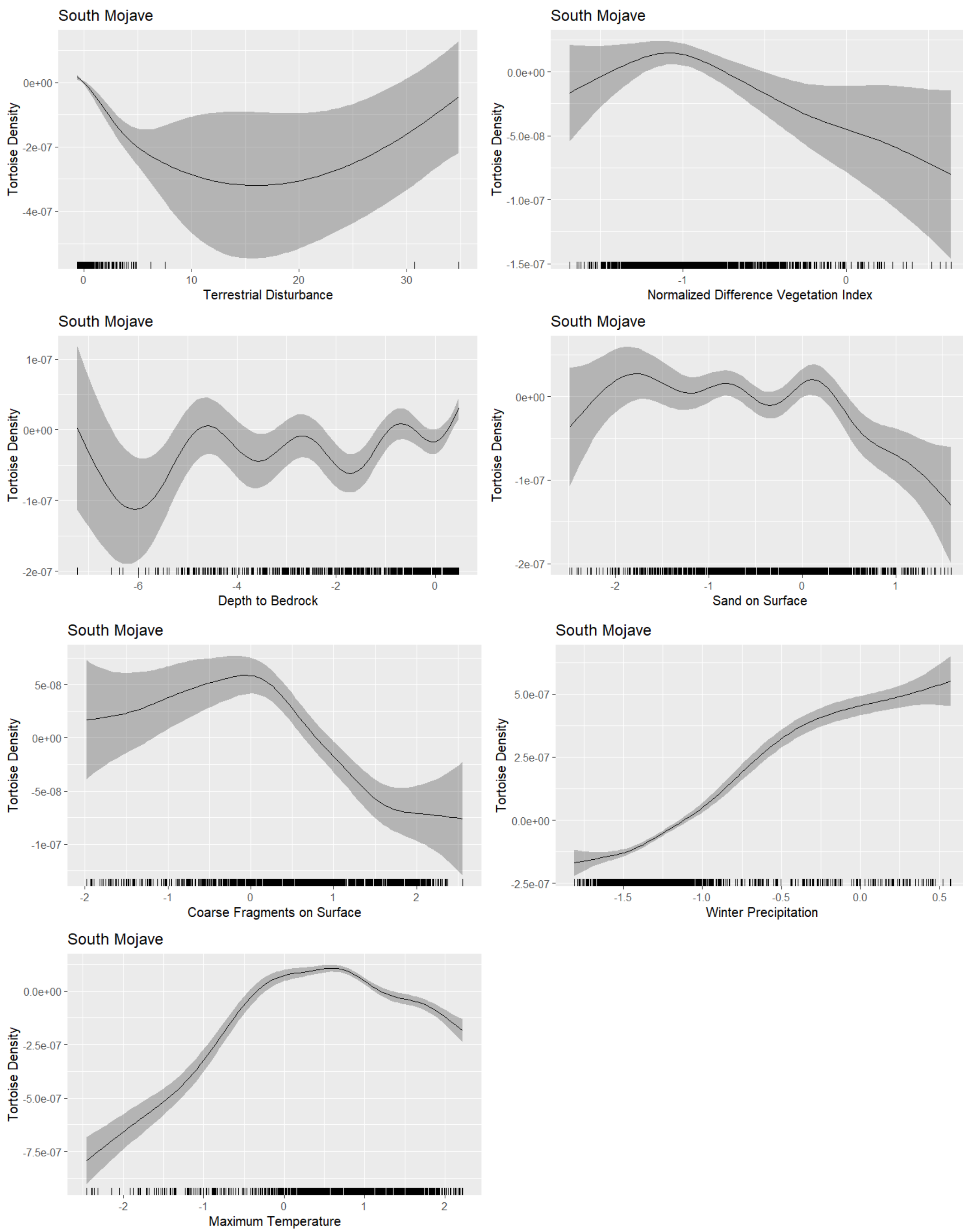

Figure 15: South Mojave tortoise density interactions with covariates. Gray regions represent uncertainty due to lack of data points.

Chapter 2: Using UAVs to obtain remotely sensed imagery for measuring habitat suitability indicators of the Mojave Desert Tortoise

Due to the patchy nature of tortoises distributed throughout their habitat, I sought to examine influential factors on tortoise densities at multiple scales. At the landscape scale, remote sensing imagery derived from satellites allows for the analysis of explanatory environmental covariates in relation to range wide tortoise densities. At finer scales, detailed data have been collected that give insights into tortoise health and potentially smaller scale patterns in habitat preferences (Figure 16). The AIM strategy for vegetation monitoring was adopted by the Bureau of Land Management (BLM) to create a standardized monitoring protocol for assessing the conditions and trends of natural resources on public lands (Toevs 2011). Using UAVs, I can characterize finer scale data similar to AIM data on vegetation and soils that influence individual tortoises more directly. Some knowledge already exists regarding habitat requirements of desert tortoises. At low elevations, desert tortoise habitat is typically characterized by creosote bush (*Larrea tridentata*) and white bursage shrubs (*Ambrosia dumosa*), while at higher elevation ranges habitat consists of Joshua tree (*Yucca brevifolial*) and Mojave Yucca (*Y. schidigera*) woodlands, though at these sites tortoise densities begin to diminish as blackbrush (*Coleogyne ramossisima*) begins to dominate the landscape (Nussear and Tuberville 2014, Berry and Murphy 2019). Though imagery obtained with UAVs is typically not used to quantify densities of specific plant species, other habitat characteristics such as percent perennial cover, annual growth, shrub cover, and soil moisture are readily derived from imagery obtained in this manner. A recent study used drone imagery combined with existing rangeland monitoring programs to estimate inter-canopy gaps, vegetation height and structure, and fractional cover. These flights were conducted 40m above the ground and consisted of one vertical mission and four missions to collect 30-degree oblique images (Gillan et al. 2020).

One of the first steps toward bridging the gap between data collected using transect field methods and data collected using satellite imagery is to determine if the measurements of habitat characteristics obtained from UAV imagery correlate with the data obtained through measurements using the AIM protocol. For instance, if shrub cover percentage obtained through the AIM gap intercept method is equivalent to the shrub cover percentage derived from UAV imagery, then UAVs could be advantageous for obtaining fine scale data, as they can cover more of the landscape than field transect methods could feasibly cover. Field estimates remain important toward calibrating the data, but UAV acquired data may provide a more accurate means of assessing vegetation at broader scales. Numerous studies have attempted the extrapolation of field measurement data to a larger area. For instance, one study used the line-intercept method to measure perennial vegetation and multiplied maximum height by intercept distance (intercept start and end of each plant along the transect) to obtain a 2-dimensional index of biomass in units/m^2 (Webb 2003). Similar methods can be applied to the BLM AIM data and derive measurements comparable with UAV imagery to determine suitability of such methods.

The relationship between satellite imagery and UAV imagery is much easier to link as similar methods are used for collecting satellite imagery as are used when collecting imagery through UAVs. For instance, the normalized difference vegetation index (NDVI) is derived from a calculation using near-infrared and red imagery bands, both of which can be obtained from both satellite and UAV sensors. Differences do exist however between sensor bands, and the aggregation that occurs due to differential pixel sizes. One study used MODIS satellite enhanced vegetation index combined with field measurements to obtain estimates of perennial vegetation cover, however this was only able to produce results with a 250m resolution (Wallace et al. 2008). This resolution would be sufficient for range wide analyses, but to understand habitat characteristics within 1km by 1km plots we would benefit from finer resolution. With this, it is evident that all three methods (field measurements, UAV imagery, and satellite imagery) are equally important considerations in our analysis of the influences of environmental covariates on tortoise distributions.

Data obtained through on the ground field methods have the potential to provide a greater understanding of tortoise population health indicators (such as densities across the landscape) in relation to environmental covariates. This is because field measurements reveal detailed data on plant species biomass and composition as well as soil structure and stability. If data obtained through field methods can be related to UAV derived measurements, then there is potential to assess environmental variables in relation to tortoise densities and behaviors beyond the small scales that are possible using transect based methods.

Research Questions:

- Can remote sensing imagery obtained with UAVs supplement on the ground field data collection methods, and bridge the gap between fine scale data and satellite-based imagery?

Methods:

UAV flights were conducted where AIM plots occur in order to calibrate field-measurements with image-derived indicators. There are 10 plots where I conducted UAV flight missions, 6 of these plots are 800 meters by 800 meters in size while 4 plots are 400 meters by 400 meters in size (Table 6). Each flight covered the same region of the AIM surveys as well as areas where tortoises have been monitored. Flights were conducted at the maximum legal height of approximately 400 feet. I used a DJI Matrice M200 and the Android application UgCS for DJI to create a connection between our drone and tablet to create and monitor flight missions. A Micasense Red Edge MX multispectral camera was used for capturing imagery which was then compiled and processed using Pix4D on a Windows Server based PC. Approximately 8,000 to 15,000 images were collected for each individual plot for each month.

TABLE 6: STUDY PLOTS WHERE UAV IMAGERY WAS OBTAINED ALONGSIDE BLM AIM DATA COLLECTION.

Study Plots	Size
McCullough Pass	800x800 meters
Sheep Mountain	800x800 meters
Silver State	800x800 meters
Coyote Springs North	800x800 meters
Coyote Springs Center	800x800 meters
Coyote Springs South	800x800 meters
Stump Springs Zone 1	400x400 meters
Stump Springs Zone 2	400x400 meters
Stump Springs Zone 3	400x400 meters
Stump Springs Zone 4	400x400 meters

The AIM protocol consists of 4 AIM points per each of six tortoise plots: Coyote Springs (3 plots), McCullough Pass, Sheep Mountain, and Silver State, and 1 AIM point for each of four tortoise plots at Stump Springs. At each randomly generated AIM point location three 25 meter long transects are placed at 0 °, 120 °, and 240 °. Along these transects field crews conduct gap intercept measurements for shrub cover, line point intercepts (LPI) for quantifying vegetation and soil cover, species Inventory, and forb diversity. Additionally, crews assess soil stability and infiltration through digging a soil pit and capture site photographs.

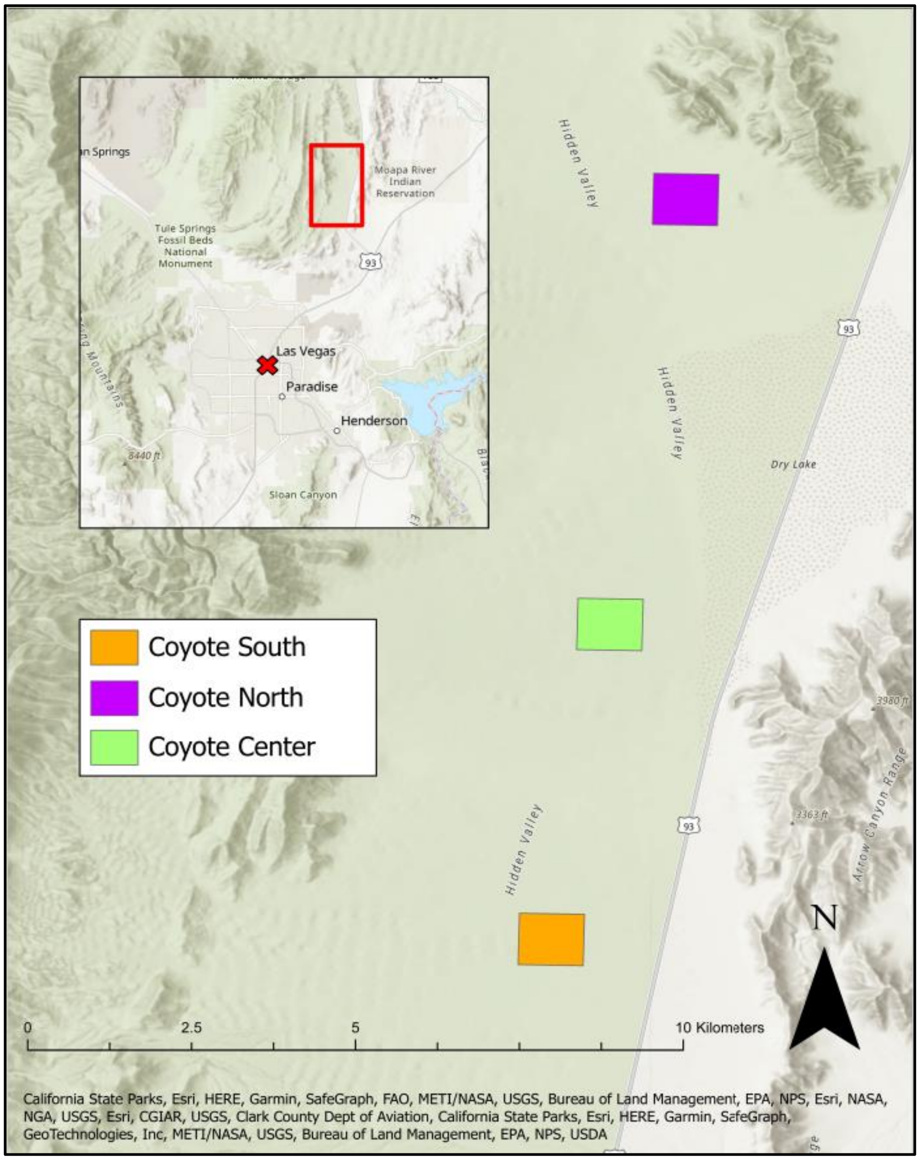

Figure 16: Figure 16: 1 km^2 AIM locations for Coyote Spring North, Central, and South.

To compare UAV imagery with field derived AIM data I focused on comparing the ability of UAV imagery to capture shrub cover, which could have implications for suitability of tortoise habitat, as this represents cover for thermal protection as well as from predators. Analyses at the individual plant species level were not the focus of this project but are possible with higher resolution imagery and additional field validated training data. Shrub cover was estimated using a supervised classification method. To conduct this classification, I created approximately 4000 to 5000 training polygons for each plot representing shrub and soil classes in the program ArcGIS pro. Once I created training classes, I used an RGB (red, green, blue), an NDVI image, and a plant height layer (calculated by subtracting the digital surface model from the digital terrain model calculated in Pix4d) to run a random forest classification using the RandomForest package (4.7-1.1) in R. This was then projected onto the full study area to produce a surface representing shrub and soil.

The AIM protocol measures gaps between shrubs along 25-meter transects. To obtain shrub cover for our comparison with the UAV derived data, I took the inverse of these gap values to convert gaps into shrub intersections and compared this to shrub cover from the random forest classifications. To obtain average shrub cover for AIM transects I took the total length of shrubs along a single transect in centimeters divided by 2500cm (the total length of the transect). Due to both human and GPS error, the location of the 25-meter transects that are used for each return visit to the same AIM plot for several months out of the year are not always in the exact same location. To calculate the potential for error in comparing the AIM and UAV derived shrub cover values I created a 5-meter buffer (representing the error possible using handheld consumer grade GPSs) around the start point of each transect and digitized 100 random points in this circle from which I created 100 random transect lines with the same direction and length as the AIM transects. This was used to obtain the frequency of potential shrub cover values that could be measured on the AIM transects for comparison with the AIM data (Figures 17, 18, 19, and 20). For this part of the analysis, I set any values of the shrub cover raster layer representing soil to null. I then converted the raster into polygons to depict only shrubs across the plot. Finally, I used the intersect tool in ArcGIS pro to intersect the one hundred lines for each transect with the shrub cover polygon to obtain the estimates of shrub cover values in centimeters for each of the 100 simulated transects (Figure 21).

Results:

The analysis evaluating shrub cover captured with UAV imagery against shrub cover obtained from AIM data reveal that, although AIM data is capturing a portion of the picture, there is a great deal of heterogeneity across the landscape that is being missed when collecting data in this manner. Additionally, it is clear that there is often an over- or under-estimation of shrub cover when only taking into consideration shrub cover captured along several 25 meter transects (Figures 22, 24, and 26). In March of 2022 at McCullough Pass the data reveal that the AIM shrub cover was overestimated along all three transects relative to the shrub cover captured from the UAV (Figure 21). At Sheep Mountain in March shrub cover was overestimated by the AIM data along 2 of 9 transects while the rest revealed underestimates by the AIM data (Figure 22). On this plot transects 3, 7, 8, and 9 reveal a significant under estimation of shrub cover in relation to what was captured using the UAV. Transect 3 for the AIM data had a mean shrub cover of just 0.0188cm across the single 2500 centimeter transect while the UAV mean estimate from 100 transects (each 2500 centimeters in length) was 0.2252cm. At

Silver State in March of 2022 there was an even distribution of over and underestimates by the AIM data relative to the UAV data, with transects 7, 10, and 12 having nearly the exact same mean estimates between AIM and UAV data (Figure 23). At Coyote Springs north 4 of 6 transects depicted significant underestimations of shrub cover by the AIM data relative to the UAV data (Figure 24). Similarly, at Stump Springs in March of 2022 most of the AIM data (7 out of 9 transects) appeared to underestimate shrub cover (Figure 25). Similar to the March results, in April of 2022 the AIM transect data at McCullough revealed mostly overestimates of shrub cover (9 of 12 transects) relative to the UAV shrub cover (Figure 26). However, for the rest of the plots in April of 2022 the AIM data most often underestimates shrub cover relative to the UAV data (Figures 27, 28, 29, and 30). In May of 2022 exactly half of the transects at McCullough Pass display an underestimation of shrub cover by the AIM data relative to the UAV data (Figure 31). Moreover, 30 of the 51 transects across all plots in May reveal an underestimation of shrub cover by the AIM transect data, with some of the AIM values showing significant deviations from the UAV shrub cover estimates (Figures 31, 32, 33, 34, and 35). For instance, at Silver State in May of 2022 transect 3 had a mean shrub cover of 0.0944cm from the AIM data for a single 2500cm long transect while the UAV estimated mean from 100 transects was 0.3239cm (Figure 33). These trends continued in September of 2022 with the AIM transect data having underestimated shrub cover along 44 of 51 transects across all plots relative to the UAV shrub cover data (Figures 36, 37, 38, 39, and 40). T-tests evaluating mean UAV shrub cover values against mean AIM shrub cover values can be found in Index I.

Discussion:

Field methods such as the AIM protocol are effective for collecting detailed plant data, however they come with limitations as demonstrated by the analyses here. To be able to rely on the extrapolation of AIM data to larger areas it is crucial that methods are consistent and that measurements are accurate. The shrub cover measurements obtained through UAV imagery reveal that there is great variability of shrub cover throughout Mojave desert tortoise habitat even amongst plots that are just several kilometers apart. Although the mean shrub cover values obtained from the AIM protocol often falls within these boundaries there is still a great deal of heterogeneity not being captured by this method. Additionally, the shrub cover measurements obtained through the AIM protocol most often underestimate the shrub cover relative to the measurements obtained with the UAV. This discrepancy in shrub cover measurements is likely due to the difficulty of placing tape measures in straight lines across shrubs and rough terrain. Though human error is always a factor in obtaining data through field methods this issue can be mitigated by using more sturdy measurement tools such as poles rather than the tape measures that are able to bend and move so easily. The data obtained using UAVs demonstrates an effective method of obtaining shrub cover across larger regions than could be obtained using the AIM protocol. Using UAVs to obtain habitat imagery at these scales can aid in evaluating how tortoise densities vary with differing shrub cover values as well as other habitat characteristics.

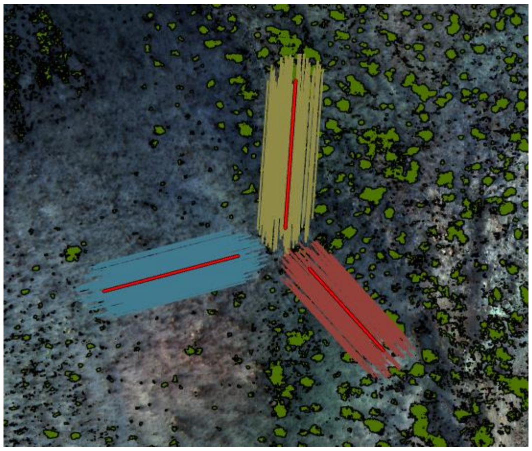

FIGURE 17: MCCULLOUGH PASS AIM TRANSECTS (RED) MARCH 2022

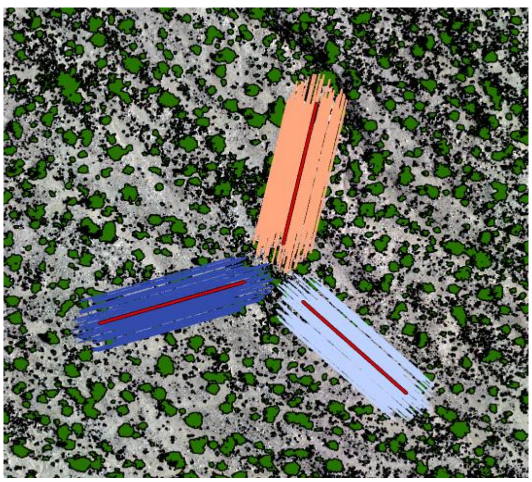

FIGURE 18: SILVER STATE AIM TRANSECTS (RED) MAY 2022

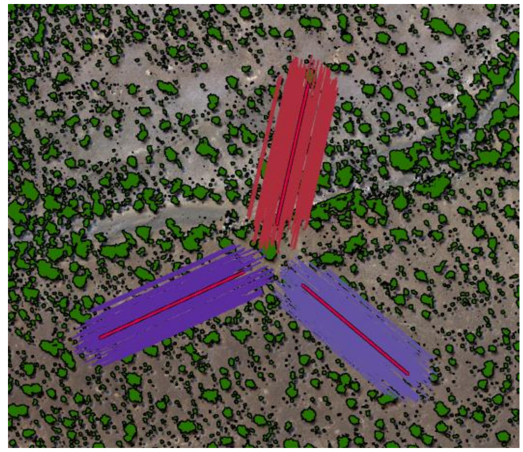

FIGURE 19: SHEEP MOUNTAIN AIM TRANSECTS (RED) APRIL 2022

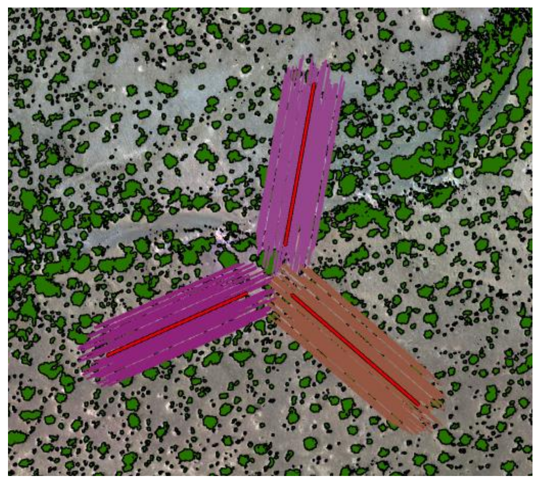

FIGURE 20: SHEEP MOUNTAIN AIM TRANSECTS (RED) SEPTEMBER 2022

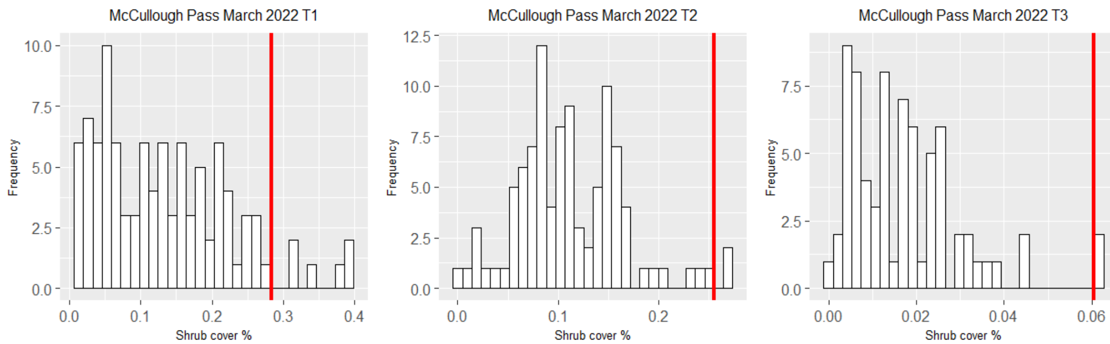

Figure 21: Figure 18 McCullough Pass March UAV Shrub Cover % Versus AIM Shrub Cover % (red line)

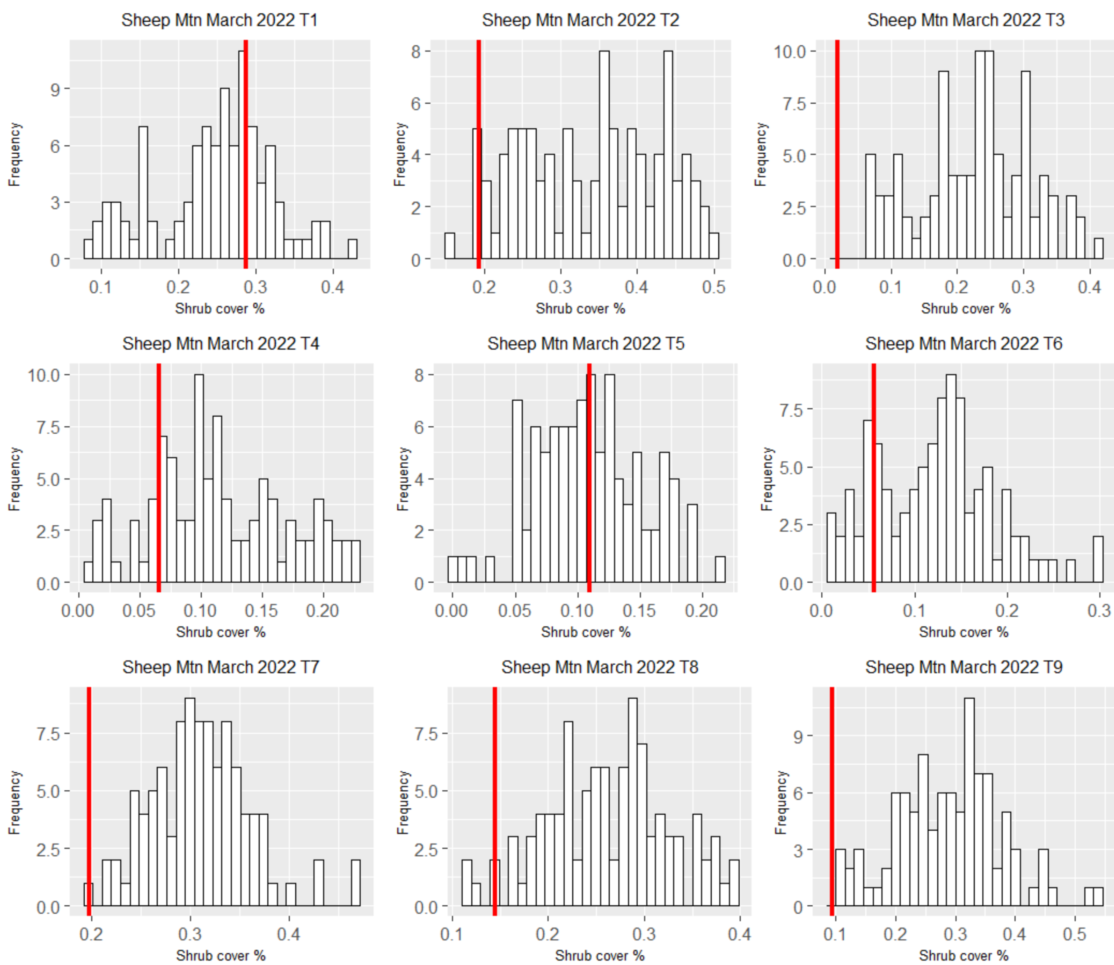

Figure 22: Sheep Mountain March UAV Shrub Cover % Versus AIM Shrub Cover % (red line)

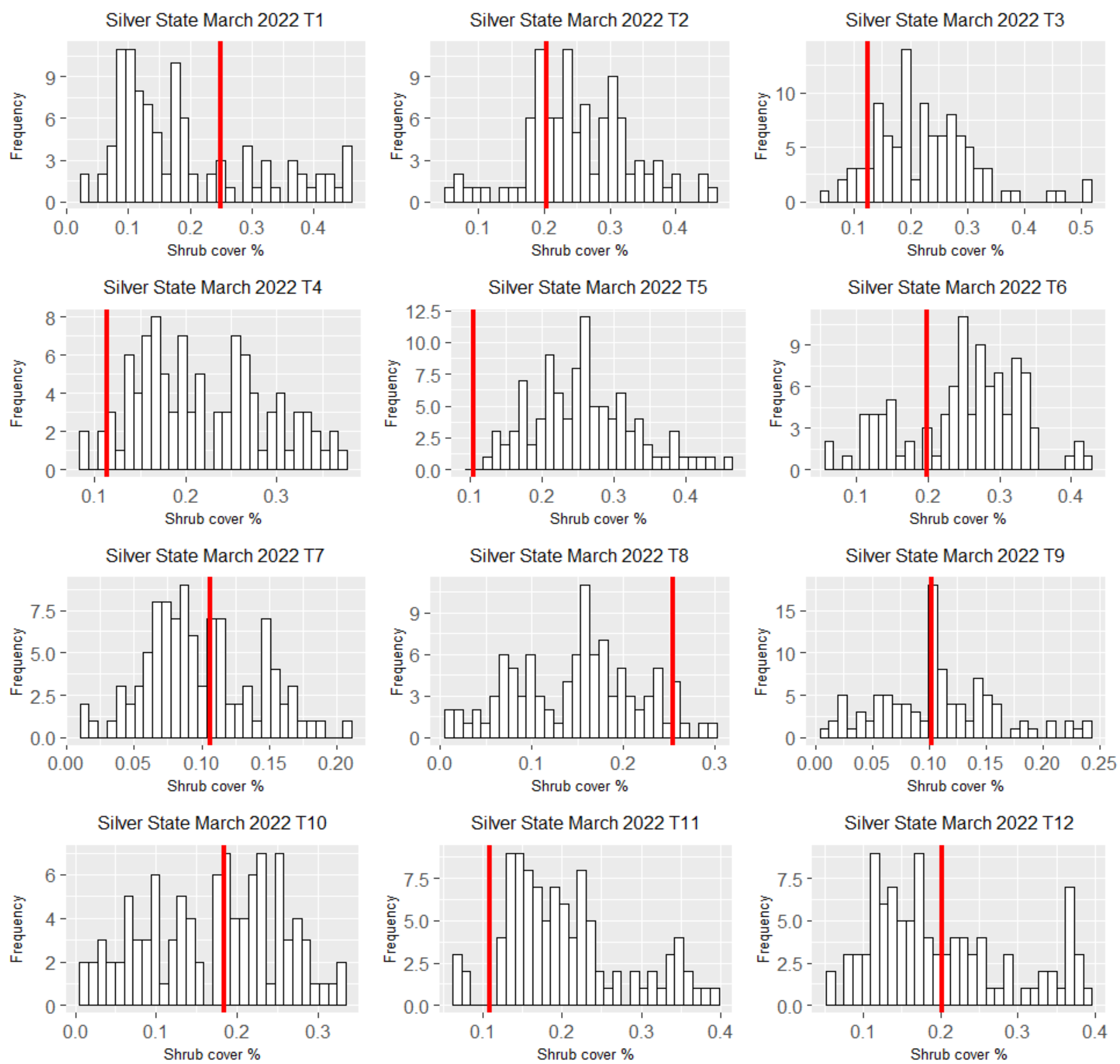

FIGURE 23: SILVER STATE MARCH UAV SHRUB COVER % VERSUS AIM SHRUB COVER % (RED LINE)

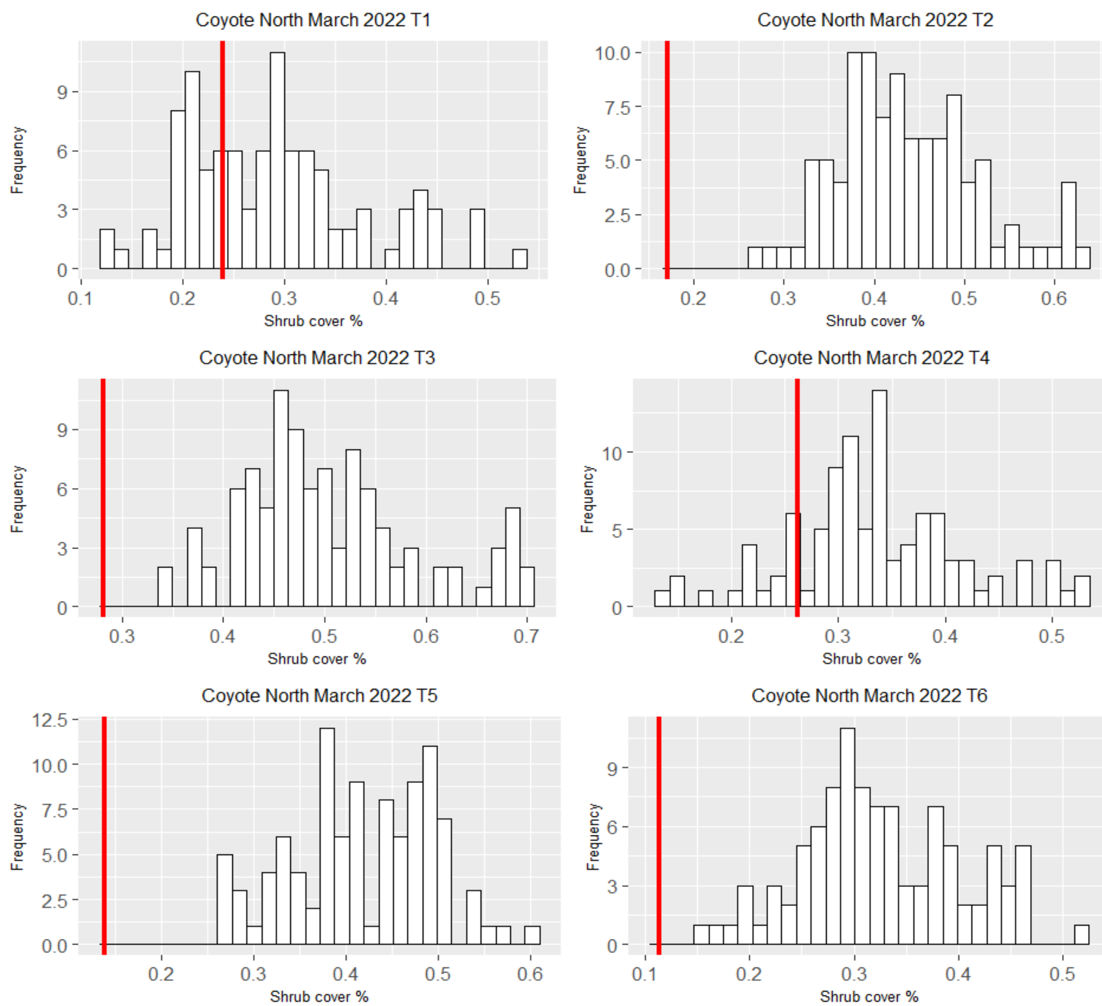

FIGURE 24: COYOTE SPRINGS MARCH UAV SHRUB COVER % VERSUS AIM SHRUB COVER % (RED LINE)

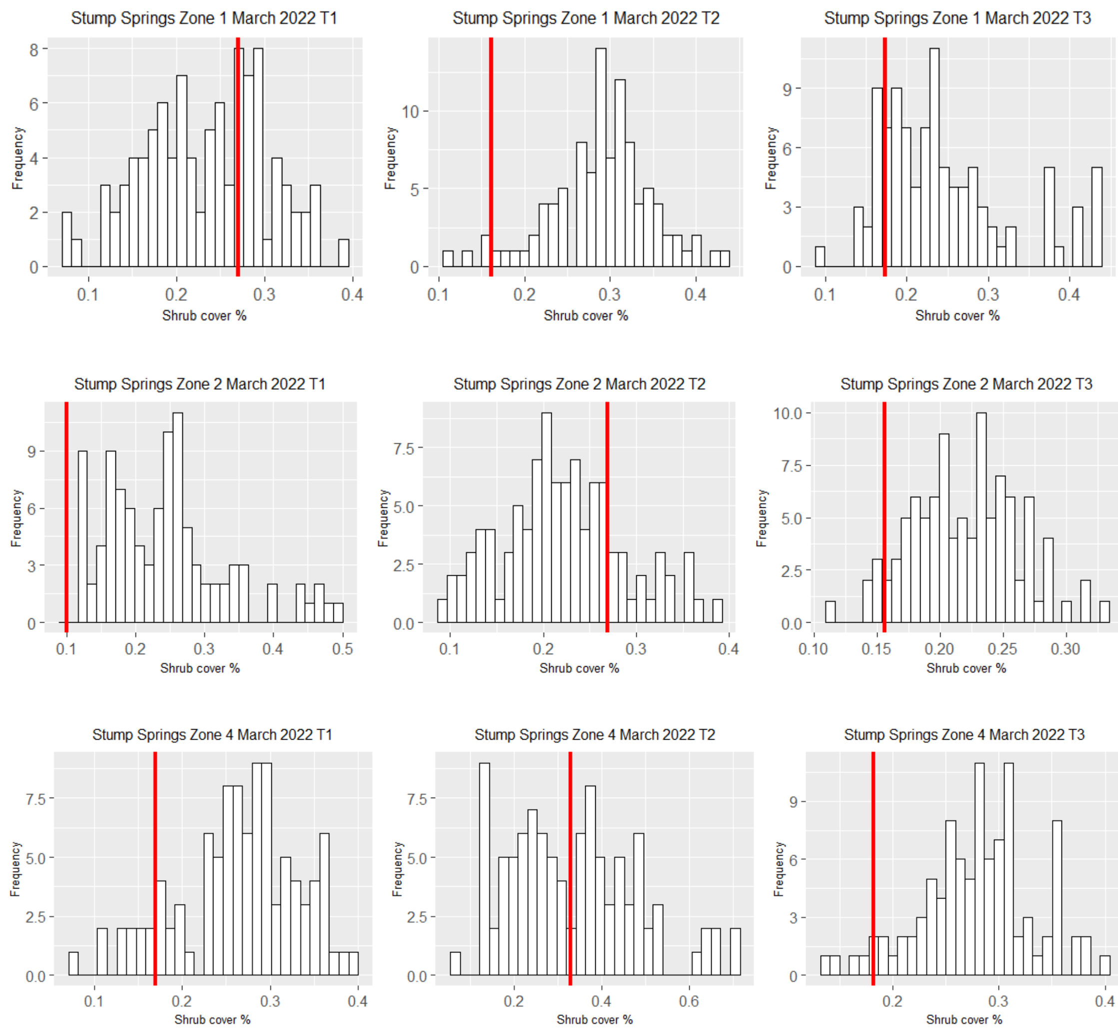

FIGURE 25: STUMP SPRINGS MARCH UAV SHRUB COVER % VERSUS AIM SHRUB COVER % (RED LINE)

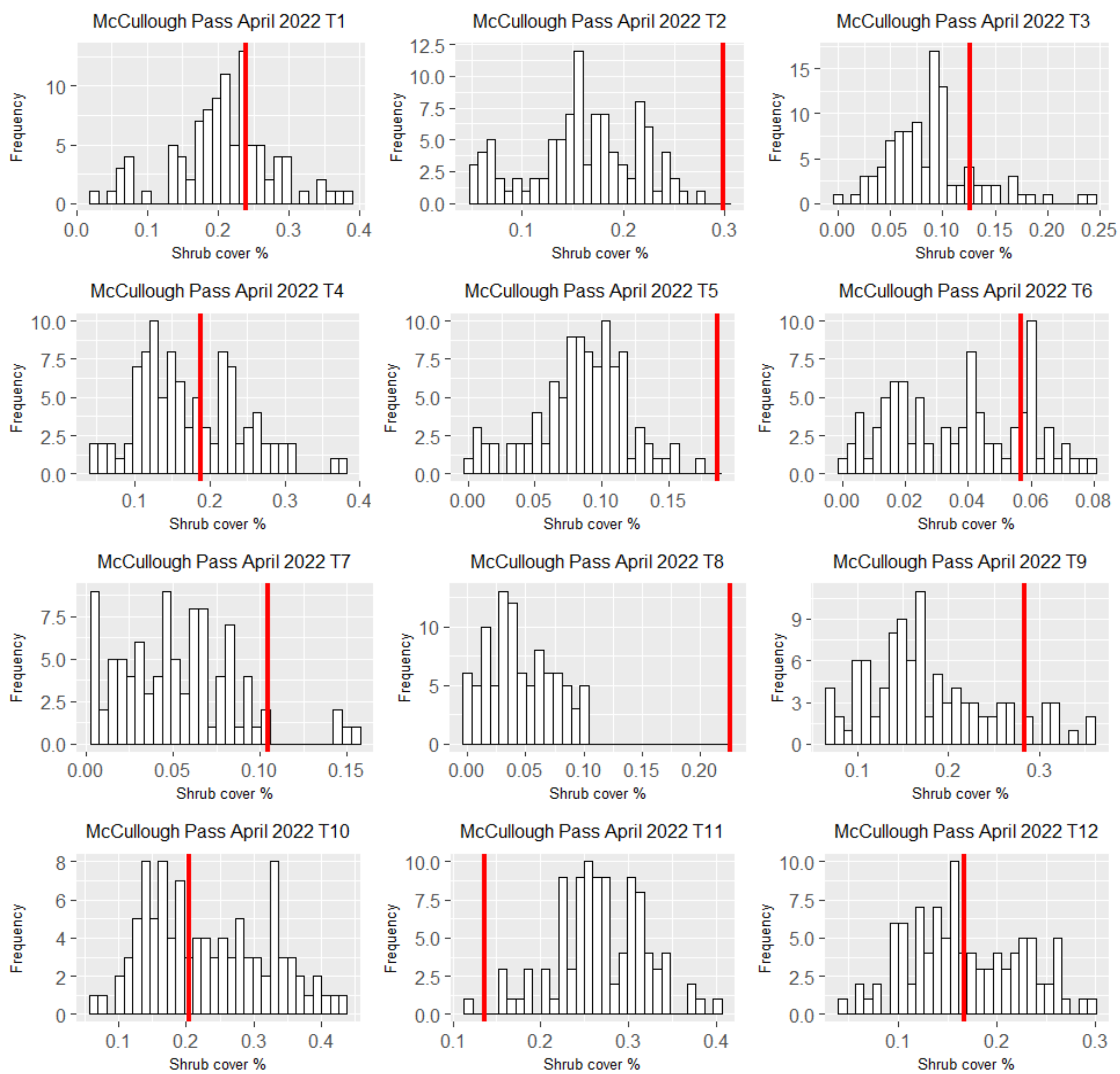

FIGURE 26: MCCULLOUGH PASS APRIL UAV SHRUB COVER % VERSUS AIM SHRUB COVER % (RED LINE)

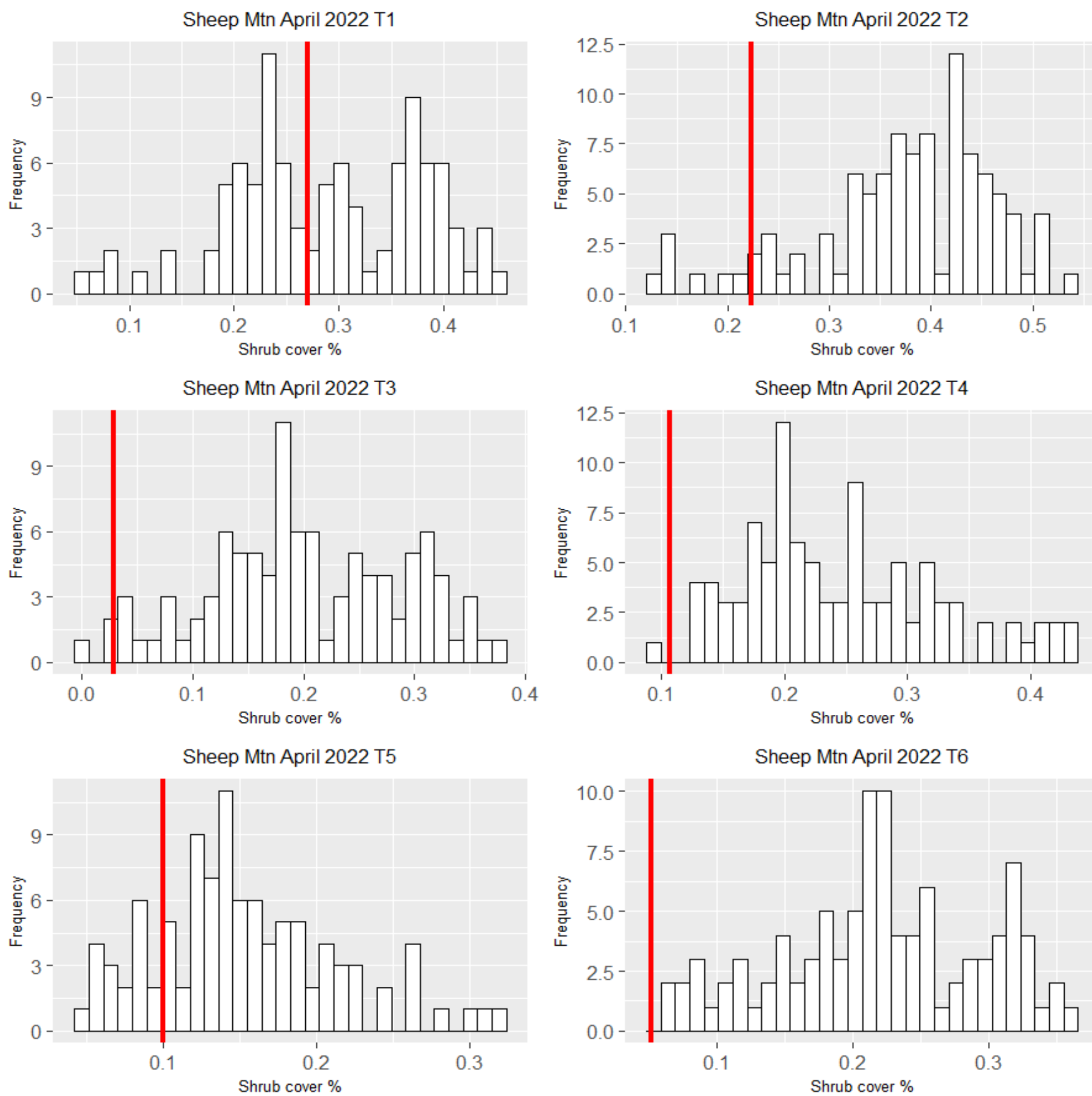

Figure 27: Sheep Mountain April UAV Shrub Cover % Versus AIM Shrub Cover % (red line)

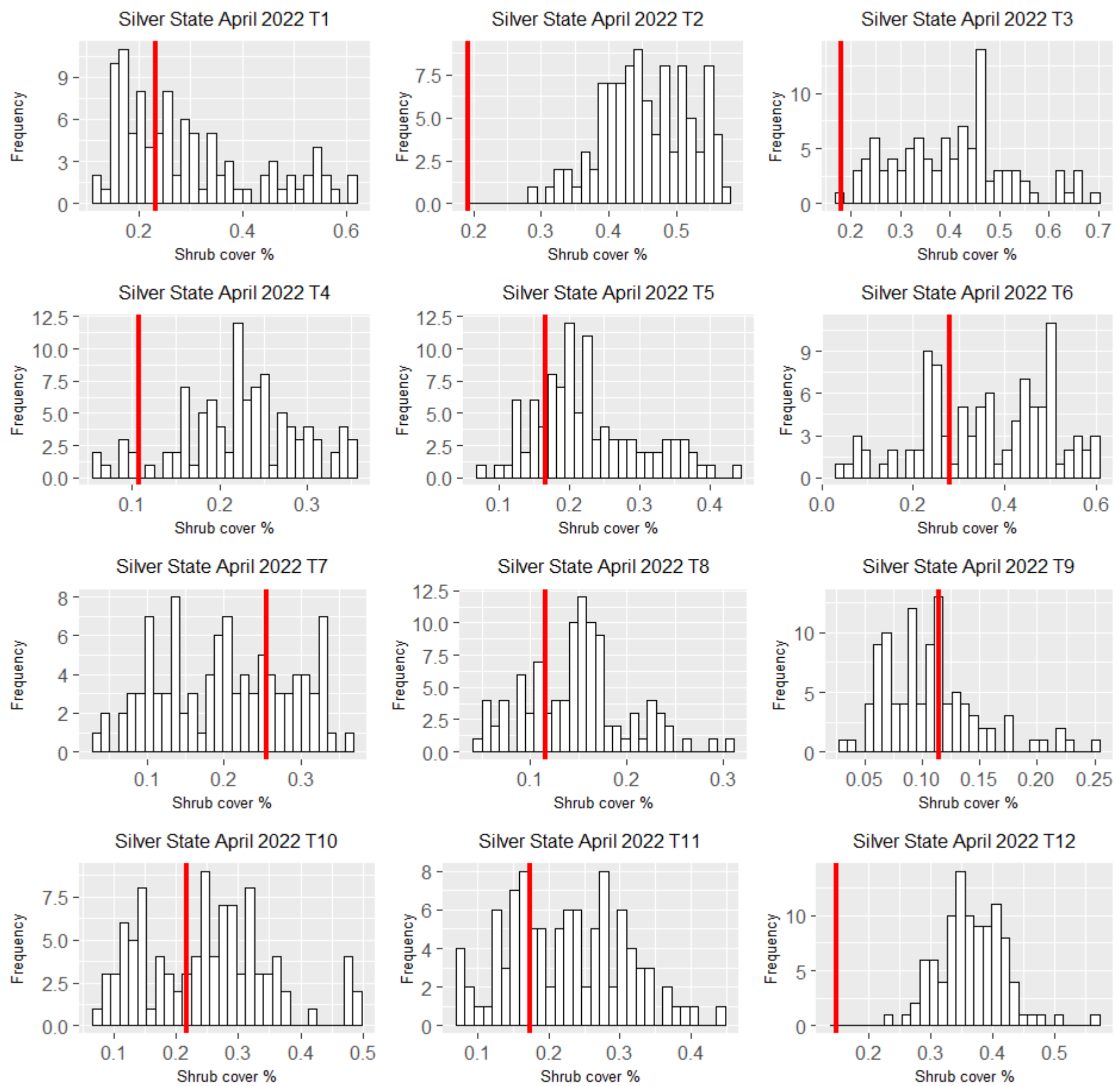

FIGURE 28: SILVER STATE APRIL UAV SHRUB COVER % VERSUS AIM SHRUB COVER % (RED LINE)

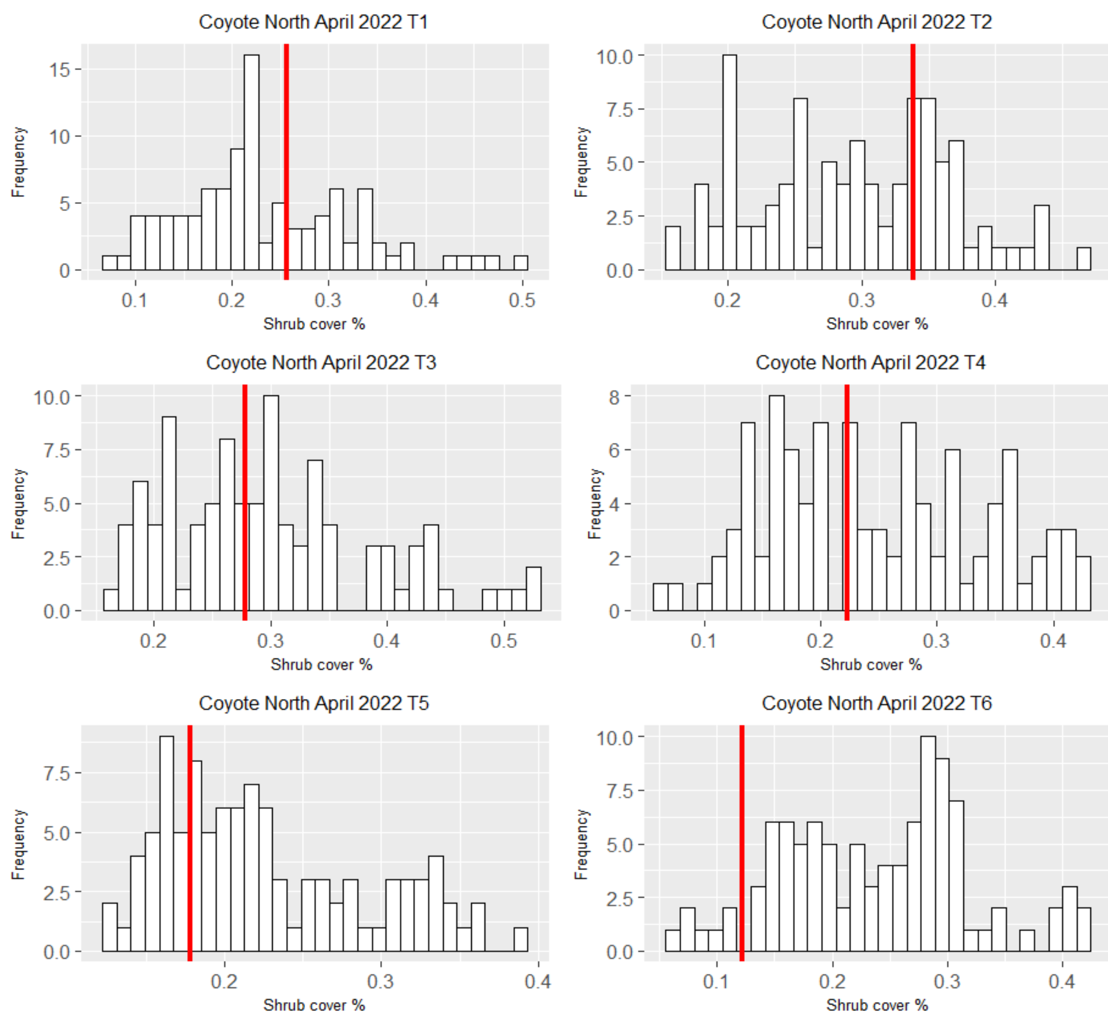

Figure 29: Coyote Springs April UAV Shrub Cover % Versus AIM Shrub Cover % (red line)

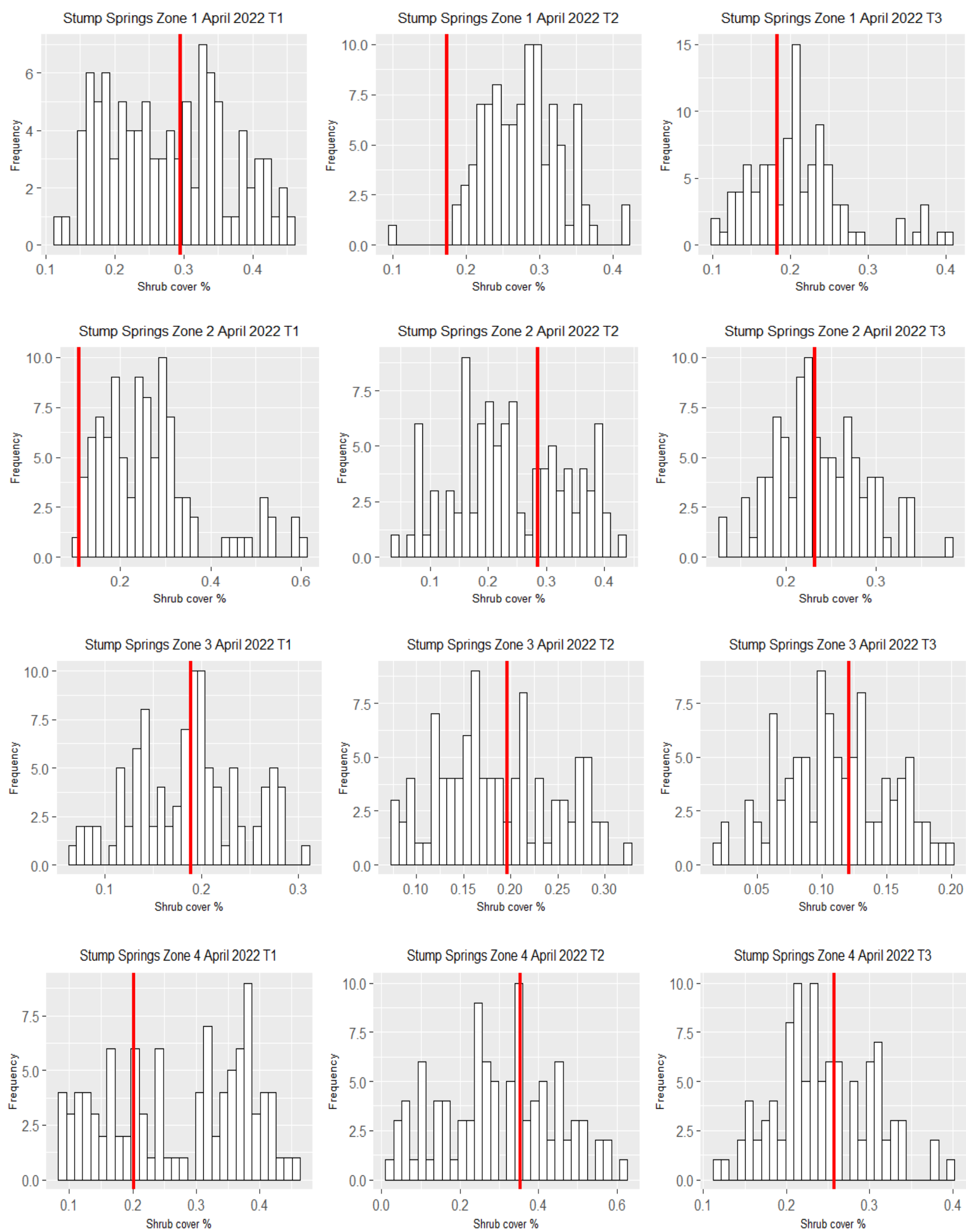

FIGURE 30: STUMP SPRINGS APRIL UAV SHRUB COVER % VERSUS AIM SHRUB COVER % (RED LINE)

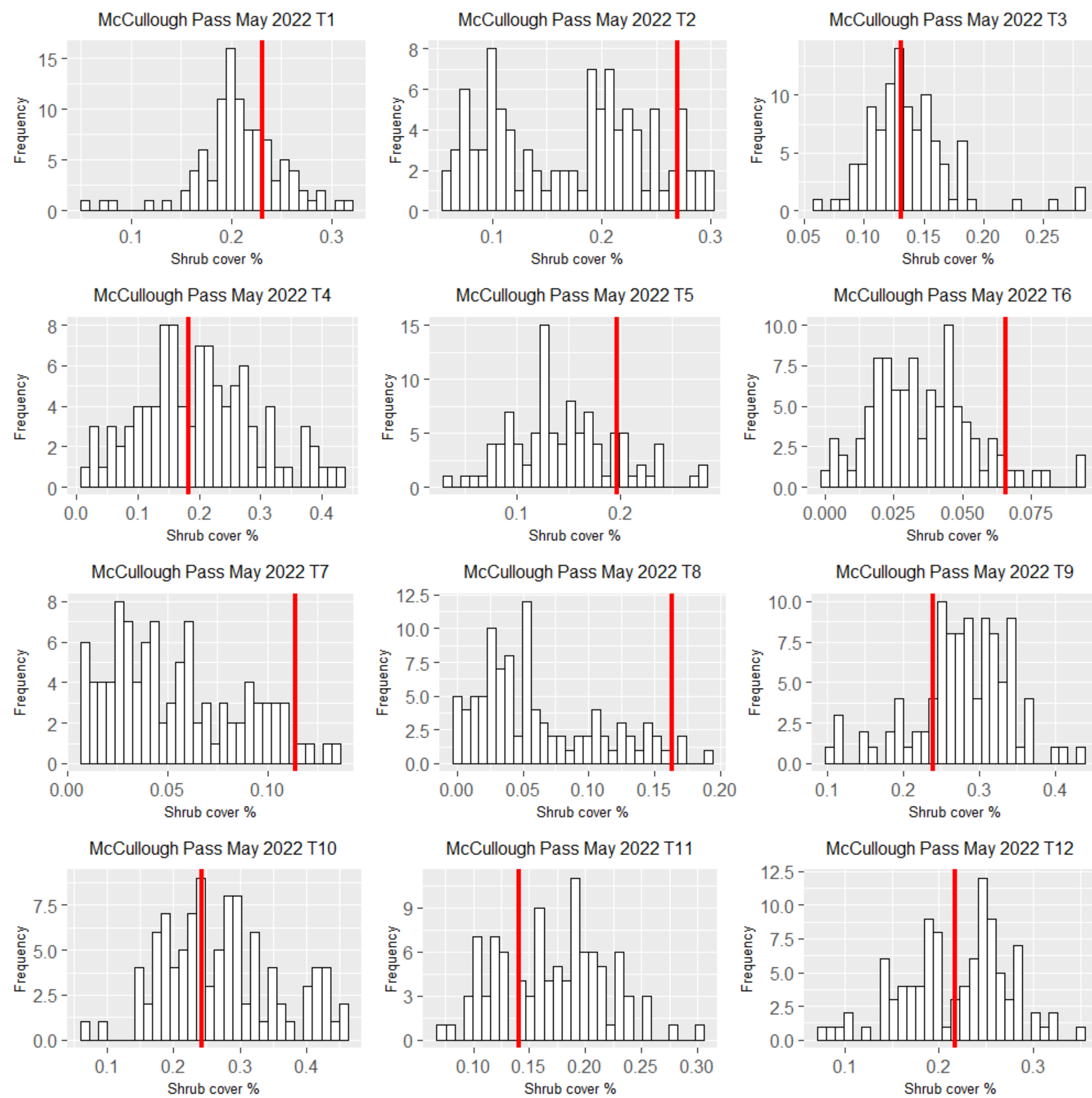

FIGURE 31: MCCULLOUGH PASS MAY UAV SHRUB COVER % VERSUS AIM SHRUB COVER % (RED LINE)

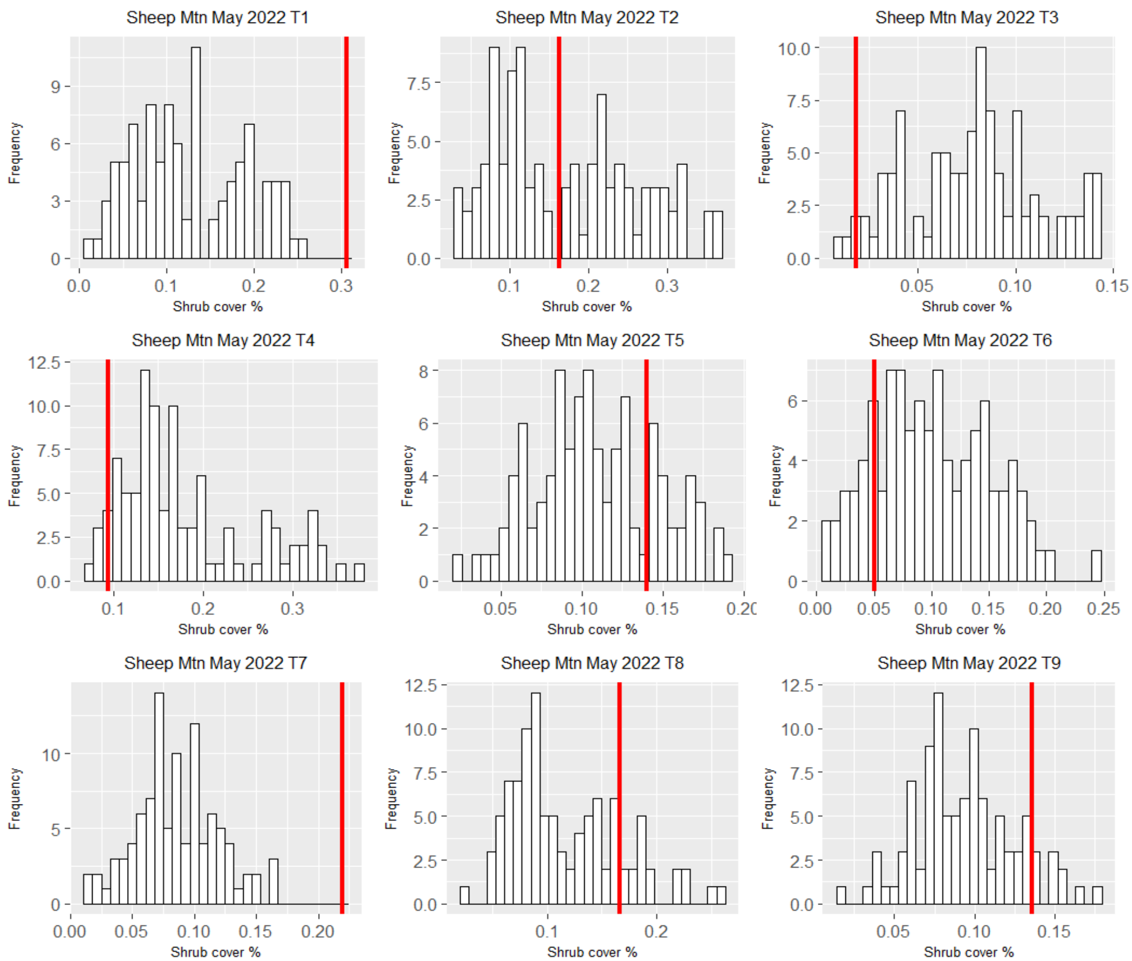

Figure 32: Sheep Mountain May UAV Shrub Cover % Versus AIM Shrub Cover % (red line)

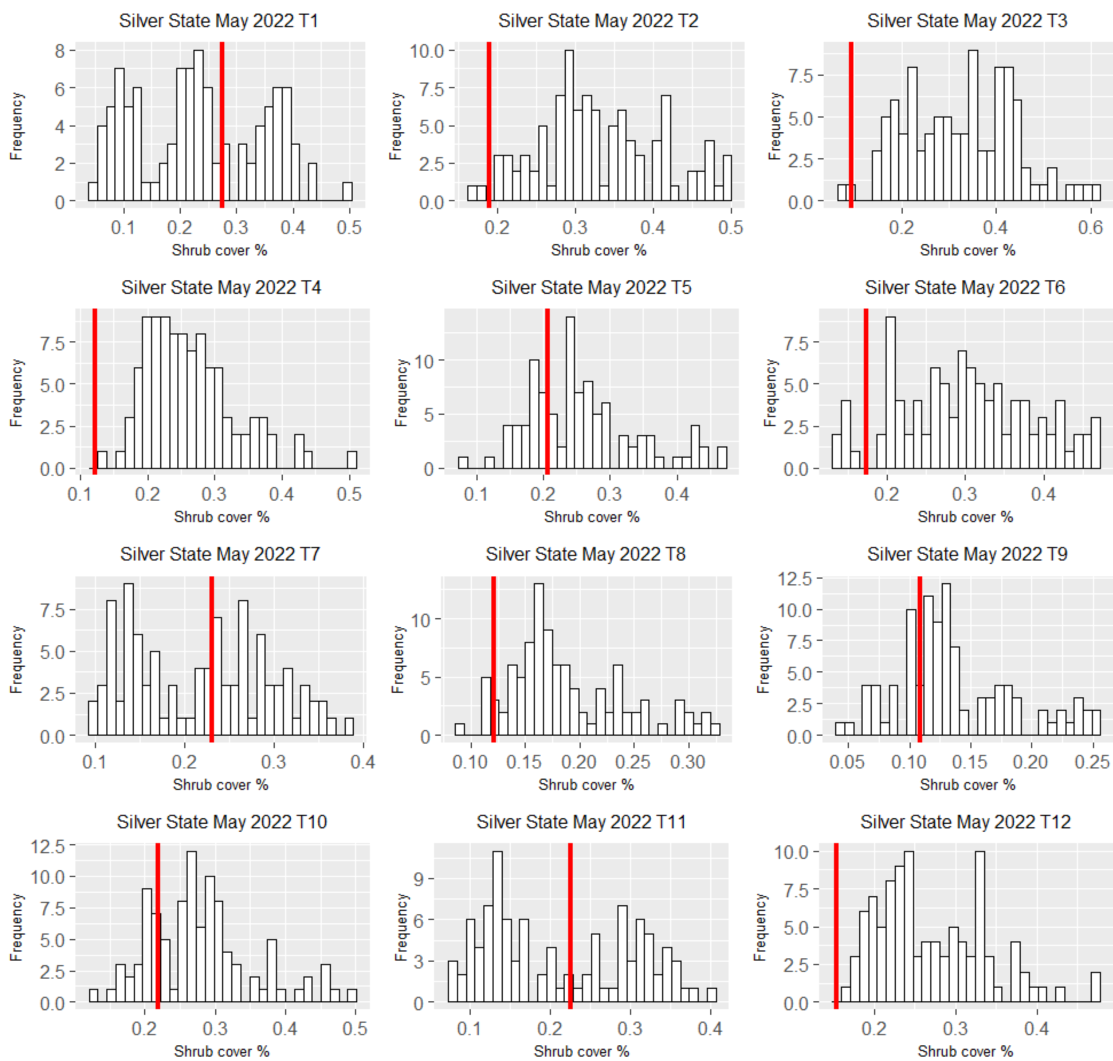

FIGURE 33: SILVER STATE MAY UAV SHRUB COVER % VERSUS AIM SHRUB COVER % (RED LINE)

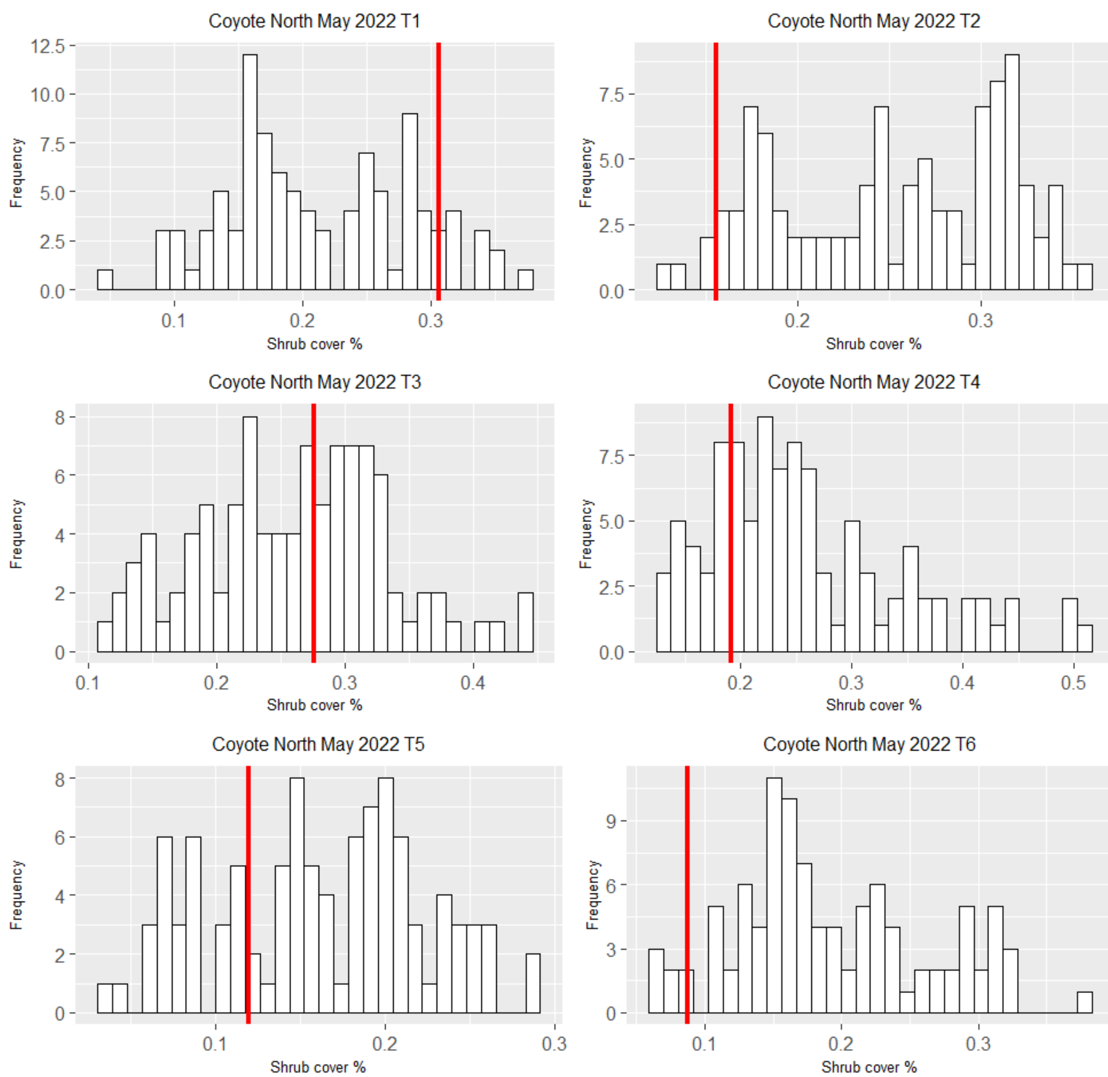

FIGURE 34: COYOTE SPRINGS MAY UAV SHRUB COVER % VERSUS AIM SHRUB COVER % (RED LINE)

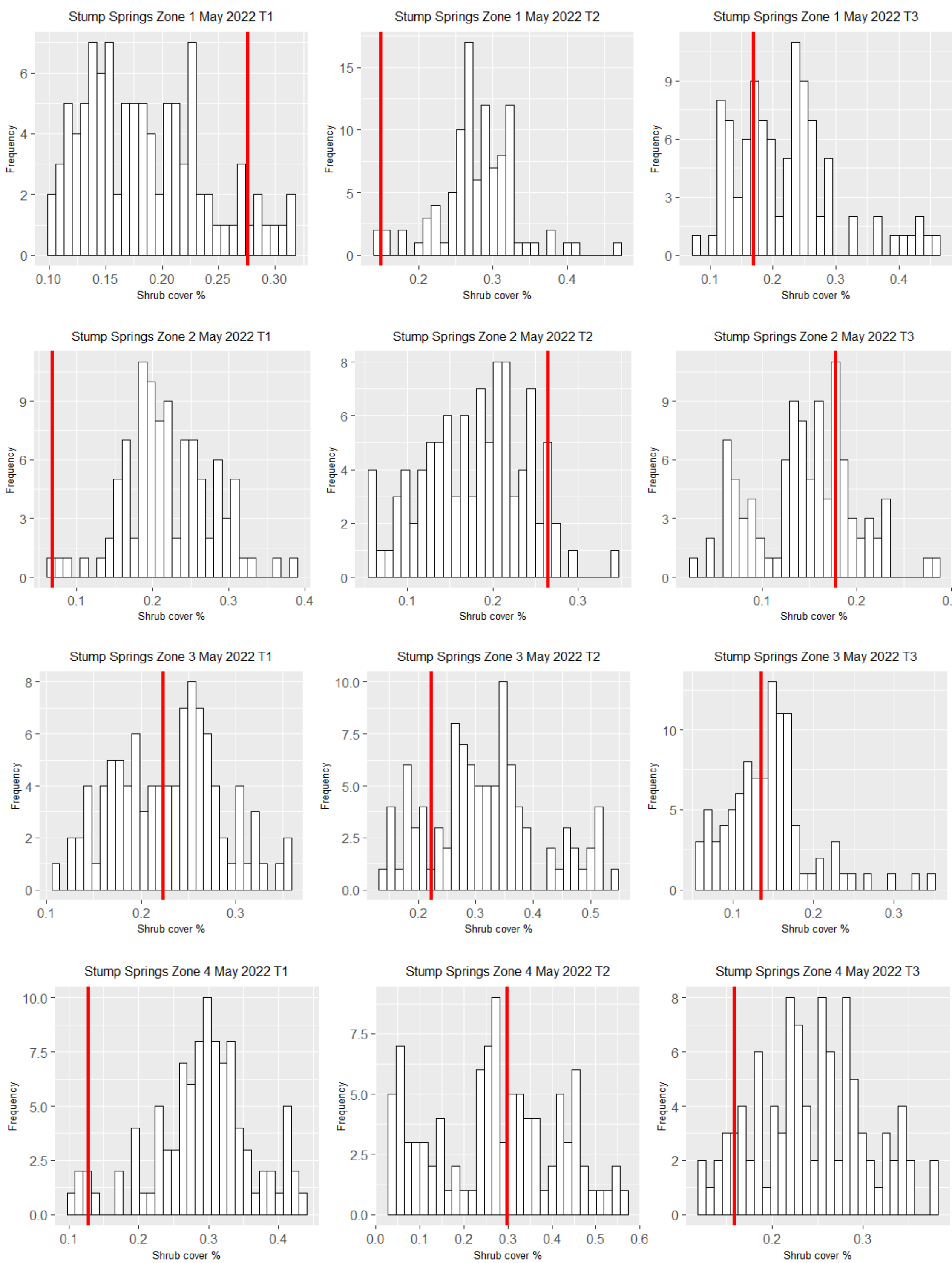

FIGURE 35: STUMP SPRINGS MAY UAV SHRUB COVER % VERSUS AIM SHRUB COVER % (RED LINE)

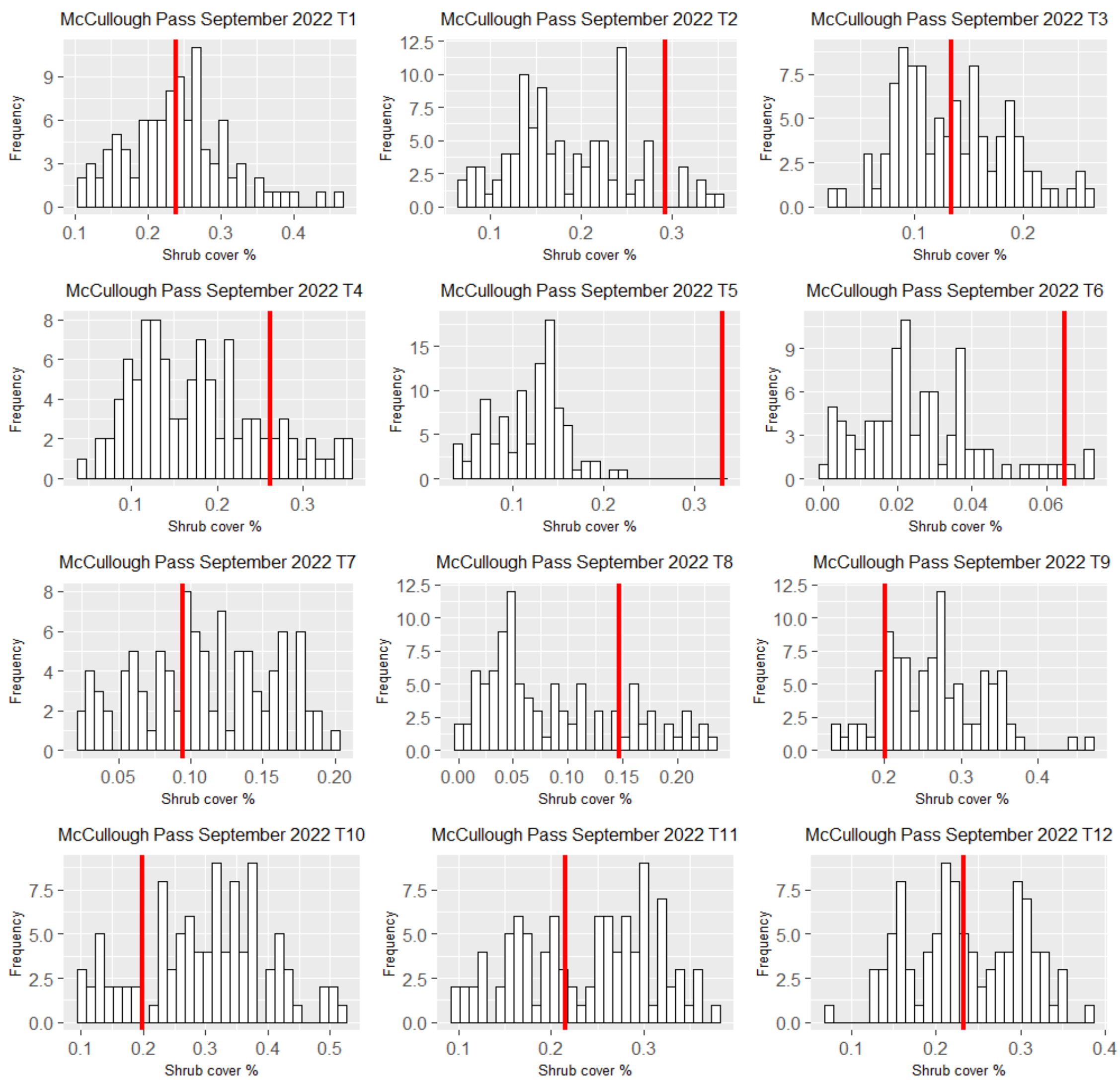

FIGURE 36: MCCULLOUGH PASS SEPTEMBER UAV SHRUB COVER % VERSUS AIM SHRUB COVER % (RED LINE)

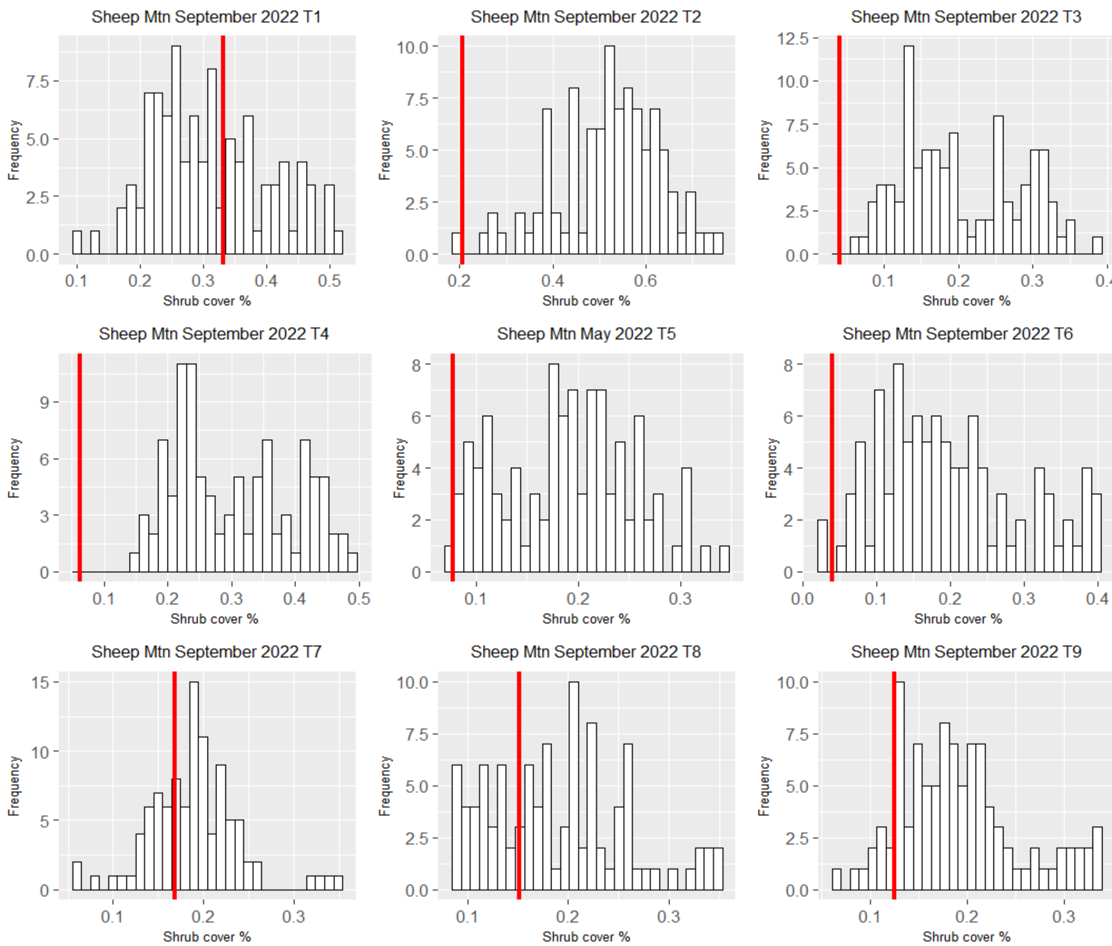

Figure 37: Sheep Mountain September UAV Shrub Cover % Versus AIM Shrub Cover % (red line)

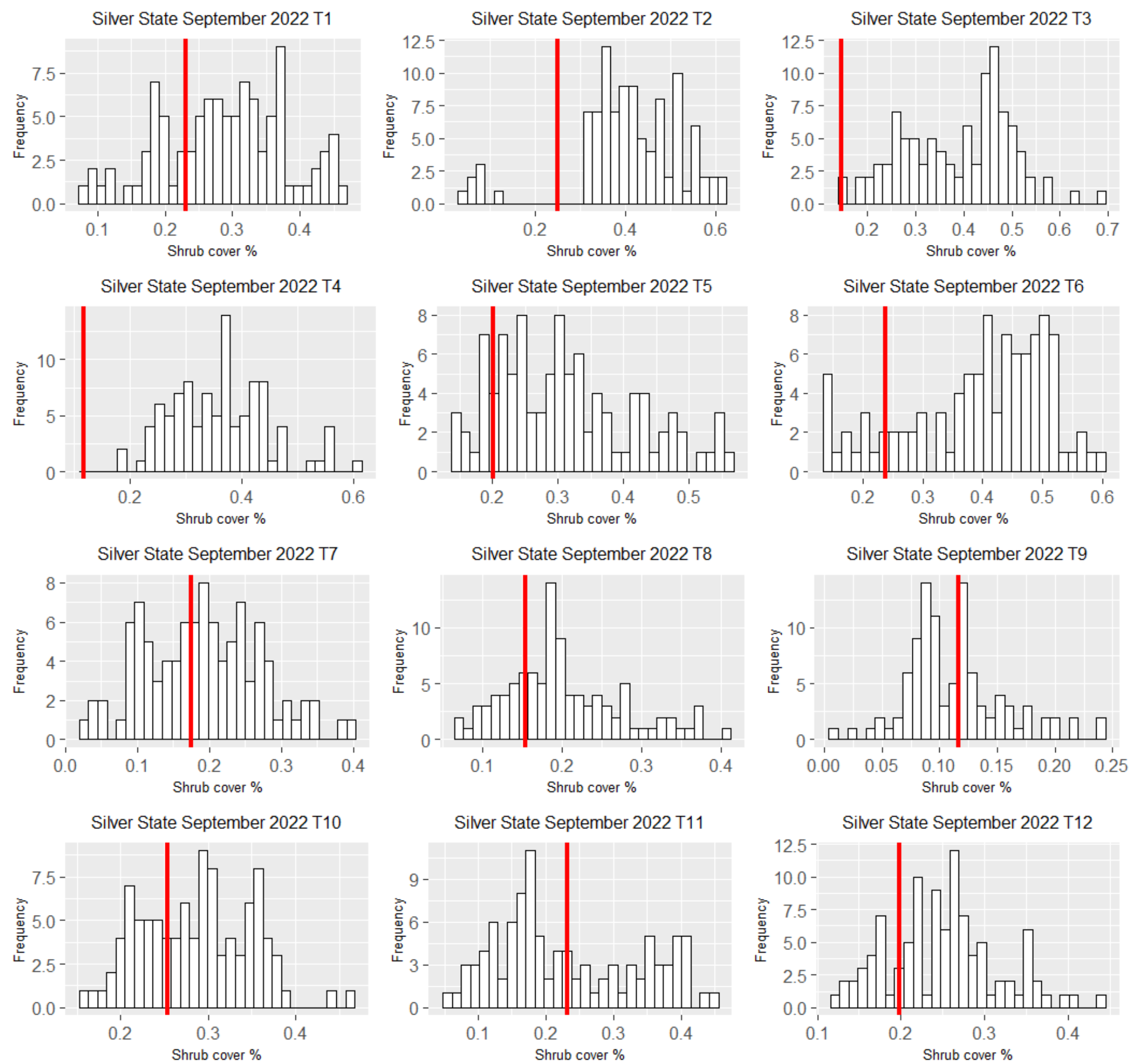

FIGURE 38: SILVER STATE SEPTEMBER UAV SHRUB COVER % VERSUS AIM SHRUB COVER % (RED LINE)

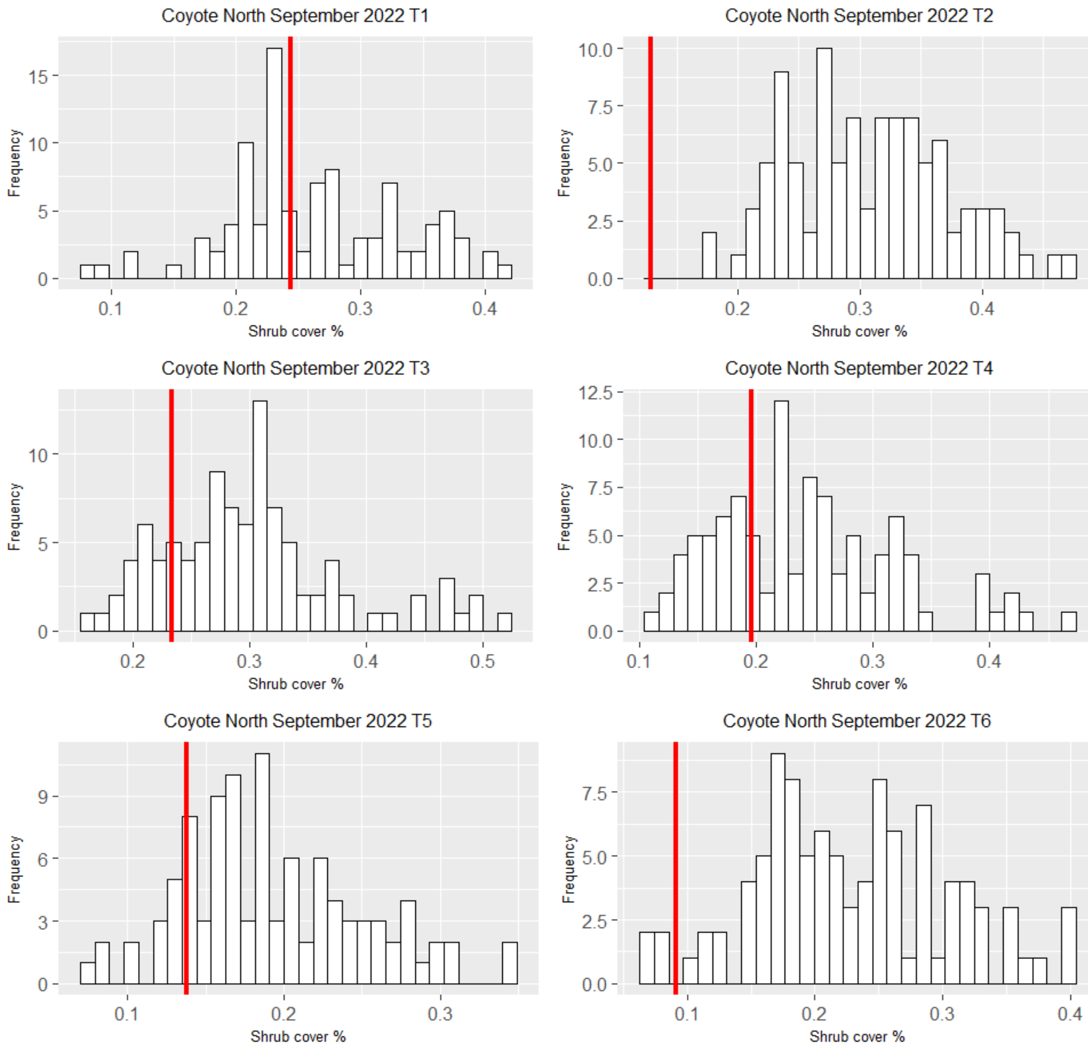

FIGURE 39: COYOTE SPRINGS SEPTEMBER UAV SHRUB COVER % VERSUS AIM SHRUB COVER % (RED LINE)

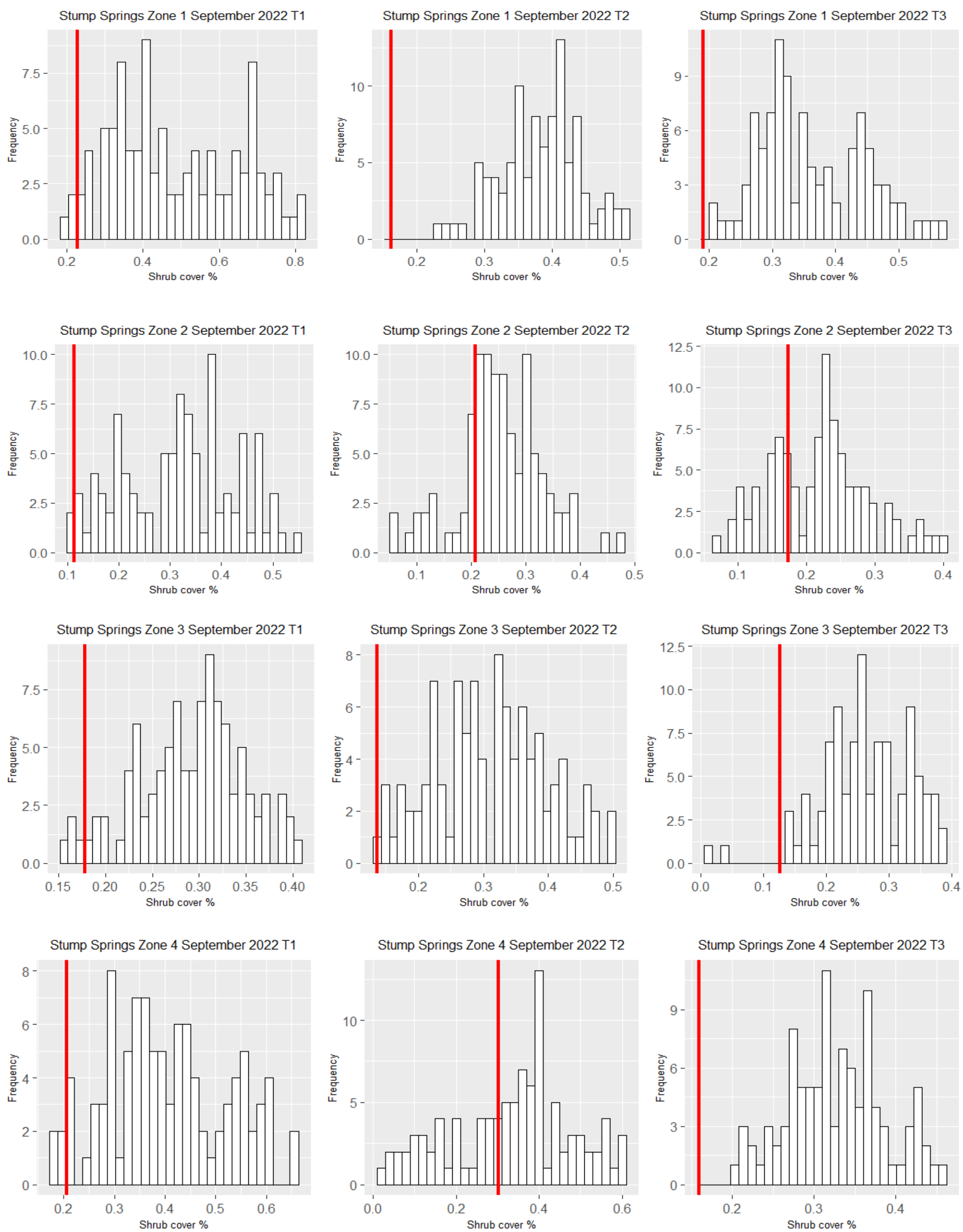

FIGURE 40: STUMP SPRINGS SEPTEMBER UAV SHRUB COVER % VERSUS AIM SHRUB COVER % (RED LINE)

Chapter 3: Localized Mojave desert tortoise density models constructed using UAV imagery and remotely sensed satellite imagery

Given the variation in densities and associated habitat selection of tortoises at different spatial scales, modeling influences on tortoise densities at local scales will help us to understand individual level habitat selection that results in local patterns of occupancy. Though AIM data are available for analyses on this spatial scale, given its inconsistency and inability to capture the heterogeneity of the landscape (even at these small spatial scales - see Chapter 2) I created generalized additive models using UAV remotely sensed imagery to evaluate densities in relation to environmental and landscape characteristics. These models may be improved upon further by combining both UAV and satellite data to increase the predictive power of models and the ability to estimate densities in not yet surveyed regions. Though several studies exist comparing the applicability of UAV imagery and satellite imagery in habitat modeling, much fewer data are available regarding the modeling power of hybrid models using both sets of data.

Previous studies on Mojave desert tortoises have revealed variation in the species densities in relation to multiple abiotic and biotic variables such as topography and temperature (Zylstra 2023). Accounting for these abiotic and biotic factors in relation to tortoise densities assists in better understanding why certain regions occupied by tortoises display greater declines in population numbers than other regions of seemingly similar habitat suitability. Moreover, habitat selection by Mojave desert tortoises has been a key focus of their conservation for many decades and despite their cryptic behavior much data are available regarding these preferences. Germano et al. (1994) described habitat use and densities of Mojave desert tortoises throughout the range of the Mojave desert. These authors addressed the variation in habitat use of tortoises across their range from bajadas and valley bottoms in the north to rocky hillsides in the south. Despite the large pool of literature, there are still few data available regarding the localized habitat preferences of tortoises on scales such as that of the 1 kilometer by 1 kilometer mark-recapture survey plots measured in the Ivanpah Valley area of the Mojave (Mitchel et al. 2021).

Research Questions:

- Can remote sensing imagery obtained using UAVs improve upon models evaluating local tortoise densities relative to significant variables of interest?
- What habitat indicators derived from UAV remote sensing imagery have the greatest influence/are better able to predict patchiness of tortoise distributions at local scales?

Methods:

To conduct this analysis of densities at the local scale, I obtained mark-recapture data from 2015, 2018, and 2021 for three of the plots that were imaged in Chapter 2: McCullough Pass, Sheep Mountain, and Silver State. These plots are south of Las Vegas and east of Primm, NV (Figure 2). To avoid duplicating individuals with multiple locations I kept point data from the most recent time an individual tortoise was seen. For example, if a tortoise was seen every three years, then I only kept the GPS point location from 2021. Once each set of points were compiled I created a smoothed density raster for each plot using the density.ppp() (version 3.0-5, spatstat.explore) function in Rstudio. Next, I generated one thousand random sample points for each image and sampled the density raster to obtain a gradient of density values as described in Chapter 1.

UAV flights were conducted at the maximum legal height of approximately 400 feet using a DJI Matrice M200. Creation and execution of flight plans were conducted using Android application UgCS for DJI and a laptop computer (also running UgCS on Apple OSX). I used a Micasense red edge MX multispectral camera for capturing images which were compiled and processed into orthophoto mosaics, and associated indices (shrub cover, plant height, elevation, and normalized difference vegetation index) using Pix4D on a Windows Server based PC. For each plot approximately 11,000 to 14,000 images were collected for each monthly flight.

Similar to the generalized additive models of Chapter 1, for this analysis I wanted to create models for these three plots where have both UAV and Satellite data area available. From the Pix4D computation I obtained elevation from the digital terrain model, normalized difference vegetation index (NDVI) was calculated using the red and near-infrared spectral bands (NDVI = (NIR-RED)/NIR+RED)), and plant heights were calculated by subtracting the digital terrain model from the digital surface model. The fourth variable of interest was shrub cover which was generated using a supervised classification in order to be as close to the ground truth as possible (See Chapter 2). I aggregated each variable derived from the 7cm resolution UAV imagery up to 5 by 6-meter cells for input into generalized additive models alongside mark-recapture tortoise point data that were summarized as the density of tortoises in a 900 m^2 area. This 5 by 6 meter grid came from a kernel density raster of mark-recapture points for each individual plot that was created by using mark-recapture points and the density.ppp() function from the spatstat.explore (version 3.0-5) package in Rstudio. Once I had this density raster for each plot, I created a gridded polygon by inputting the raster into the rasterToPolygons() function from the raster package (version 3.6-11) in Rstudio. For elevation I averaged the 7cm cells up to 5 by 6-meter cells by extracting the smaller cells into each larger grid cell and specifying the function as “mean”. Since NDVI represents the level of greenness across the landscape I kept values representing plants, so for each image I identified a threshold value above which everything was representative of vegetation. Following this I averaged the NDVI cells up to 5 by 6-meter cells just the same as elevation using the density grid. The plant height calculation created some negative values, and I thresholded these layers to only keep positive values, after which I conducted the same aggregation up to 5 by 6-meter cells as elevation and NDVI. Finally, I obtained shrub cover per 5 by 6-meter cell by taking the number of 7cm size cells representing shrubs and dividing by the total number of 7cm cells within the 5 by 6-meter grid in order to obtain a shrub cover % per 5 by 6-meter grid cell. For the satellite based generalized additive models I used the same variables used for the range wide models in Chapter 1 which were: terrestrial disturbance index, normalized difference vegetation index, depth to bedrock, sand on surface, coarse fragments on surface, winter precipitation (30 year average), and maximum temperature (30 year average) (Table 7). To compare the satellite GAM models with the UAV GAM models the imagery needed to have the exact same extent across all models. To ensure this, I averaged each set of satellite imagery across the same 5 by 6-meter grids that I used to aggregate the UAV imagery, but I did not smooth the large resolution of the imagery in order to maintain the coarse resolution for accurate comparison with the high-resolution UAV imagery. However, for the hybrid models I did smooth the satellite data using the focal() function in R with method set to lanczos and weights set to 31.

TABLE 7: ENVIRONMENTAL AND DISTURBANCE DATA USED TO MODEL MOJAVE DESERT TORTOISE DENSITIES

Description of Covariate Layer	Source of Data
Summer Maximum Temperature 30-year normal period	PRISM climate data
Winter Precipitation 30-year normal period	PRISM climate data
Terrestrial Disturbance Index	Carter and others (2020)
Normalized Difference Vegetation Index (2001-2019)	USGS Phenology
Sand on Surface	Soilgrids.org
Coarse Fragments on Surface	Soilgrids.org
Depth to Bedrock	Soilgrids.org

Results:

The best performing model based on AIC values for McCullough was the hybrid model using both satellite and UAV data while the best model for both Sheep Mountain and Silver State was the satellite model (Tables 10, 11, and 12). Similar to our landscape level analyses, these localized models reveal that individual tortoises do show preferences in habitat selection and these preferences vary or stay consistent from region to region as we saw in Chapter 1. All models where elevation is included as a covariate reveal that tortoise densities decrease with an increase in elevation, as to be expected based on tortoises known life history and behavior (Figures 46, 49, 55, 58, 64, and 67). The relationship between tortoise densities and NDVI varied between models and amongst plots as well. At McCullough Pass and Silver State both the satellite and hybrid models indicate an increase in densities with an increase in NDVI (Figures 43, 49, 61, and 67). All three models for Sheep Mountain revealed different relationships between densities and NDVI with the satellite model showing a decrease in densities with increasing NDVI, the UAV model showing an increase in densities with increasing NDVI, and the hybrid model having no clear relationship at all (Figures 52, 55 and 58). Only the UAV models for Sheep Mountain and Silver State displayed a trend relative to shrub cover with tortoise densities decreasing with an increase in shrub cover at these locations (Figures 55 and 64). Where depth to bedrock was included in the models there is a general increase in densities with increasing depth (Figures 43, 49, and 61). Among satellite models for all three plots tortoise densities showed little to no relationship with winter precipitation (Figures 43, 52, and 61). On the other hand, tortoise densities for each hybrid model showed a general increase with increasing winter precipitation with a falloff in densities at McCullough likely due to elevation (Figures 49, 58, and 67).

Discussion:

The AIC results for the McCullough models reveal the potential for improving models evaluating tortoise and other species densities relative to significant variables by including both satellite derived and UAV data. Despite the satellite models having a better AIC than the UAV models, the UAV models appear better from a landscape perspective as the predicted density maps from these models have a better resolution and more detail at these scales (Figures 41, 44, 50, 53, 59, and 62). The discrepancies in even the same variables from model to model on a single plot reveal the bias that can arise by only evaluating densities with a single set of data and/or imagery with differing resolutions. Moreover, from the UAV imagery I derived four variables of interest: elevation, NDVI, shrub cover, and plant heights. With the addition of equipment such as thermal cameras we can improve upon UAV models by including more variables at higher resolutions. These models present an introduction to our ability to improve our understanding of Mojave desert tortoise densities and distributions by the addition of UAV derived data.

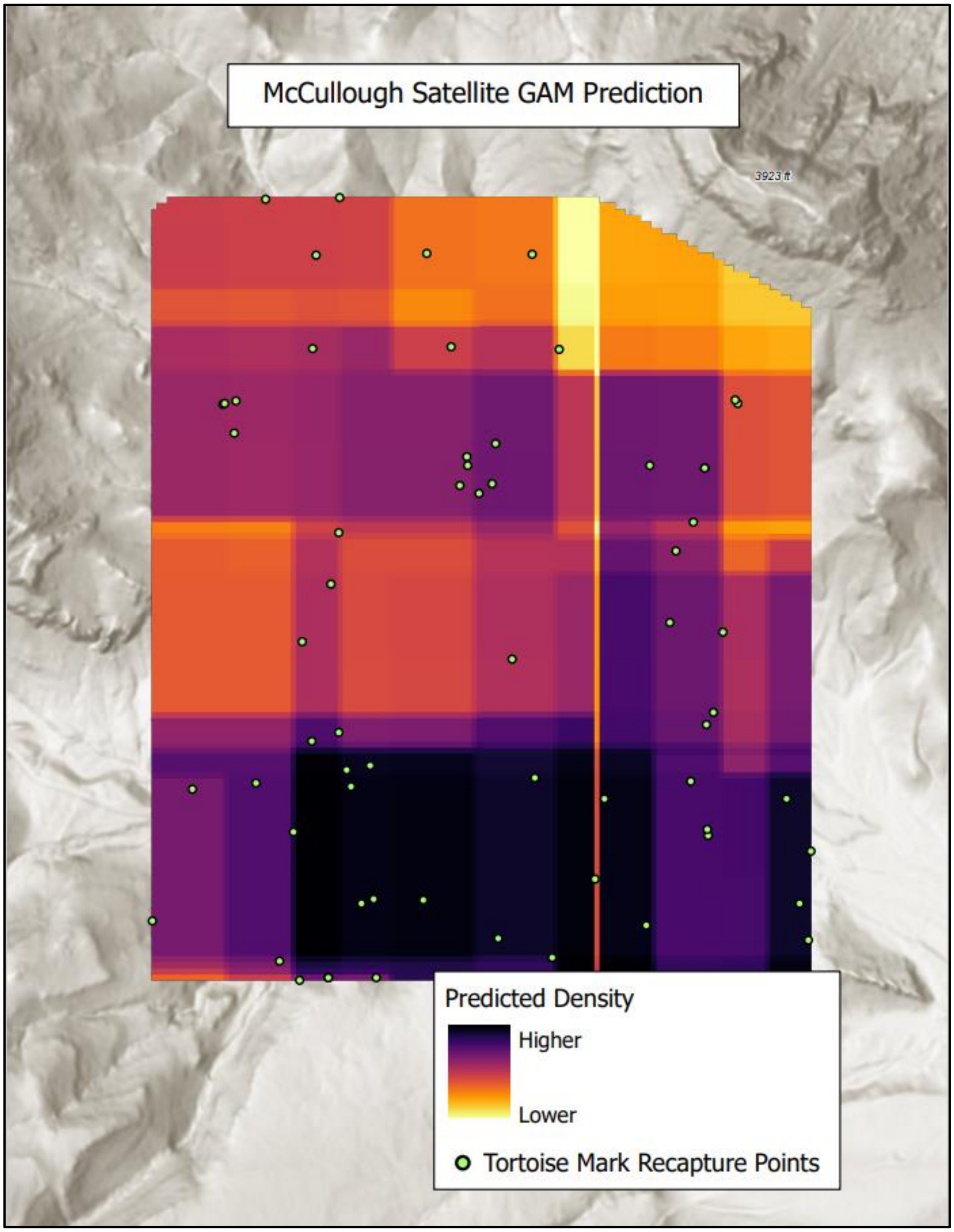

FIGURE 41: MCCULLOUGH PASS SATELLITE GENERALIZED ADDITIVE MODEL PREDICTED DENSITY MAP.

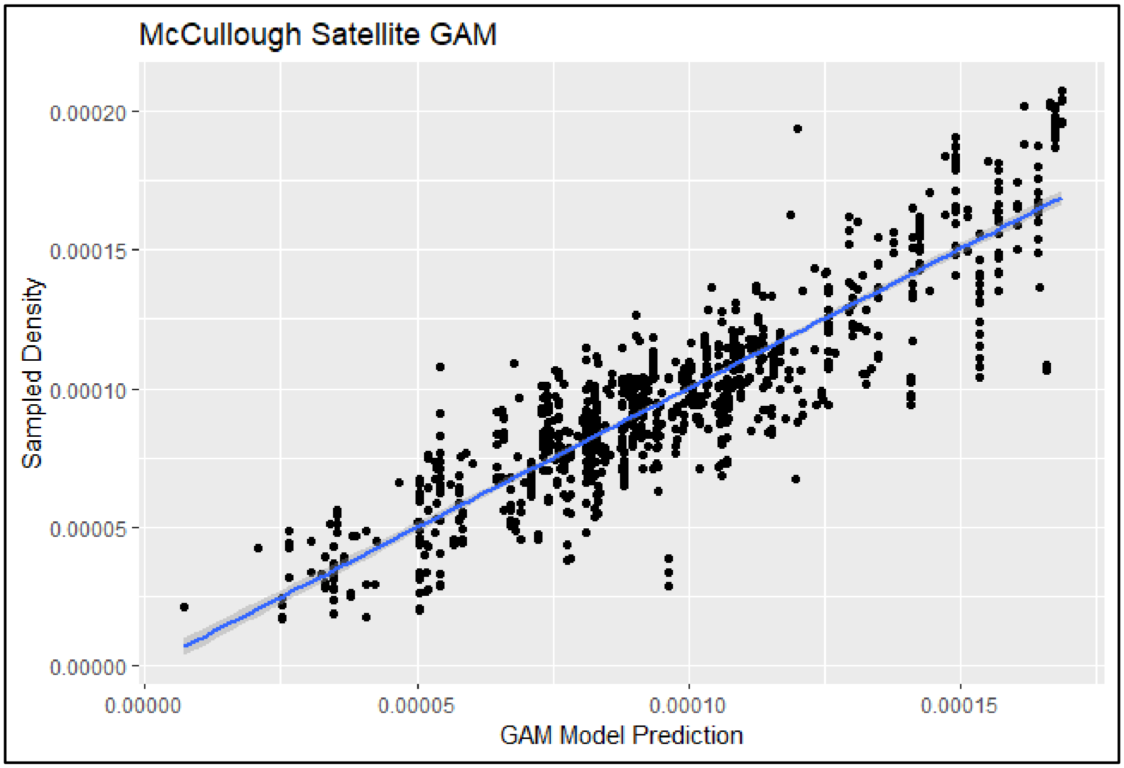

FIGURE 42: MCCULLOUGH PASS SATELLITE GAM PREDICTED DENSITY VERSUS TRUE SAMPLED DENSITY

TABLE 8: MCCULLOUGH PASS SATELLITE GENERALIZED ADDITIVE MODEL SUMMARY INCLUDING: ESTIMATED DEGREES OF FREEDOM (EDF), REFERENCE NUMBER OF DEGREES OF FREEDOM (REF.DF), F-STATISTIC (F) AND P-VALUES.

Terms	edf	Ref.df	F	p-value	
Terrestrial Disturbance Index	5.68E+00	7	8.626	< 2e-16	***
Normalized Difference Vegetation Index	6.76E+00	7	16.621	< 2e-16	***
Depth to Bedrock	5.86E+00	7	42.049	< 2e-16	***
Coarse Fragments on Surface	6.37E+00	7	14.135	< 2e-16	***
Sand on Surface	6.62E+00	7	30.967	< 2e-16	***
Winter Precipitation	5.83E+00	7	16.782	< 2e-16	***
Maximum Temperature	2.97E-05	7	0.000	0.078	
Deviance Explained = 79.7%	**R-squared (adj) = 0.789**				

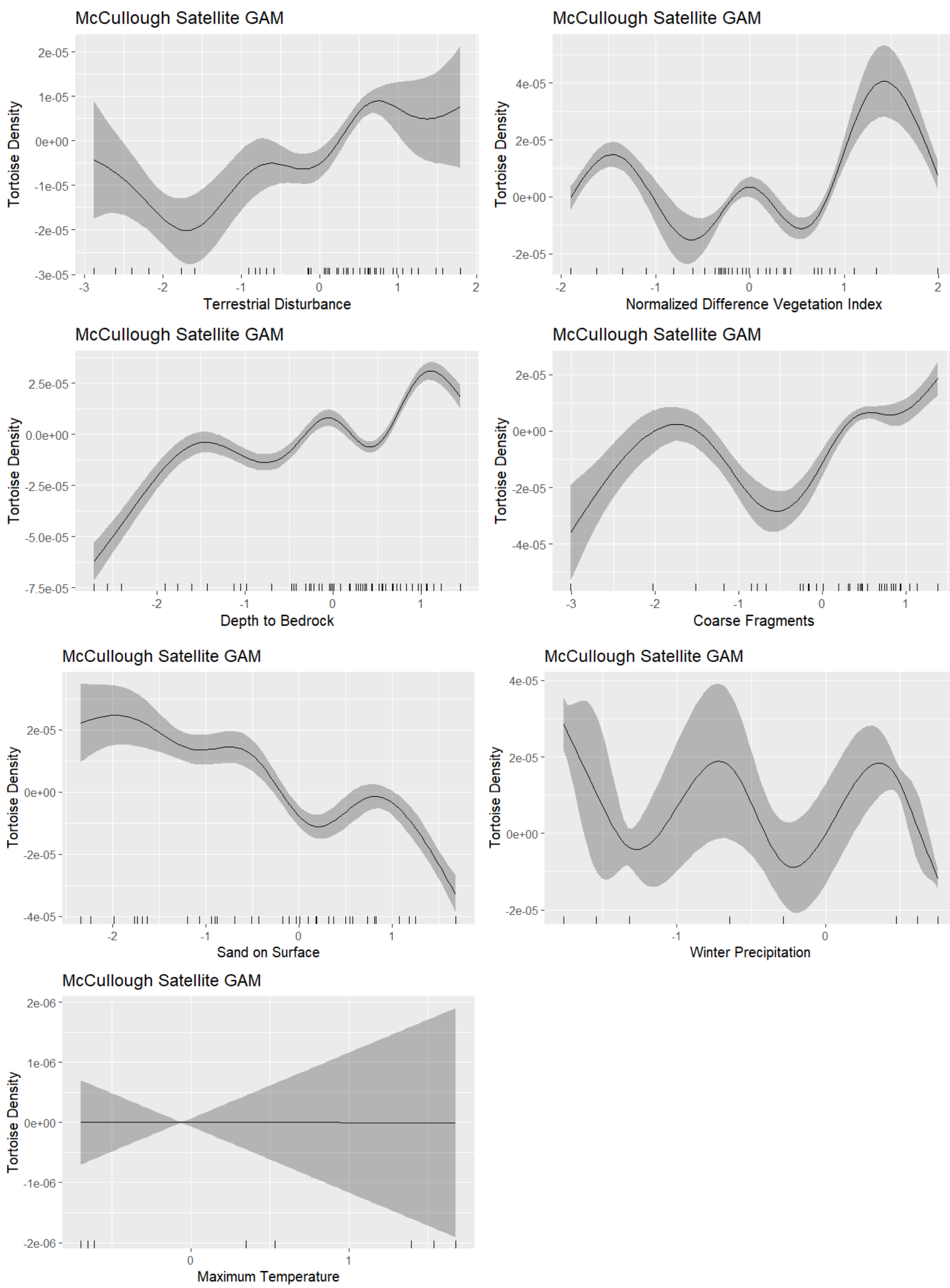

FIGURE 43: MCCULLOUGH PASS SATELLITE MODEL COVARIATE EFFECTS WITH TORTOISE DENSITIES. GRAY REGIONS REPRESENT UNCERTAINTY DUE TO LACK OF DATA POINTS.

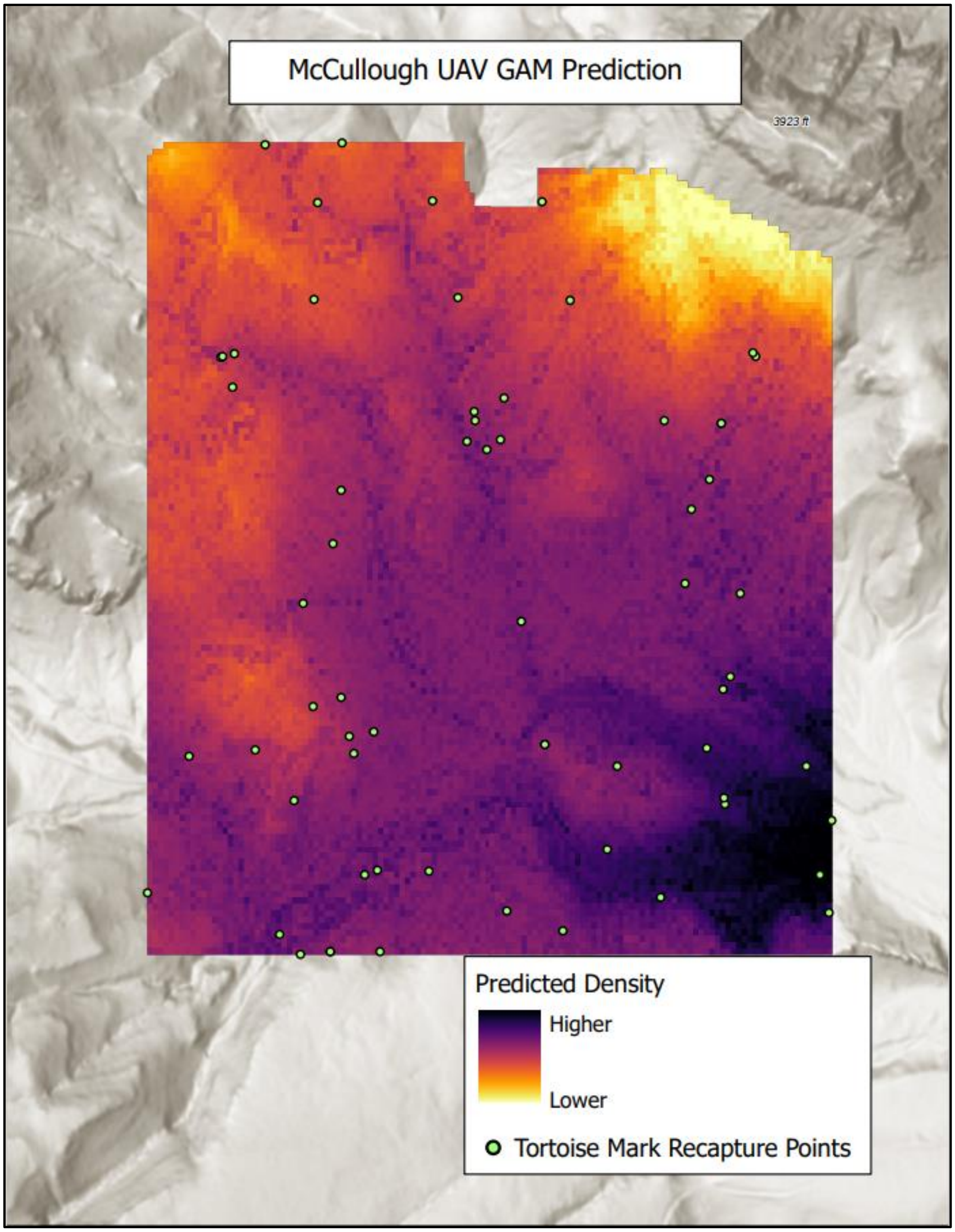

FIGURE 44: MCCULLOUGH PASS UAV GENERALIZED ADDITIVE MODEL PREDICTED DENSITY MAP.

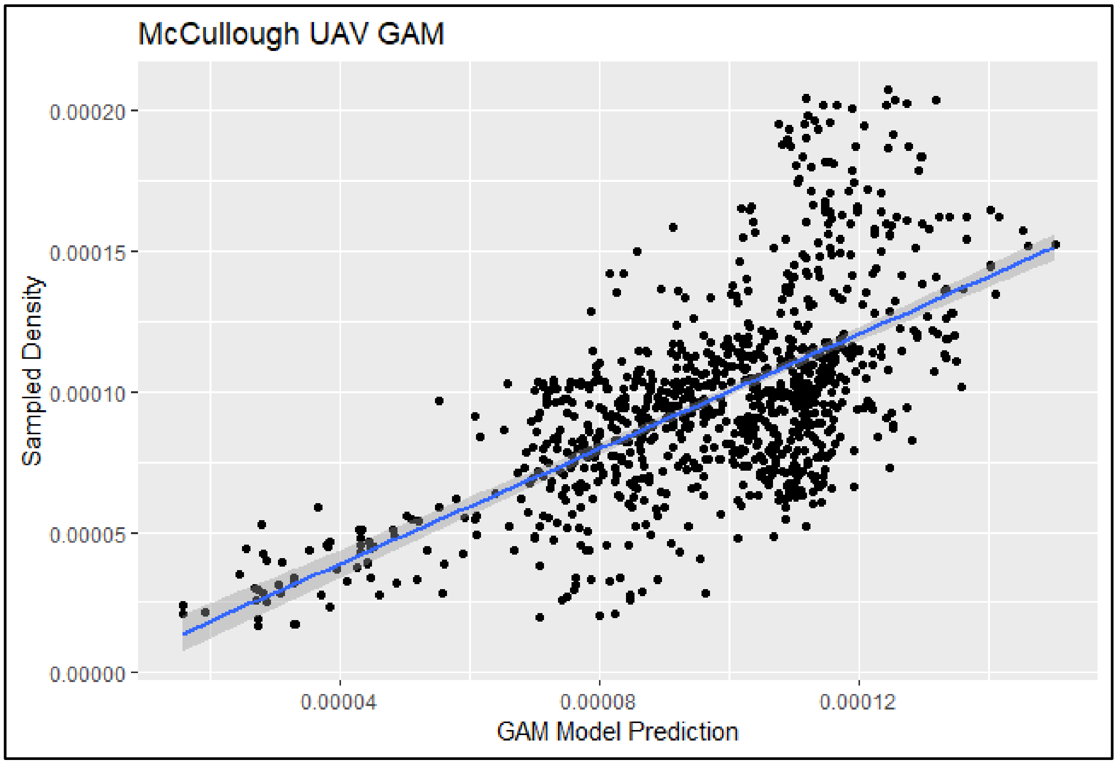

FIGURE 45: MCCULLOUGH PASS UAV GAM PREDICTED DENSITY VERSUS TRUE SAMPLED DENSITY

TABLE 9: MCCULLOUGH PASS UAV GENERALIZED ADDITIVE MODEL SUMMARY

Terms	edf	Ref.df	F	p-value	
Elevation	11.8498	29	16.196	< 2e-16	***
Normalized Difference Vegetation Index	4.8697	29	0.358	0.035739	*
Shrub Cover %	6.8676	29	0.717	0.000904	***
Plant Height	0.4042	29	0.001	0.885530	
Deviance Explained = 40.3%	**R-squared (adj) = 0.388**				

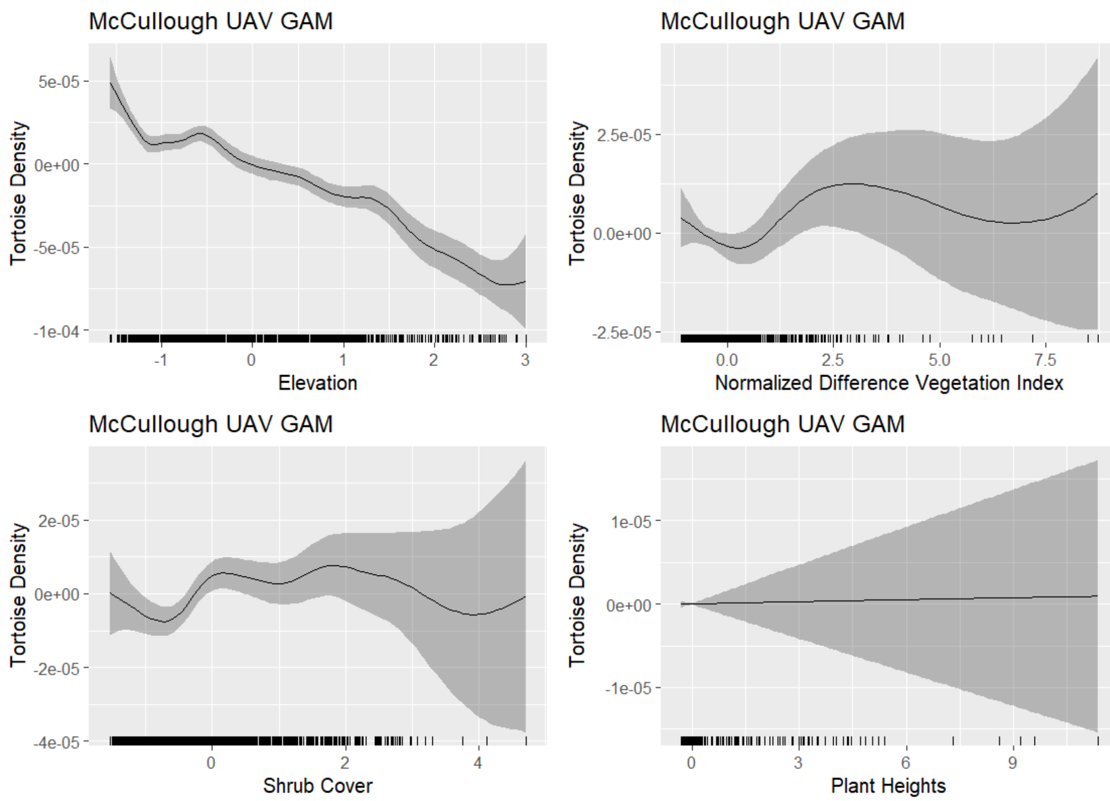

FIGURE 46: MCCULLOUGH PASS UAV MODEL COVARIATE EFFECTS WITH TORTOISE DENSITIES. GRAY REGIONS REPRESENT UNCERTAINTY DUE TO LACK OF DATA POINTS.

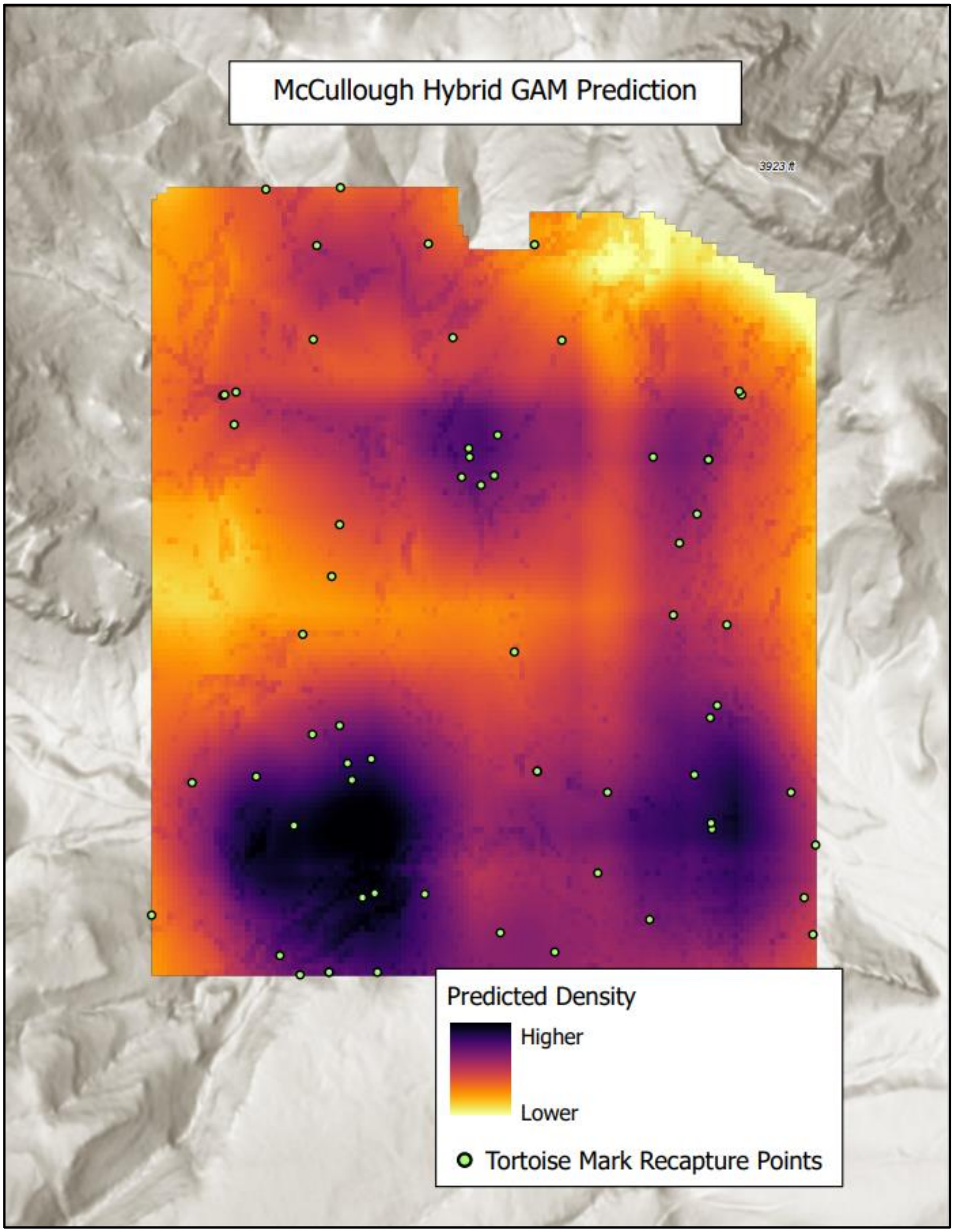

FIGURE 47: MCCULLOUGH PASS HYBRID GENERALIZED ADDITIVE MODEL PREDICTED DENSITY MAP.

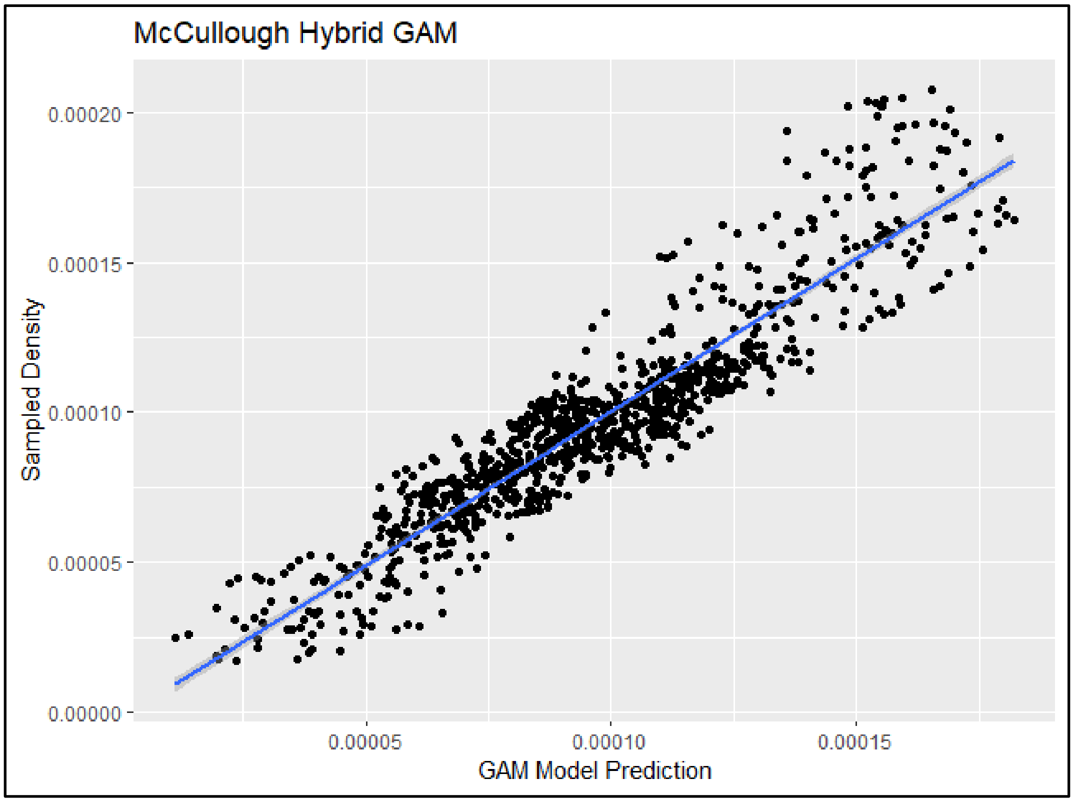

FIGURE 48: MCCULLOUGH PASS HYBRID GAM PREDICTED DENSITY VERSUS TRUE SAMPLED DENSITY

TABLE 10: MCCULLOUGH PASS HYBRID GENERALIZED ADDITIVE MODEL SUMMARY INCLUDING: ESTIMATED DEGREES OF FREEDOM (EDF), REFERENCE NUMBER OF DEGREES OF FREEDOM (REF.DF), F-STATISTIC (F) AND P-VALUES.

Terms	**edf**	**Ref.df**	**F**	**p-value**	
Terrestrial Disturbance Index	3.431	4	106.401	< 2e-16	***
Depth to Bedrock	3.997	4	105.310	< 2e-16	***
Coarse Fragments on Surface	3.017	4	45.166	< 2e-16	***
Sand on Surface	3.525	4	339.477	< 2e-16	***
Winter Precipitation	2.068	4	103.140	< 2e-16	***
Maximum Temperature	3.971	4	84.336	< 2e-16	***
UAV Elevation	2.867	4	31.090	< 2e-16	***
UAV Normalized Difference Vegetation Index	2.993	4	8.851	< 2e-16	***
UAV Shrub Cover	0.853	4	1.230	0.00311	**
UAV Plant Height	1.186	4	1.042	0.02535	*
Deviance Explained = 85.6%	**R-squared (adj) = 0.852**				

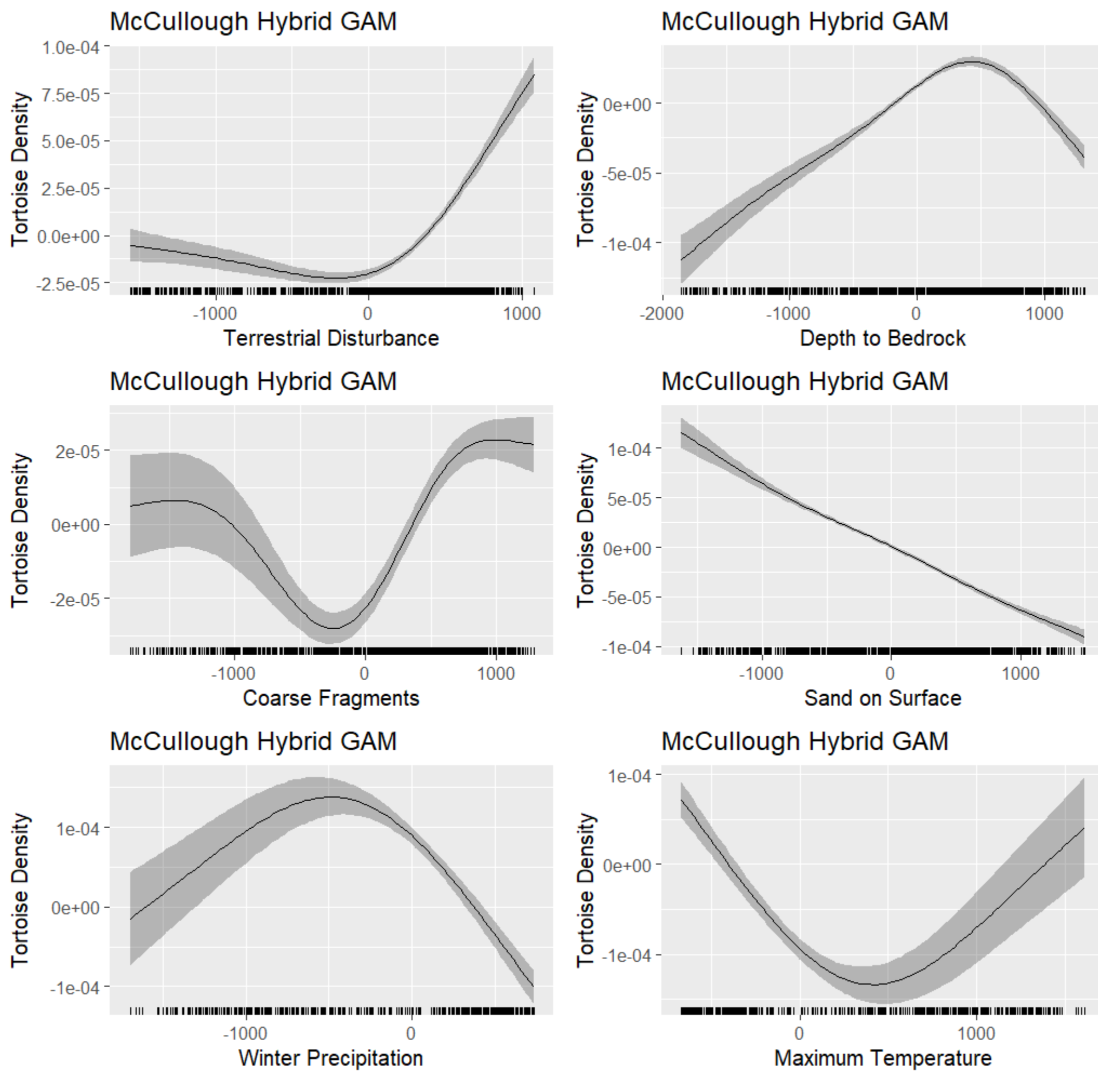
McCullough Hybrid GAM
Tortoise Density
1.0e-04
7.5e-05
5.0e-05
2.5e-05
0.0e+00
-2.5e-05
-1000
0
1000
Terrestrial Disturbance
McCullough Hybrid GAM
Tortoise Density
0e+00
-5e-05
-1e-04
-2000
-1000
0
1000
Depth to Bedrock
McCullough Hybrid GAM
Tortoise Density
2e-05
0e+00
-2e-05
-1000
0
1000
Coarse Fragments
McCullough Hybrid GAM
Tortoise Density
1e-04
5e-05
0e+00
-5e-05
-1e-04
-1000
0
1000
Sand on Surface
McCullough Hybrid GAM
Tortoise Density
1e-04
0e+00
-1e-04
-1000
0
Winter Precipitation
McCullough Hybrid GAM
Tortoise Density
1e-04
0e+00
-1e-04
0
1000
Maximum Temperature

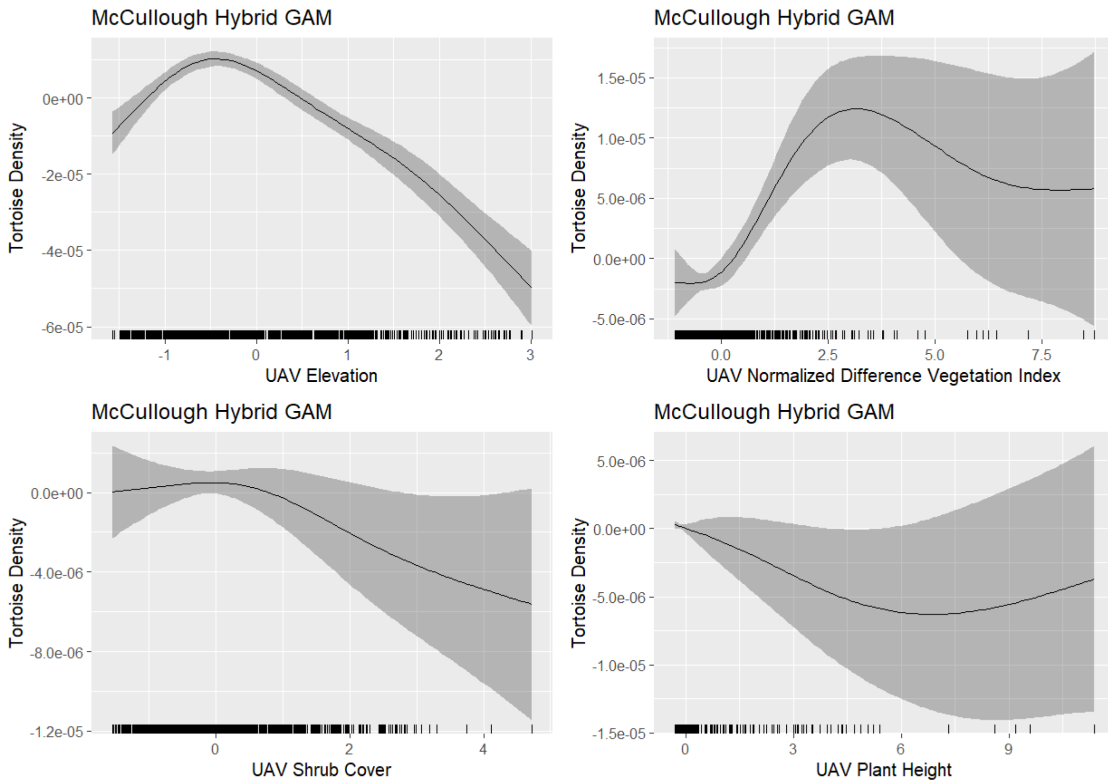

FIGURE 49: MCCULLOUGH PASS HYBRID MODEL COVARIATE EFFECTS WITH TORTOISE DENSITIES. GRAY REGIONS REPRESENT UNCERTAINTY DUE TO LACK OF DATA POINTS.

TABLE 11: MCCULLOUGH PASS ALL DENSITY MODELS AIC VALUES.

Model	Degrees of freedom	AIC
McCullough Hybrid GAM	29.9071	-18659.99
McCullough Satellite GAM	39.11246	-18588.93
McCullough UAV GAM	25.99124	-17308.94

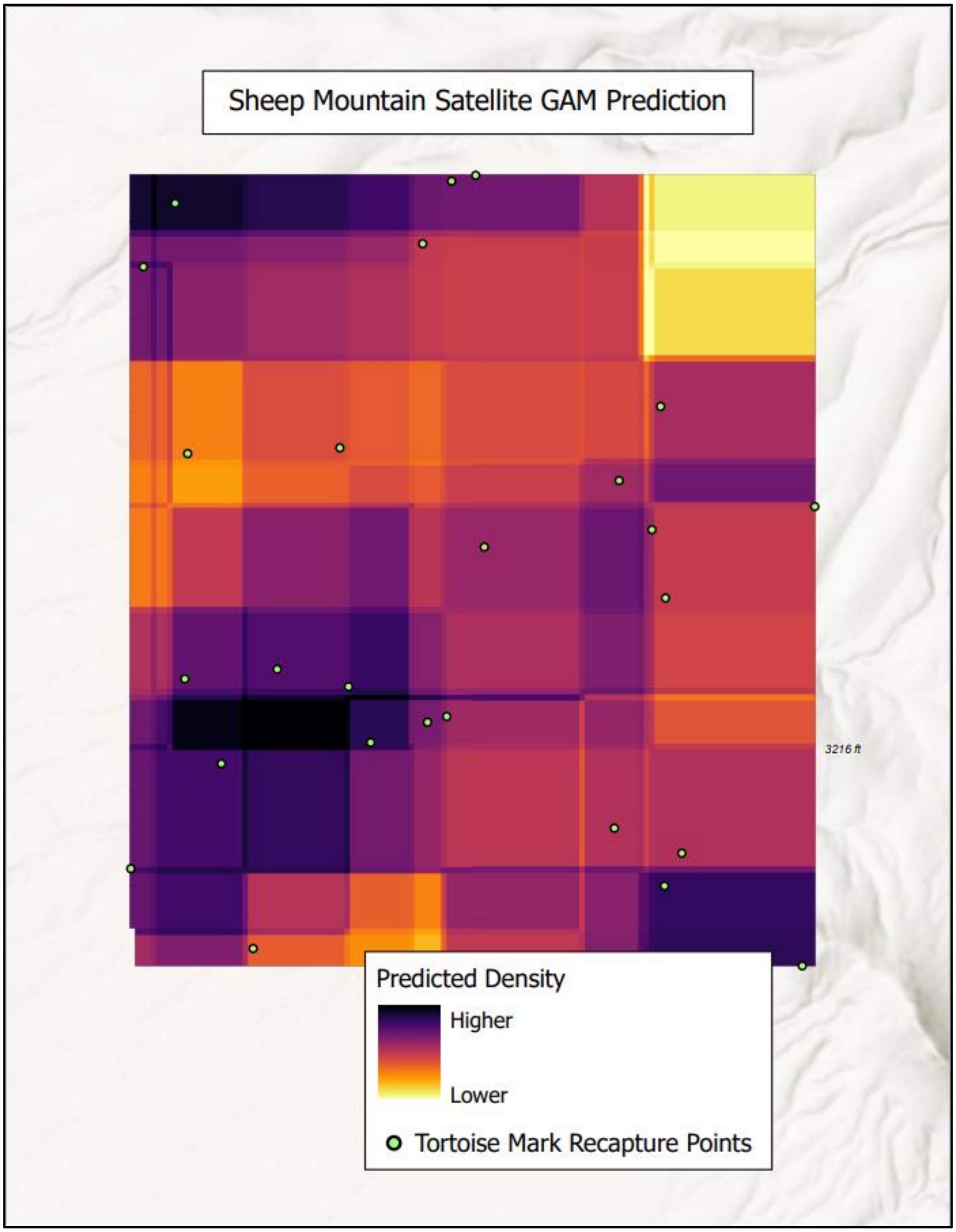

FIGURE 50: SHEEP MOUNTAIN SATELLITE GENERALIZED ADDITIVE MODEL PREDICTED DENSITY MAP.

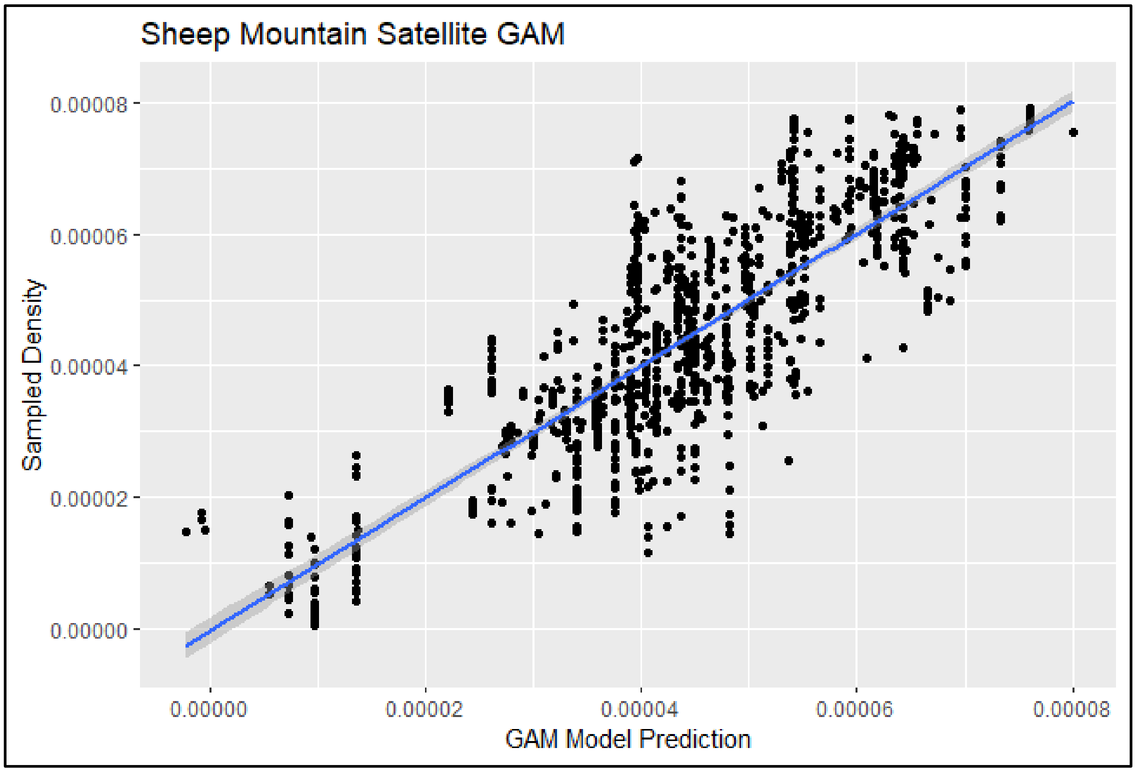

Figure 51: Sheep Mountain satellite GAM predicted density versus true sampled density

Table 12: Sheep Mountain satellite generalized additive model summary including: estimated degrees of freedom (EDF), reference number of degrees of freedom (Ref.df), F-statistic (F) and p-values.

Terms	edf	Ref.df	F	p-value	
Terrestrial Disturbance Index	4.8661	6	36.206	< 2e-16	***
Normalized Difference Vegetation Index	5.9150	6	42.440	< 2e-16	***
Coarse Fragments on Surface	4.1821	6	32.017	< 2e-16	***
Sand on Surface	5.0063	6	87.703	< 2e-16	***
Winter Precipitation	3.3025	6	4.094	2.08E-06	***
Maximum Temperature	0.1028	6	0.019	0.138	
Deviance Explained = 68.8%	**R-squared (adj) = 0.681**				

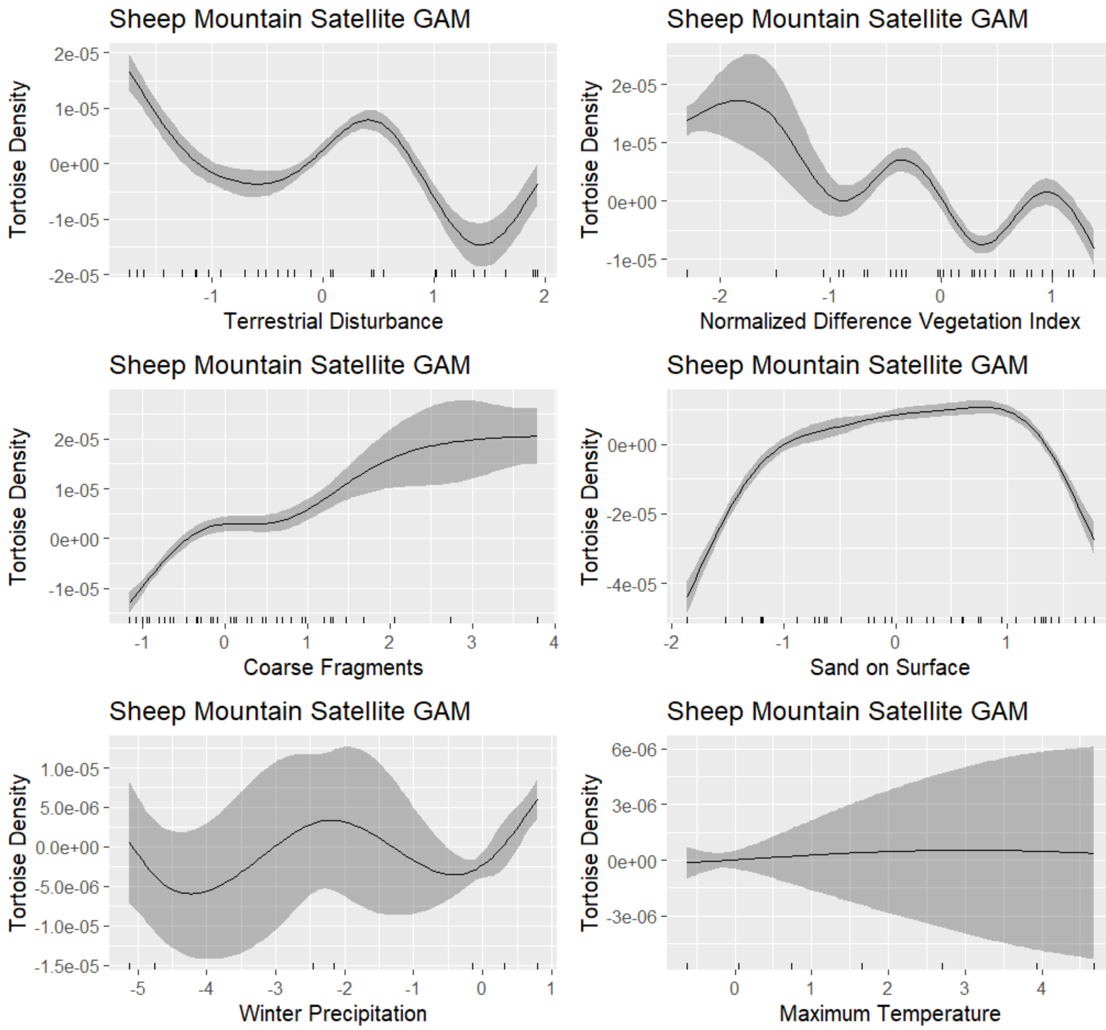

FIGURE 52: SHEEP MOUNTAIN SATELLITE MODEL COVARIATE EFFECTS WITH TORTOISE DENSITIES. GRAY REGIONS REPRESENT UNCERTAINTY DUE TO LACK OF DATA POINTS.

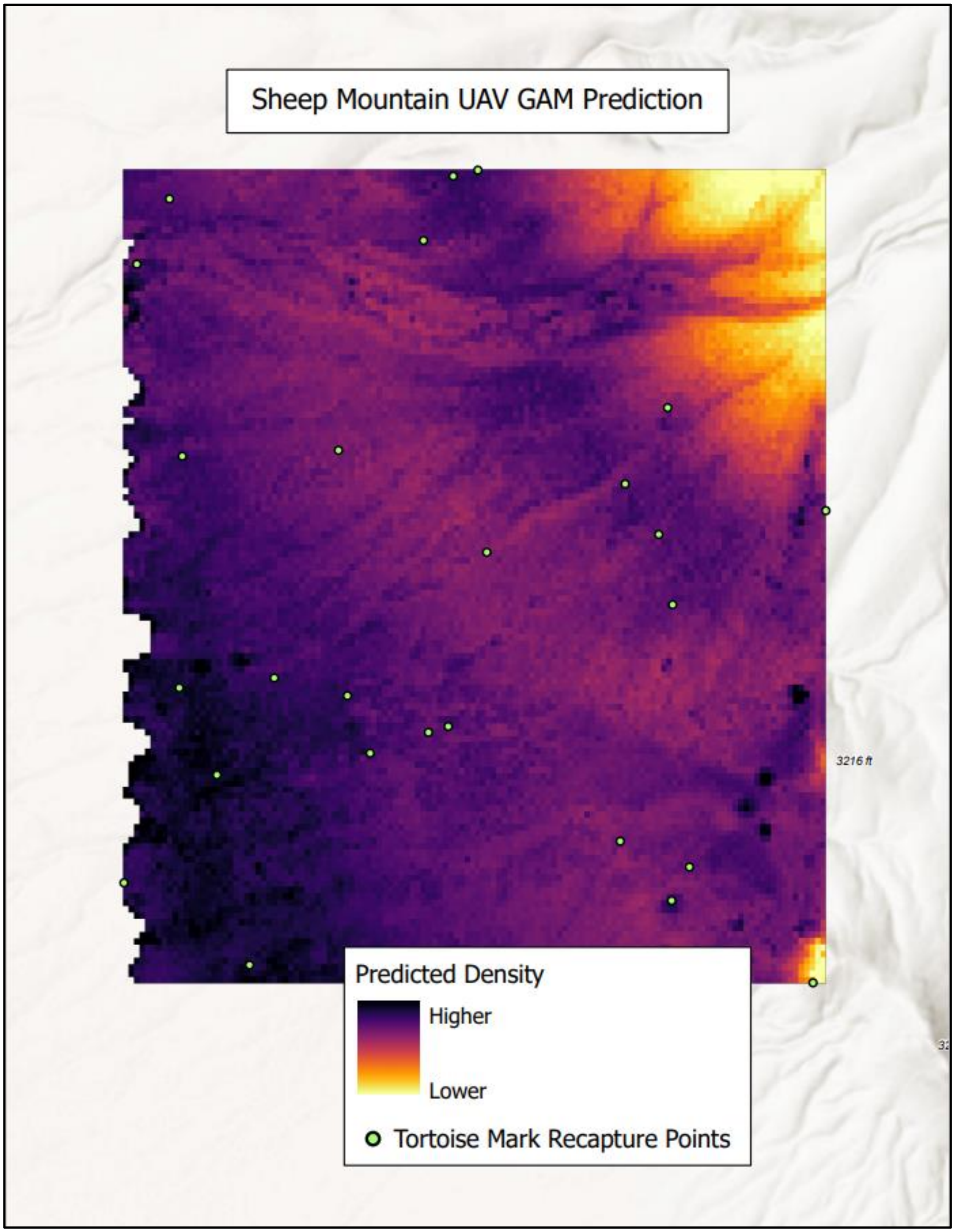

FIGURE 53: SHEEP MOUNTAIN UAV GENERALIZED ADDITIVE MODEL PREDICTED DENSITY MAP.

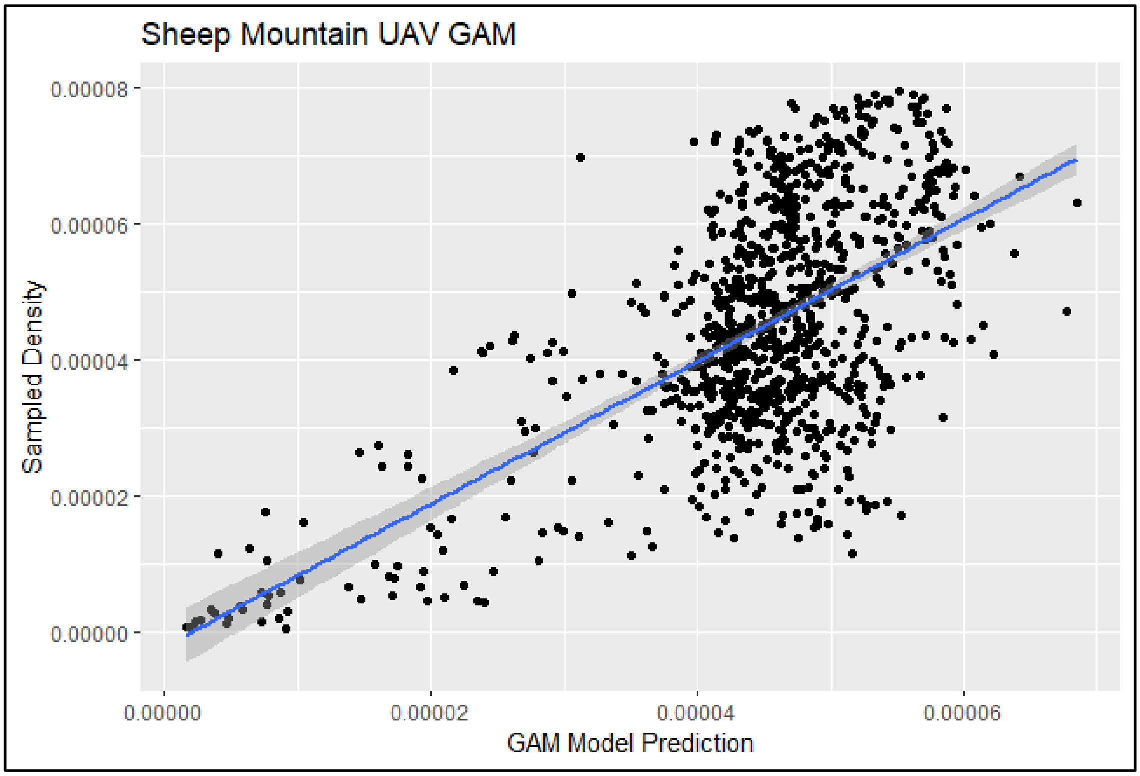

Figure 54: Sheep Mountain UAV GAM predicted density versus true sampled density

Table 13: Sheep Mountain UAV generalized additive model summary including: estimated degrees of freedom (EDF), reference number of degrees of freedom (Ref.df), F-statistic (F) and p-values.

Terms	edf	Ref.df	F	p-value	
Elevation	7.603	29	14.705	< 2e-16	***
Normalized Difference Vegetation Index	1.514	29	0.182	0.0282	*
Shrub Cover %	2.097	29	1.132	< 2e-16	***
Plant Height	4.240	29	0.273	0.0864	
Deviance Explained = 33.6%	**R-squared (adj) = 0.326**				

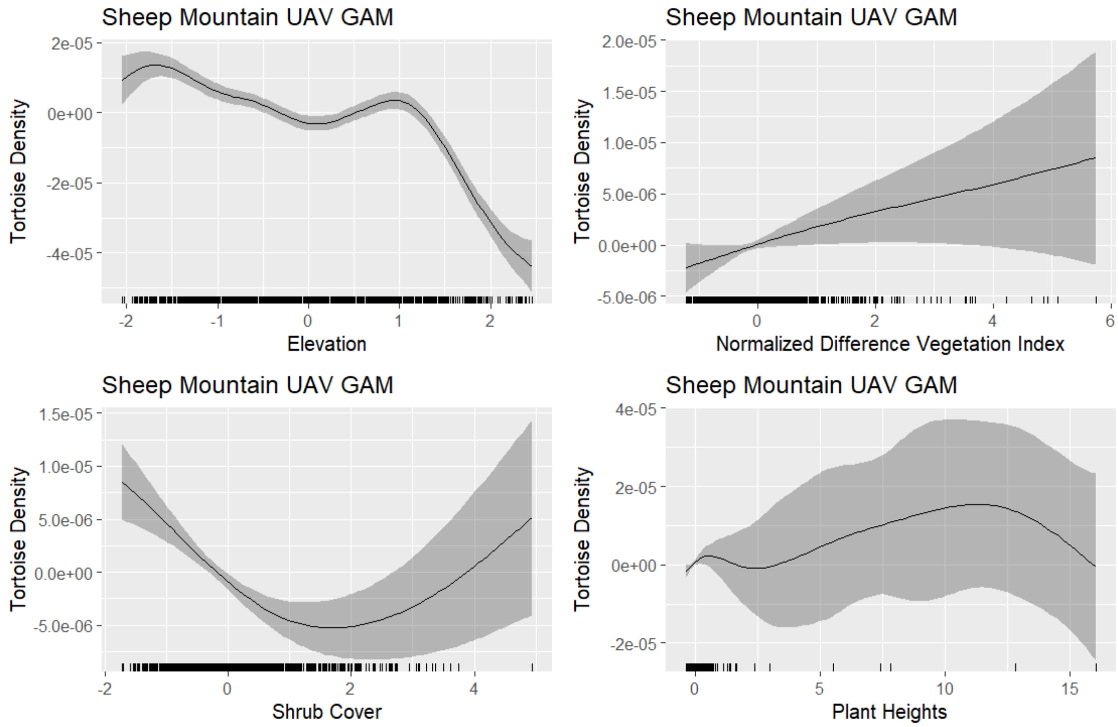

FIGURE 55: SHEEP MOUNTAIN UAV MODEL COVARIATE EFFECTS WITH TORTOISE DENSITIES. GRAY REGIONS REPRESENT UNCERTAINTY DUE TO LACK OF DATA POINTS.

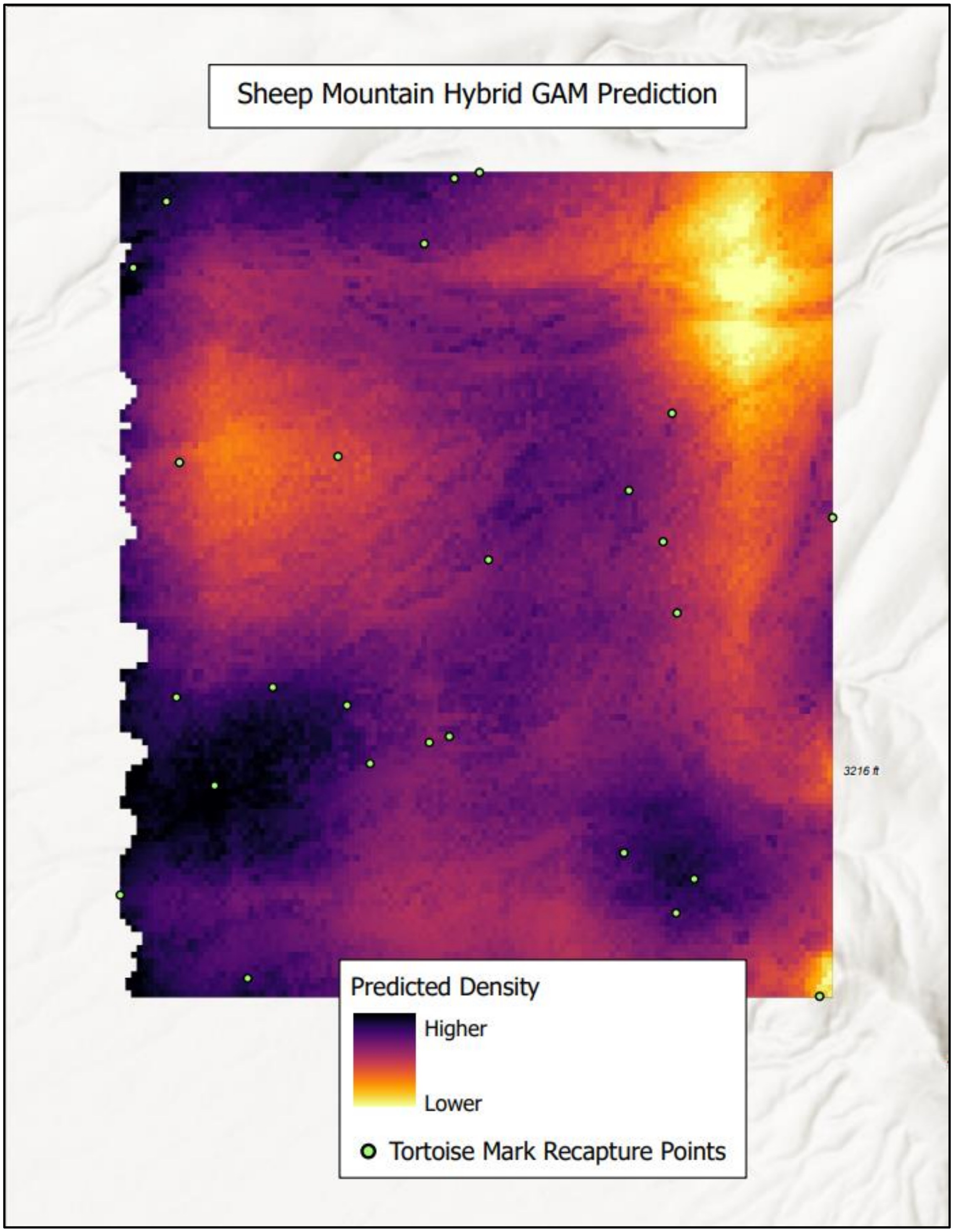

FIGURE 56: SHEEP MOUNTAIN HYBRID GENERALIZED ADDITIVE MODEL PREDICTED DENSITY MAP.

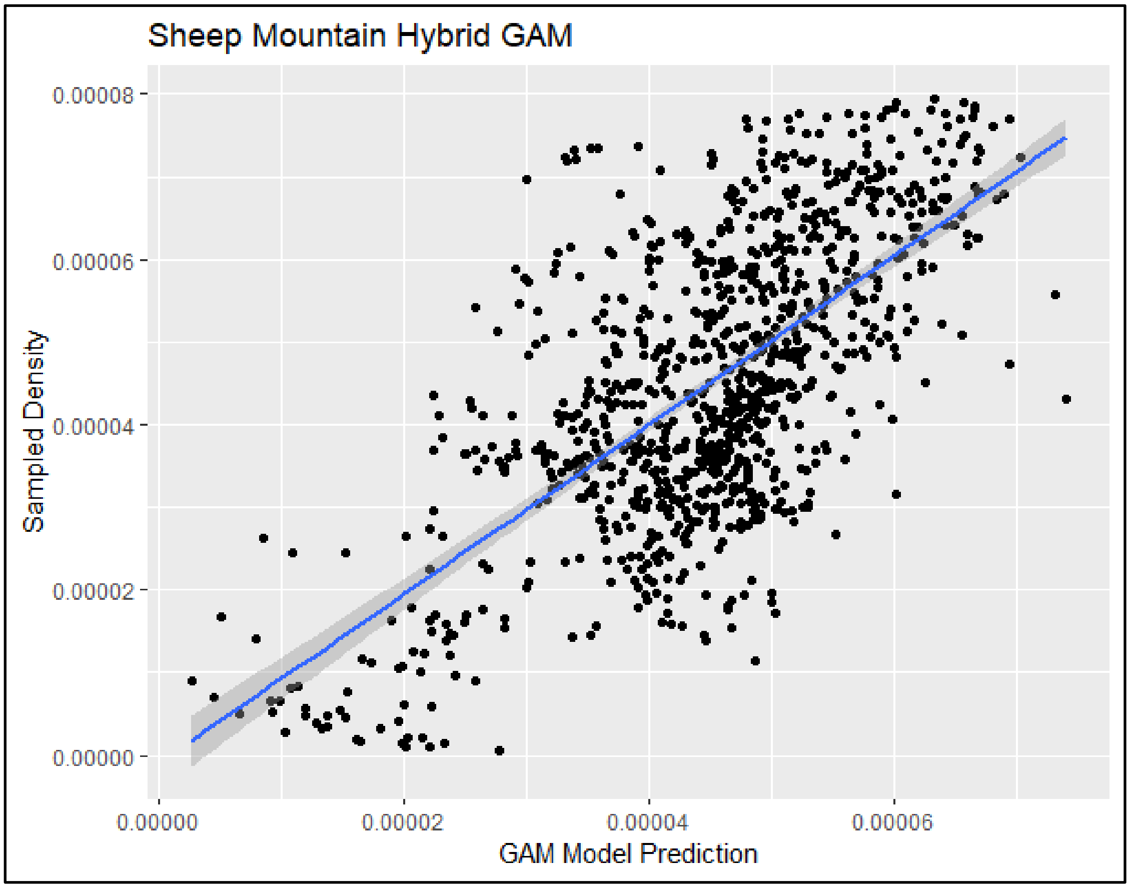

Figure 57: Sheep Mountain hybrid GAM predicted density versus true sampled density

Table 14: Sheep Mountain hybrid generalized additive model summary including: estimated degrees of freedom (EDF), reference number of degrees of freedom (Ref.df), F-statistic (F) and p-values.

Terms	edf	Ref.df	F	p-value	
Terrestrial Disturbance Index	2.9976618	3	33.642	< 2e-16	***
Coarse Fragments on Surface	1.8080225	3	7.405	2.86E-06	***
Sand on Surface	2.6483269	3	41.909	< 2e-16	***
Winter Precipitation	1.8698657	3	6.828	1.01E-05	***
Maximum Temperature	1.9161906	3	5.413	6.14E-05	***
UAV Elevation	2.4938248	3	73.947	< 2e-16	***
UAV Normalized Difference Vegetation Index	0.3265684	3	0.000	0.978	
UAV Shrub Cover	1.8948789	3	6.589	1.20E-05	***
UAV Plant Height	0.0001251	3	0.000	0.895	
Deviance Explained = 45.2%	**R-squared (adj) = 0.443**				

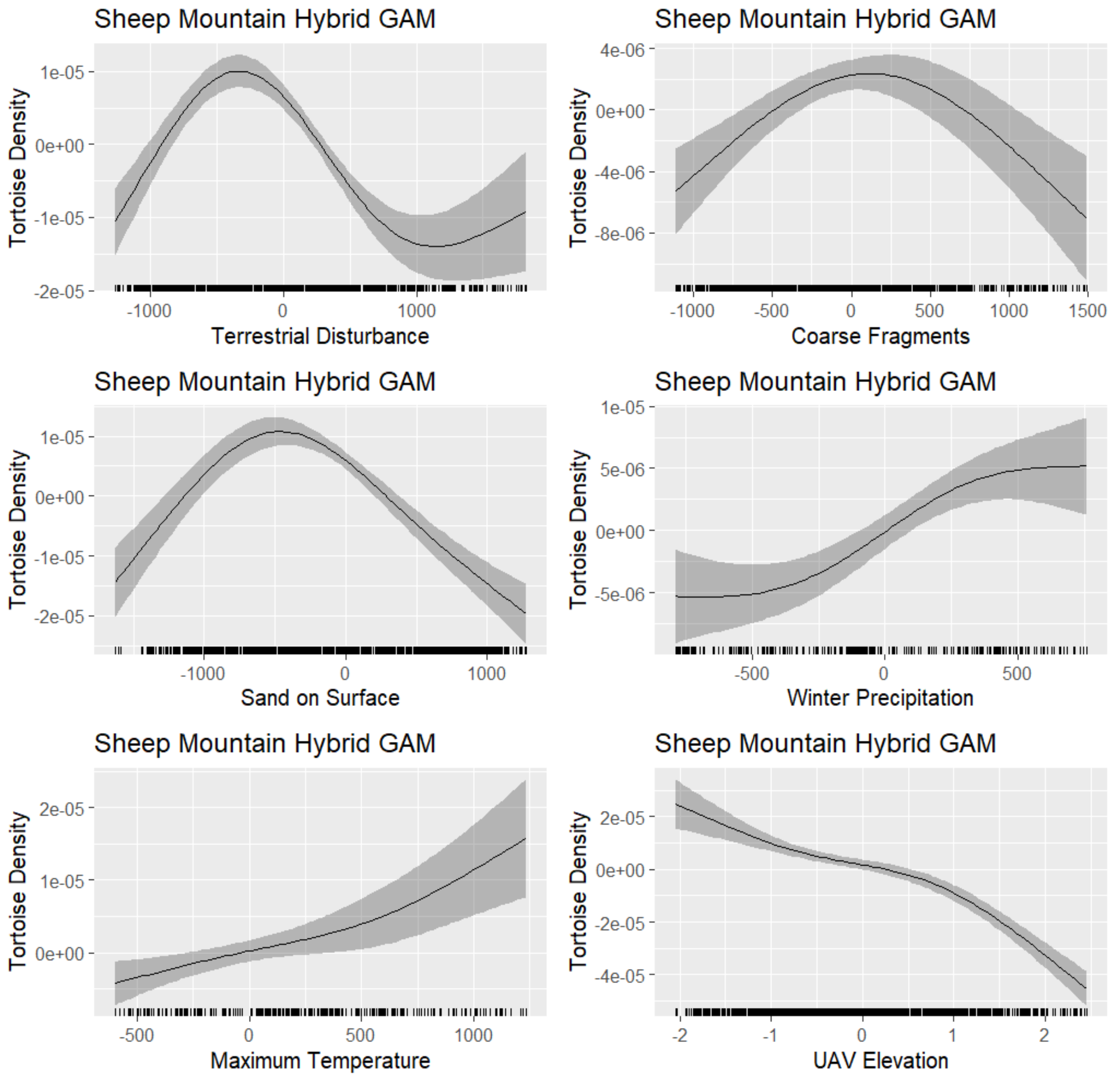
Sheep Mountain Hybrid GAM
Tortoise Density
1e-05
0e+00
-1e-05
-2e-05
-1000
0
1000
Terrestrial Disturbance
Sheep Mountain Hybrid GAM
Tortoise Density
4e-06
0e+00
-4e-06
-8e-06
-1000
-500
0
500
1000
1500
Coarse Fragments
Sheep Mountain Hybrid GAM
Tortoise Density
1e-05
0e+00
-1e-05
-2e-05
-1000
0
1000
Sand on Surface
Sheep Mountain Hybrid GAM
Tortoise Density
1e-05
5e-06
0e+00
-5e-06
-500
0
500
Winter Precipitation
Sheep Mountain Hybrid GAM
Tortoise Density
2e-05
1e-05
0e+00
-500
0
500
1000
Maximum Temperature
Sheep Mountain Hybrid GAM
Tortoise Density
2e-05
0e+00
-2e-05
-4e-05
-2
-1
0
1
2
UAV Elevation

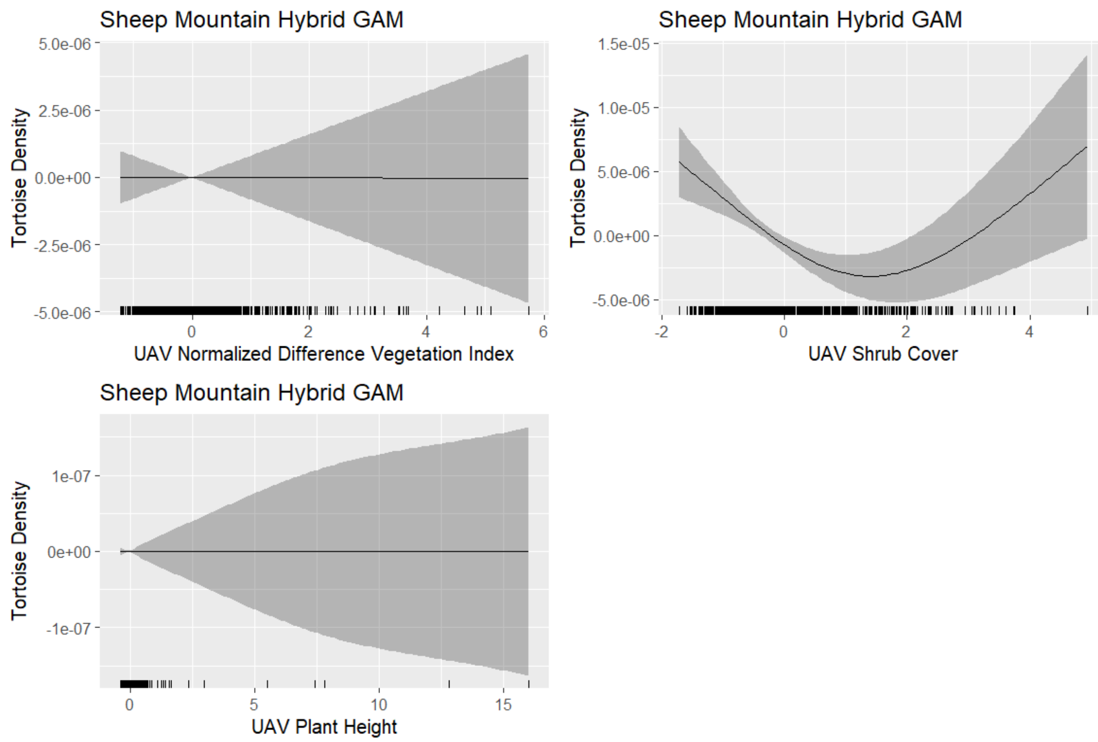

FIGURE 58: SHEEP MOUNTAIN HYBRID MODEL COVARIATE EFFECTS WITH TORTOISE DENSITIES. GRAY REGIONS REPRESENT UNCERTAINTY DUE TO LACK OF DATA POINTS.

TABLE 15: SHEEP MOUNTAIN ALL DENSITY MODELS AIC VALUES.

Model	Degrees of freedom	AIC
Sheep Mountain Satellite GAM	25.36551	-20008.36
Sheep Mountain Hybrid GAM	17.95546	-19465.66
Sheep Mountain UAV GAM	17.45362	-19276.67

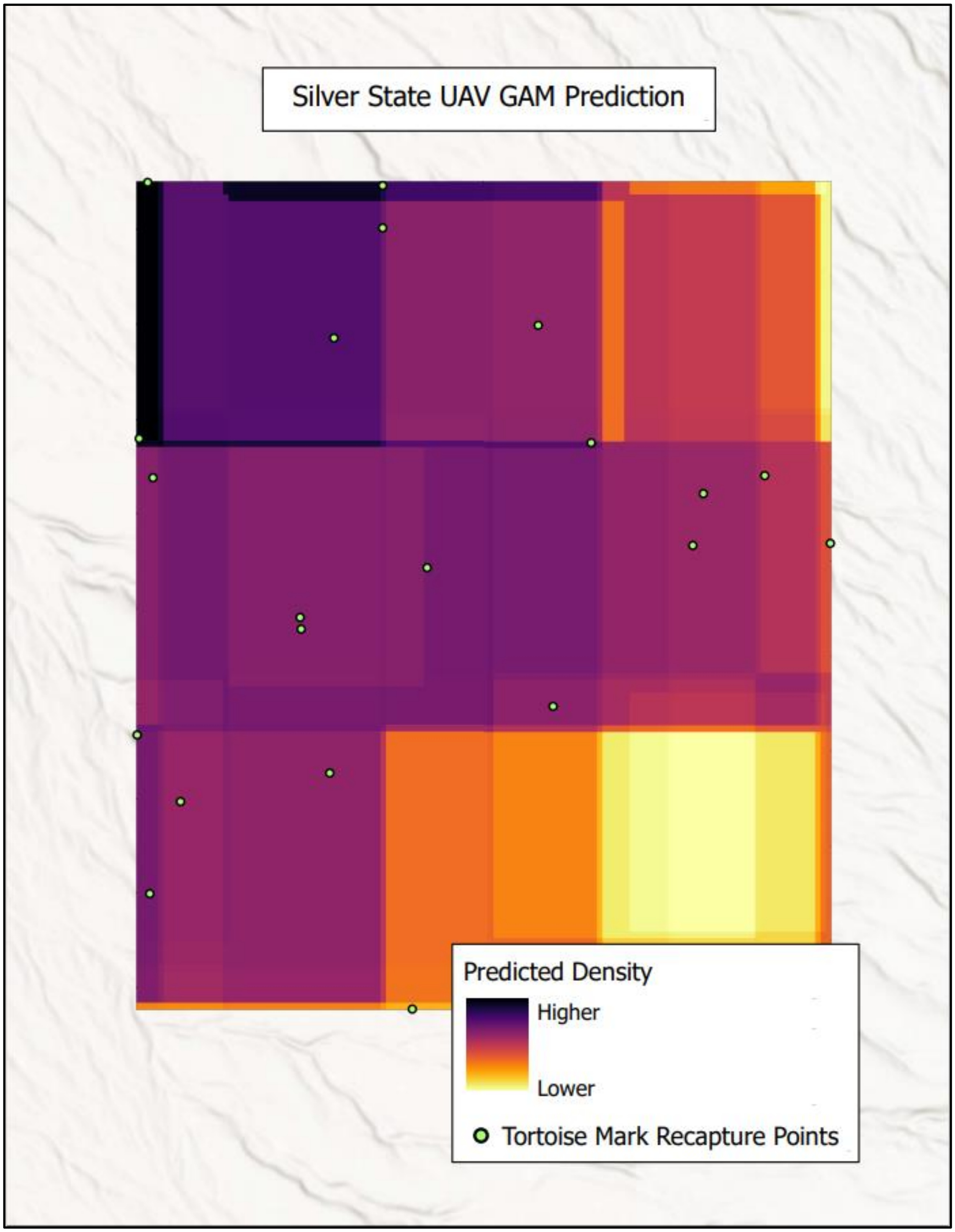

FIGURE 59: SILVER STATE SATELLITE GENERALIZED ADDITIVE MODEL PREDICTED DENSITY MAP.

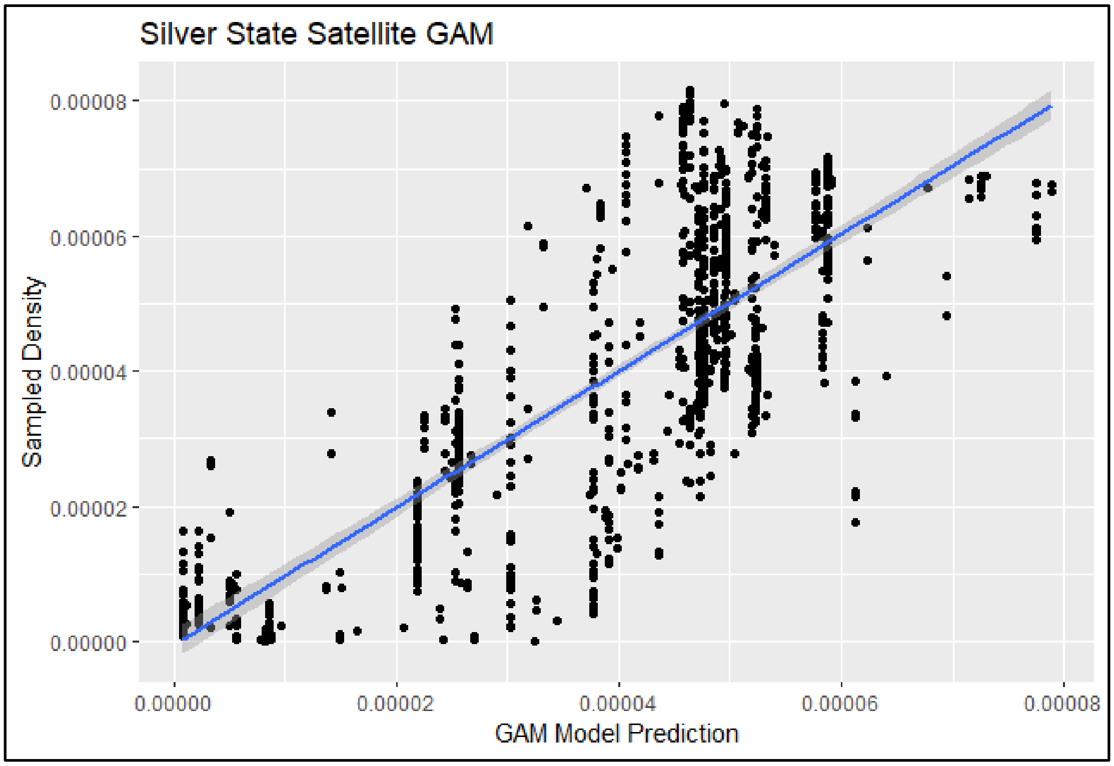

FIGURE 60: SILVER STATE SATELLITE GAM PREDICTED DENSITY VERSUS TRUE SAMPLED DENSITY

TABLE 16: SILVER STATE SATELLITE GENERALIZED ADDITIVE MODEL SUMMARY INCLUDING: ESTIMATED DEGREES OF FREEDOM (EDF), REFERENCE NUMBER OF DEGREES OF FREEDOM (REF.DF), F-STATISTIC (F) AND P-VALUES.

Terms	edf	Ref.df	F	p-value	
Normalized Difference Vegetation Index	1.88E+00	2	8.989	7.17E-05	***
Depth to Bedrock	2.00E+00	2	28.561	< 2e-16	***
Coarse Fragments on Surface	1.91E+00	2	223.240	< 2e-16	***
Sand on Surface	1.28E+00	2	97.709	< 2e-16	***
Winter Precipitation	2.99E-05	2	0.000	0.1556	
Maximum Temperature	6.56E-01	2	1.153	0.0472	*
Deviance Explained = 59%	**R-squared (adj) = 0.587**				

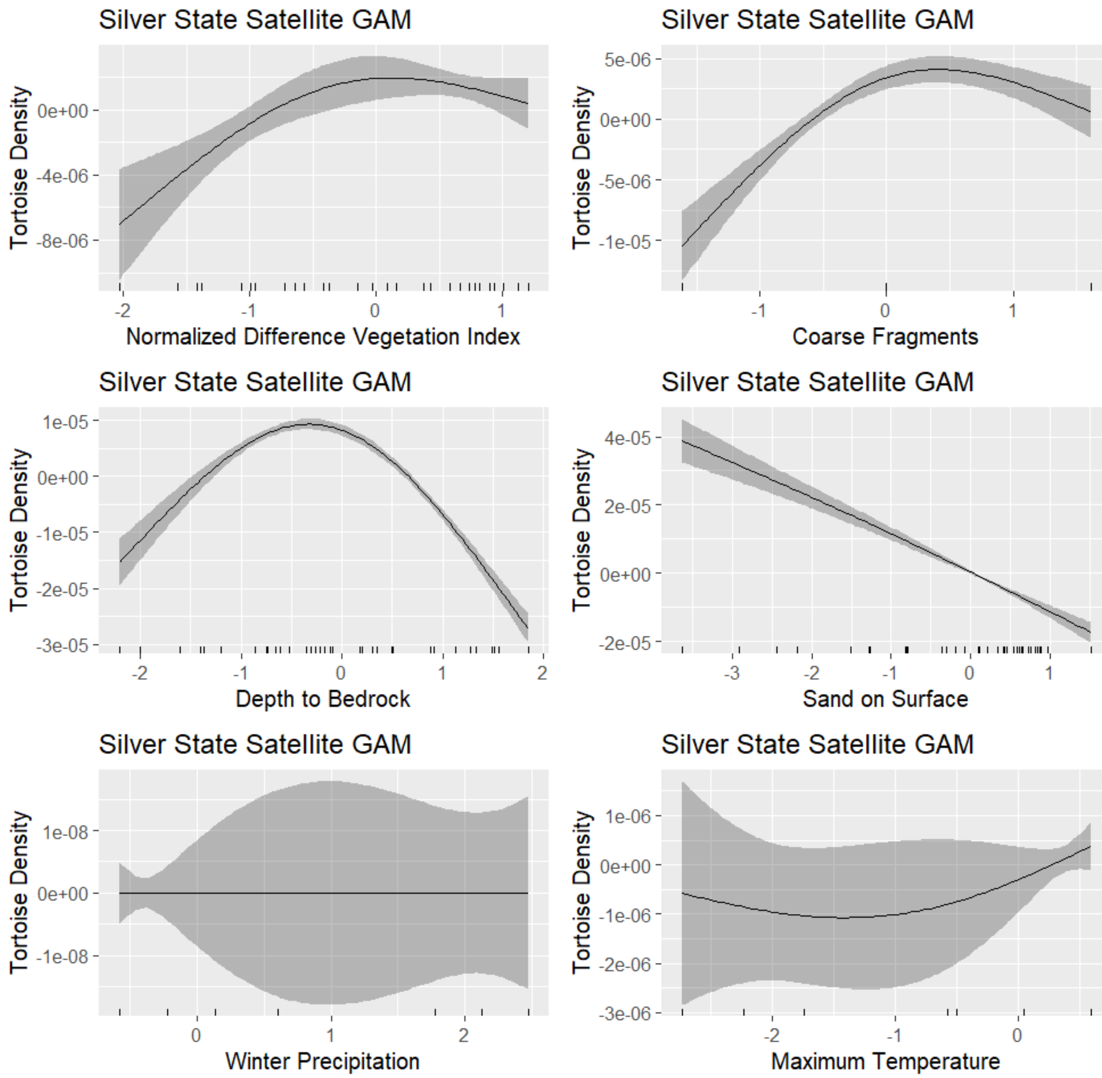

FIGURE 61: SILVER STATE SATELLITE MODEL COVARIATE EFFECTS WITH TORTOISE DENSITIES. GRAY REGIONS REPRESENT UNCERTAINTY DUE TO LACK OF DATA POINTS.

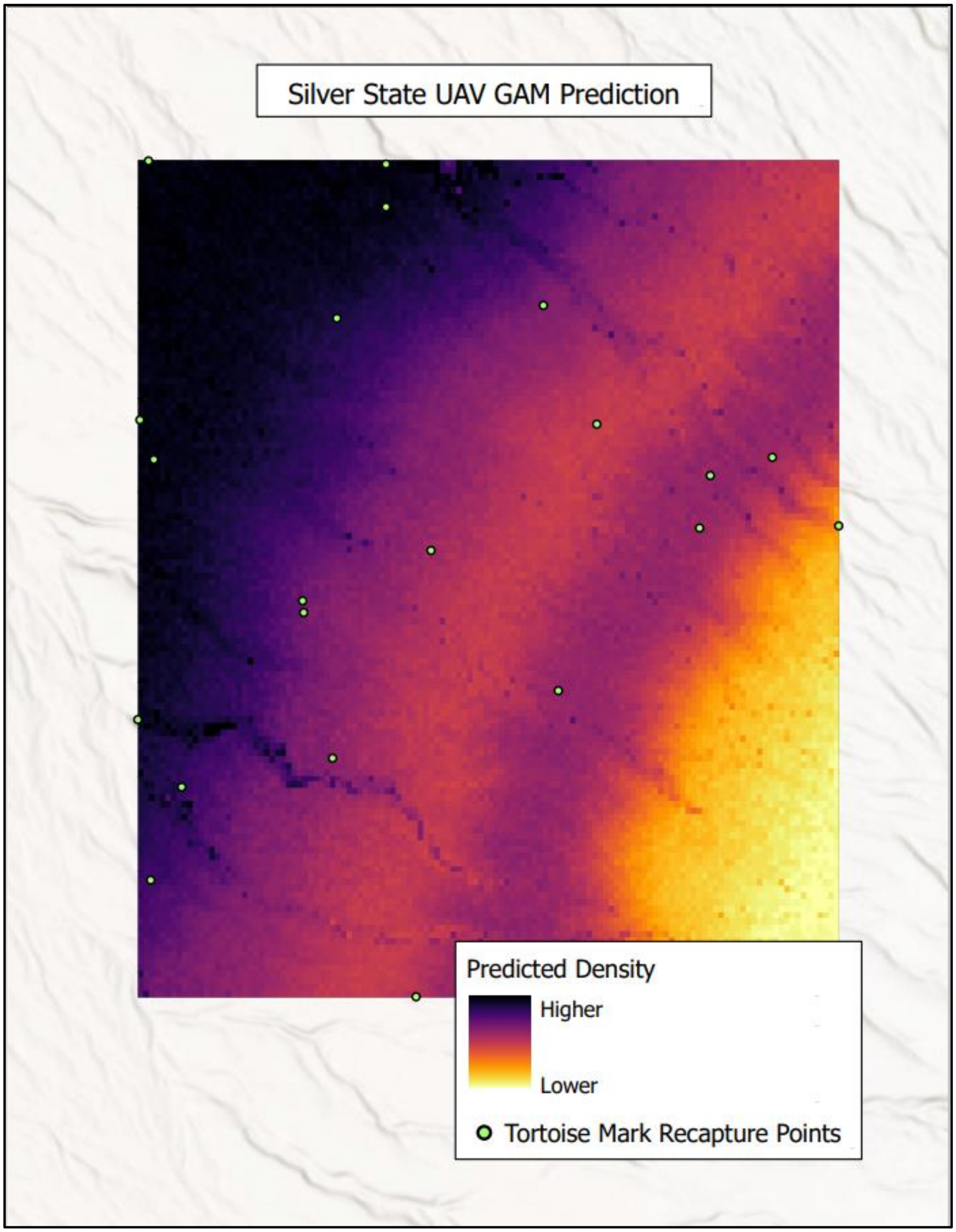

FIGURE 62: SILVER STATE UAV GENERALIZED ADDITIVE MODEL PREDICTED DENSITY MAP.

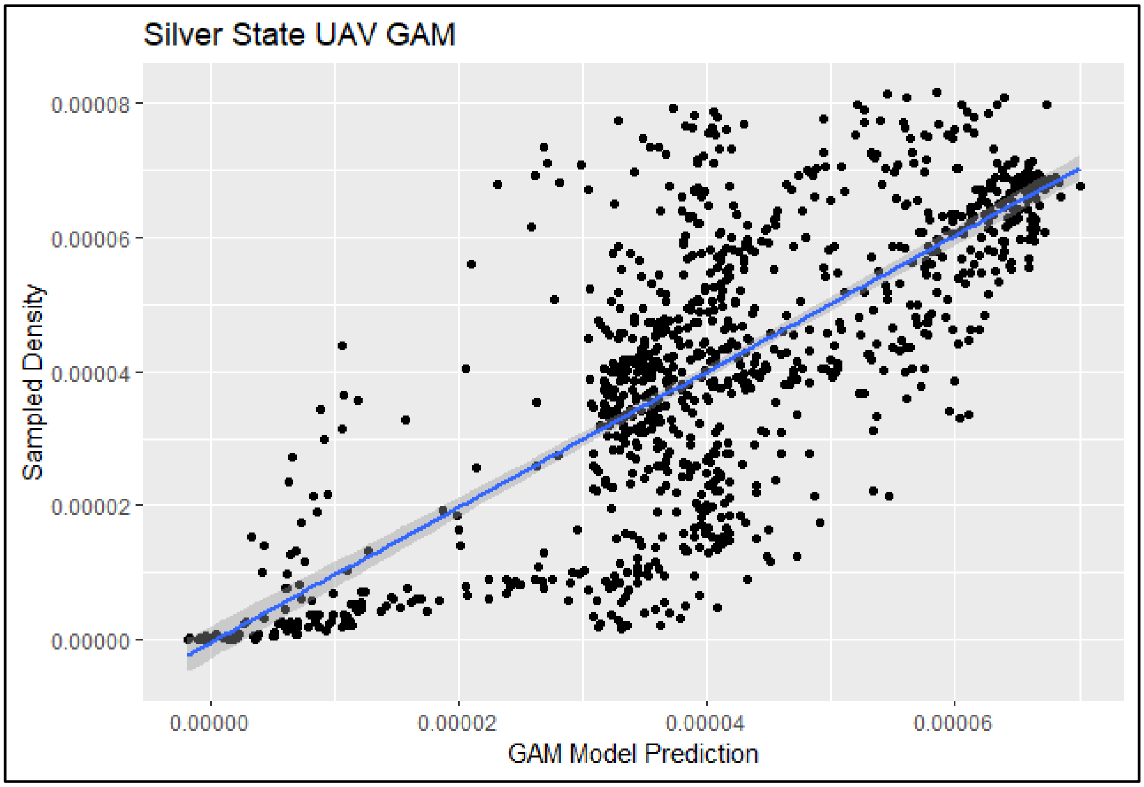

FIGURE 63 SILVER STATE UAV GAM PREDICTED DENSITY VERSUS TRUE SAMPLED DENSITY

TABLE 17: SILVER STATE UAV GENERALIZED ADDITIVE MODEL SUMMARY INCLUDING: ESTIMATED DEGREES OF FREEDOM (EDF), REFERENCE NUMBER OF DEGREES OF FREEDOM (REF.DF), F-STATISTIC (F) AND P-VALUES.

Terms	**edf**	**Ref.df**	**F**	**p-value**	
Elevation	12.248	29	40.357	< 2e-16	***
Normalized Difference Vegetation Index	6.266	29	0.239	0.279	
Shrub Cover %	4.168	29	0.137	0.403	
Plant Height	1.070	29	0.039	0.332	
Deviance Explained = 55.8%	**R-squared (adj) = 0.547**				

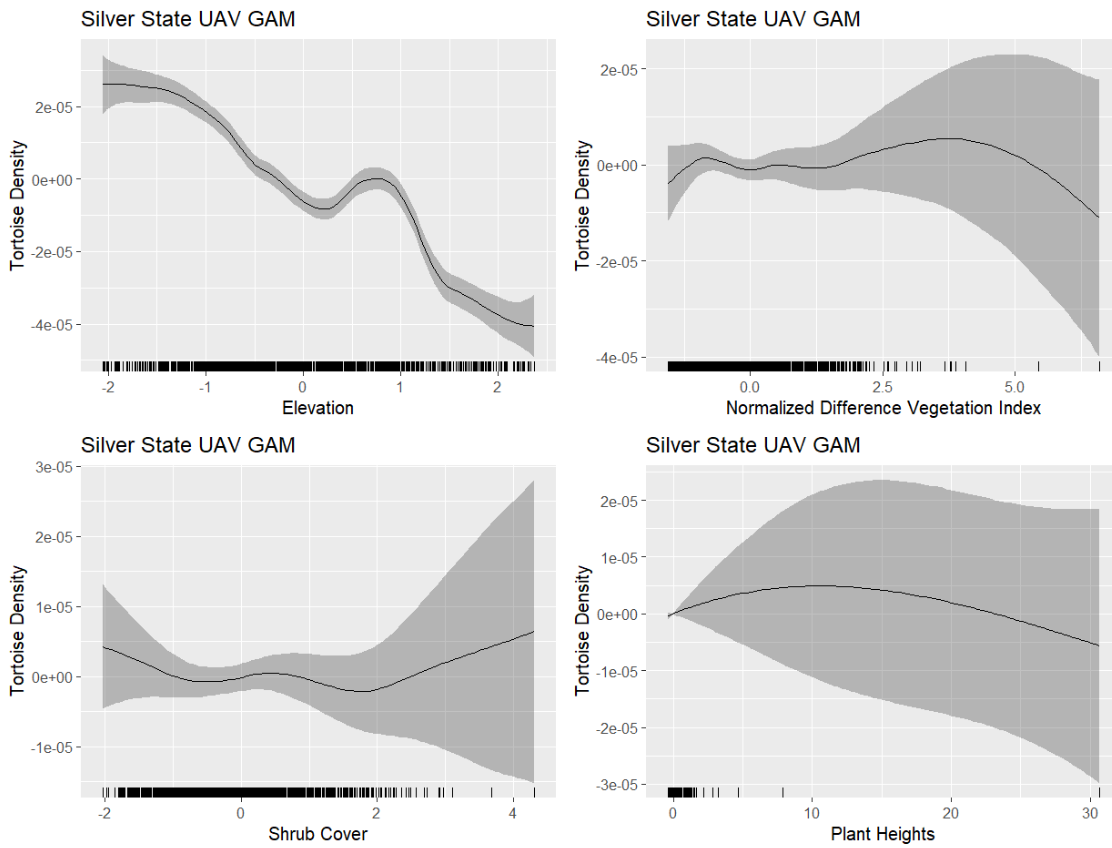

Figure 64: Silver State UAV model covariate effects with tortoise densities. Gray regions represent uncertainty due to lack of data points.

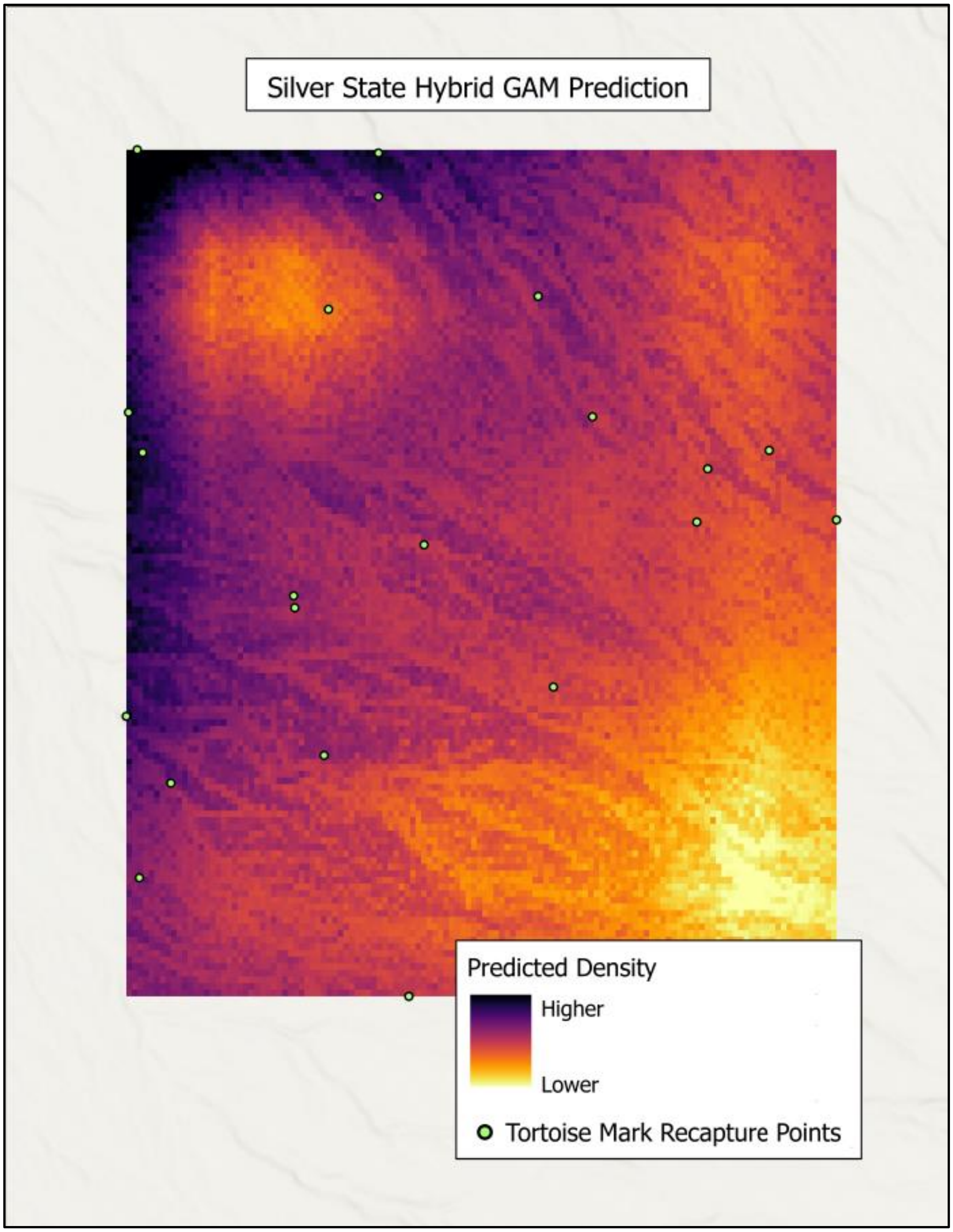

FIGURE 65: SILVER STATE HYBRID GENERALIZED ADDITIVE MODEL PREDICTED DENSITY MAP.

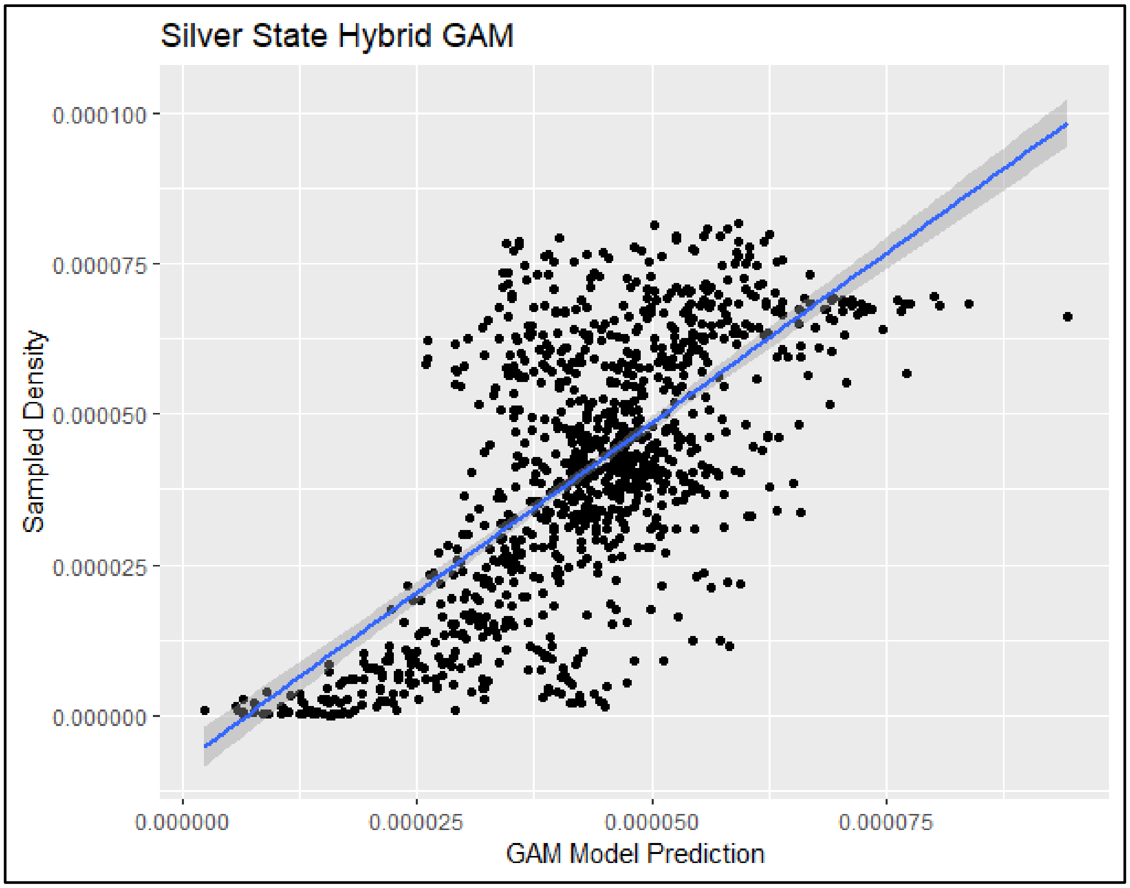

Figure 66: Silver State hybrid GAM predicted density versus true sampled density

Table 18: Silver State hybrid generalized additive model summary including: estimated degrees of freedom (EDF), reference number of degrees of freedom (Ref.df), F-statistic (F) and p-values.

Terms	edf	Ref.df	F	p-value	
Coarse Fragments on Surface	1.8309854	3	5.990	4.71E-05	***
Sand on Surface	2.6516525	3	32.258	< 2e-16	***
Winter Precipitation	1.9089319	3	0.673	0.3214	
Maximum Temperature	1.9055381	3	1.889	0.0373	*
UAV Elevation	2.9984816	3	57.144	< 2e-16	***
UAV Normalized Difference Vegetation Index	0.8030371	3	0.755	0.0921	
UAV Shrub Cover	2.0204717	3	13.502	< 2e-16	***
UAV Plant Height	0.0001249	3	0.000	0.7721	
Deviance Explained = 40.3%	**R-squared (adj) = 0.394**				

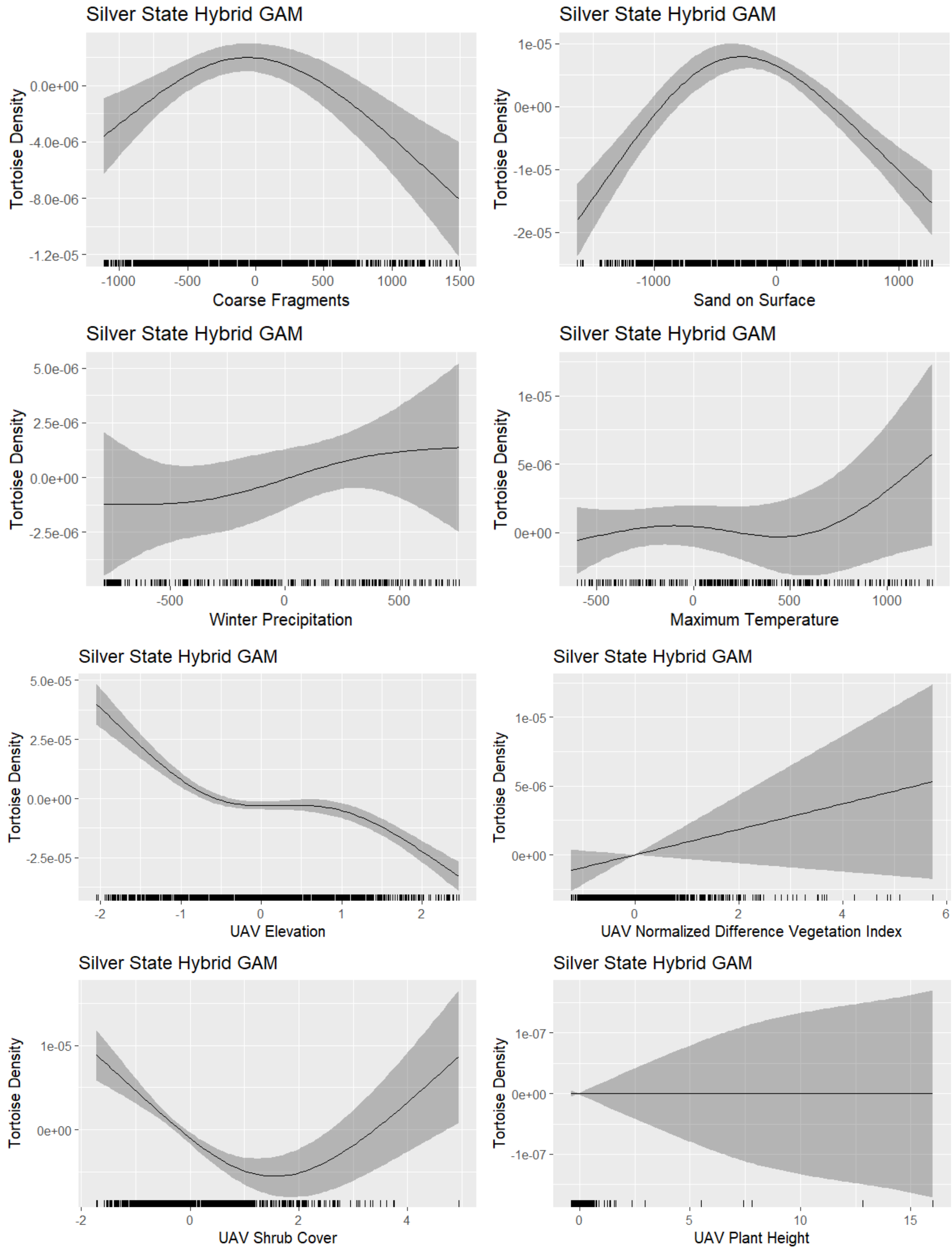

FIGURE 67: SILVER STATE HYBRID MODEL COVARIATE EFFECTS WITH TORTOISE DENSITIES. GRAY REGIONS REPRESENT UNCERTAINTY DUE TO LACK OF DATA POINTS.

TABLE 19: SILVER STATE ALL DENSITY MODELS AIC VALUES.

Model	Degrees of freedom	AIC
Silver State Satellite GAM	9.719774	-19474.07
Silver State Hybrid GAM	16.119223	-19383.48
Silver State UAV GAM	25.751293	-19365.37

Discussion

The Mojave Desert tortoise, like other reptiles and amphibians across many different landscapes, is threatened by numerous circumstances including disturbance, drought, predation, and increasing urbanization just to list a few. Characterizing densities of the desert tortoise based on habitat characteristics is crucial to informing future management and conservation decisions. When the Mojave desert tortoise was listed as threatened on the endangered species list in 1990 one of the criteria for determining whether this protection could be removed was that tortoises must be well distributed across the range (Averill-Murray et al. 2012). Thus, the need to improve models evaluating tortoise densities throughout suitable habitat so that we may better understand why tortoises are dense in certain areas but sparse in others. Given the inevitability of a rapidly changing ecosystem, understanding spatial variation of species in relation to key environmental variables will prove valuable in managing the species habitat and distributions. The variables used in the models presented here were informed by previous studies on Mojave desert tortoises such as the species distribution model constructed by Nussear and others (2009) revealing regions of habitat suitability across the range of the desert tortoise. The models I've constructed take these analyses a step further by not only evaluating what environmental variables have a significant influence on tortoise distributions but also how tortoises respond to these variables. Various methods exist for analyzing species densities, and the methods used in this project are suitable for beginning to understand the processes influencing tortoise distributions. The models presented here have the potential to be applied to data collected at multiple scales and with varying collection methods as well as to historical data. With the advancement of remote sensing imagery collected with UAVs, density models such as this have the potential to be significantly improved upon, as they are more reflective of the local landscape experienced by tortoises. Satellite imagery proves useful for range wide analyses but may not be as interpretable at finer scales. For example, NDVI derived from satellite imagery returns a coarse image that is not precisely reflective of the vegetation present at local scales and in many instances this NDVI satellite covariate revealed differing responses from tortoise densities compared to the UAV derived shrub cover covariate. Field based methods provide extremely fine scale and detailed data; however, these methods cannot capture the heterogeneity of the landscape, nor can they be applied across large regions due to limitations of time and resources. With data collected using UAVs we have the potential to analyze species densities at finer scales in relation to significant variables and begin to bridge the gap between remotely sensed satellite imagery and data collected through field-based methods. Though these methods hold a great deal of potential they are also fairly knew and much more research must be done before the data collected through the use of

UAVs can be solely relied upon for input into species models. For instance, obtaining specific plant species compositions across the landscape would require longer flight times due to the need to reduce the height and speed at which the UAV is flown and even this data is not yet capable of being as precise as on the ground field methods. Other studies have already begun to reveal the potential of UAV remotely sensed imagery in evaluating species' habitat and densities. Fritz and others (2018) found that predictor variables derived from fine scale imagery obtained using UAVs played a significant role in describing the variance of a bird community in eastern Qinghai-Tibetan Plateau. A combination of data collected at various scales for input into species density analyses will provide conservation managers with the greatest possible understanding of the processes influencing the patchy distribution of desert tortoises throughout the Mojave Desert from fine to large spatial scales.

References

Allison, L. J., & McLuckie, A. M. (2018). Population trends in Mojave Desert tortoises (Gopherus agassizii). *Herpetological Conservation and Biology*, *13*(2), 433-452.

Anderson, R., Gordon, D., Crawley, M. & Hassel, M. (1982). Variability in the abundance of animal and plant species. Nature 296, 245–248.

Apps, C.D., McLellan, B.N., Proctor, M.F., Stenhouse, G.B. and Servheen, C. (2016), Predicting spatial variation in grizzly bear abundance to inform conservation. Jour. Wild. Mgmt., 80: 396-413.

Averill-Murray, R. C., Darst, C. R., Field, K. J., & Allison, L. J. (2012). A new approach to conservation of the Mojave Desert Tortoise. *BioScience*, *62*(10), 893–899. https://doi.org/10.1525/bio.2012.62.10.9

Baddeley, A., Rubak, E., & Turner, R. (2016). *Spatial point patterns: Methodology and applications with R*. CRC Press Taylor & Francis Group.

Buckland, S. T., Anderson, D. R., Burham, K. P., Laake, J. L., Borchers, D. L., & Thomas, L. (2004). *Advanced distance sampling: Estimating abundance of biological populations*. Oxford University Press.

Bury, R. B. (1982) *North American Tortoises: Conservation and Ecology.* U.S. Dept. of the Interior, Fish and Wildlife Service.

Buzas, Martin A., (1971), Analyses of Species Densities by the Multivariate General Linear Model, *Limnology and Oceanography*, 4, doi: 10.4319/lo.1971.16.4.0667.

Corn, P.S. (1994) Recent trends of desert tortoise populations in the Mojave Desert. Pages 85-93 in Bury, R. B. and Germano D. J., editors. Biology of North American tortoises. National Biological Survey, Fish and Wildlife Research 13.

Drake, K. K., Bowen, L., Nussear, K. E., Esque, T. C., Berger, A. J., Custer, N. A., ... & Lewison, R. L. (2016). Negative impacts of invasive plants on conservation of sensitive desert wildlife. Ecosphere, 7(10), e01531.

Fritz, A., Li, L., Storch, I., Koch, B., 2018. UAV-derived habitat predictors contribute strongly to understanding avian species–habitat relationships on the eastern Qinghai-tibetan plateau. Remote Sen. Ecol. Conserv. 4, 53–65.

Germano, D. J., Bury, R. B., Esque, T. C., Fritts, T. H., & Medica, P. A. (1994). Range and habitats of the desert tortoise. *Biology of North American Tortoises*, *13*, 73-84.

Gillan, J. K., Karl, J. W., & van Leeuwen, W. J. (2020). Integrating drone imagery with existing rangeland monitoring programs. *Environmental monitoring and assessment*, *192*(5), 1-20.

Hengl, T., Sierdsema, H., Radović, A., & Dilo, A. (2009). Spatial prediction of species' distributions from occurrence-only records: Combining point pattern analysis, ENFA and regression-kriging. *Ecological Modelling*, *220*(24), 3499–3511.

ISRIC World Soil Information (2020), Soil Grids web portal, accessed June 13, 2021, from https://soilgrids.org/.

MacKenzie, D. I., Nichols, J. D., Royle, J. A., Pollock, K. H., Bailey, L. L., & Hines, J. E. (2006). *Occupancy estimation and modeling inferring patterns and dynamics of species* (1). Elsevier.

Mitchell, C. I., Shoemaker, K. T., Esque, T. C., Vandergast, A. G., Hromada, S. J., Dutcher, K. E., Heaton, J. S., and Nussear, K. E. (2021). Integrating telemetry data at several scales with spatial capture–recapture to improve density estimates. Ecosphere 12(8):e03689.

Nagendra, H., Rocchini, D. High resolution satellite imagery for tropical biodiversity studies: the devil is in the detail. *Biodivers Conserv* **17**, 3431–3442 (2008). https://doi.org/10.1007/s10531-008-9479-0

Nielson T, Bradford J, Holbrook WS and Seyfried M (2021) The Effect of Aspect and Elevation on Critical Zone Architecture in the Reynolds Creek Critical Zone Observatory: A Seismic Refraction Study. *Front. Water* 3:670524. doi: 10.3389/frwa.2021.670524

Nussear, K. E., Esque, T. C., Inman, R. D., Gass, L., Thomas, K. A., Wallace, C. S., ... & Webb, R. H. (2009). *Modeling habitat of the desert tortoise (Gopherus agassizii) in the Mojave and parts of the Sonoran Deserts of California, Nevada, Utah, and Arizona* (No. 2009-1102). US Geological Survey.

Nussear, K.E. & Tracy, C.R. (2007), CAN MODELING IMPROVE ESTIMATION OF DESERT TORTOISE POPULATION DENSITIES?. Ecological Applications, 17: 579-586.

Nussear, K. E., & Tuberville, T. D. (2014). Habitat characteristics of North American tortoises. In *Biology and conservation of North American tortoises*. chapter, Johns Hopkins University Press, 77-84

PRISM Climate Group (2012), Norm81m. PRISM normals, 1981–2010, Corvallis (OR): Oregon State University, accessed July 5, 2022, from http://prism.oregonstate.edu/.

U.S. Geological Survey (2019), Remote Sensing Phenology, accessed June 16, 2021, from https://www.usgs.gov/special-topics/remote-sensing-phenology.

Roff, D. A., (1973) On the accuracy of some mark-recapture estimators. *Oecologia 12, 15-34.*

Smith, A., B. Page, K. Duffy, and R. Slotow. (2012). Using Maximum Entropy modeling to predict the potential distributions of large trees for conservation planning. Ecosphere 3(6):56.

Toevs G. R, Karl J.W., Taylor J.J., Spurrier C.S., Karl M.S., Bobo M.R., & Herrick J.E., (2011). Consistent indicators and methods and a scalable sample design to meet assessment, inventory, and monitoring information needs across scales. Rangelands 33 (4), 14-20

US Fish and Wildlife Service. (2021). Status of the Desert Tortoise and Its Critical Habitat. *US Fish and Wildlife Service: Reno, NV, USA*, 25.

Wallace, S.A., Webb, R.H. & Thomas, K.A. (2008). Estimation of perennial vegetation cover distribution in the Mojave Desert using MODIS-EVI data. GIScience & Remote Sensing, 45(2), 167-187.

Webb, R. H., Murov, M. B., Esque, T. C., Boyer, D. E., DeFalco, L. A., Haines, D. F., ... & Medica, P. A. (2003). *Perennial vegetation data from permanent plots on the Nevada Test Site, Nye County, Nevada* (No. 2003-336). US Geological Survey.

De Boer W.F., van Langevelde F., Prins H.H.T., De Ruiter P.C., Blanc J., Vis M.J.P., Gaston K.J., Hamilton I.D. (2013) Understanding spatial differences in African elephant densities and occurrence, A continent-wide analysis. Biological Conservation, 159 , pp. 468-476.

Van Horne, B. (1983). Density as a Misleading Indicator of Habitat Quality. *The Journal of Wildlife Management*, *47*(4), 893–901. https://doi.org/10.2307/3808148

Van Linn, P. F., Nussear, K. E., Esque, T. C., DeFalco, L. A., Inman, R. D., & Abella, S. R. (2013). Estimating wildfire risk on a Mojave Desert landscape using remote sensing and field sampling. *International journal of wildland fire*, *22*(6), 770-779.

Williams, S.E. and Middleton, J. (2007), Climatic seasonality, resource bottlenecks, and abundance of rainforest birds: implications for global climate change. Diversity and Distributions, 14: 69-77.

Woodbury, A.M. and Hardy, R. (1948), Studies of the Desert Tortoise, Gopherus Agassizii. Ecological Monographs, 18: 145-200.

Zylstra, E. R., Allison, L. J., Averill-Murray, R. C., Landau, V., Pope, N. S., & Steidl, R. J. (2023), A spatially explicit model for density that accounts for availability: A case study with Mojave Desert Tortoises. *Ecosphere*, *14*(3). https://doi.org/10.1002/ecs2.4448

Index I

Table 20: McCullough Pass One Sample t-test March 2022 evaluating UAV mean shrub cover of 100 transects versus AIM mean shrub cover across a single transect

McCullough Pass One Sample t-test	t value	UAV Mean (100 transects) cm	AIM Mean (1 transect) cm	p-value
McCullough Pass March 2022 T1	-16.248	0.1338	0.2840	< 2.2e-16
McCullough Pass March 2022 T2	-26.421	0.1120	0.2552	< 2.2e-16
McCullough Pass March 2022 T3	-28.255	0.0173	0.0604	< 2.2e-16

Table 21: Sheep Mountain One Sample t-test March 2022 evaluating UAV mean shrub cover of 100 transects versus AIM mean shrub cover across a single transect

Sheep Mountain One Sample t-test	t value	UAV Mean (100 transects) cm	AIM Mean (1 transect) cm	p-value
Sheep Mountain March 2022 T1	-5.266	0.2472	0.2864	8.13E-07
Sheep Mountain March 2022 T2	15.893	0.3386	0.1940	< 2.2e-16
Sheep Mountain March 2022 T3	24.428	0.2252	0.0188	< 2.2e-16
Sheep Mountain March 2022 T4	8.730	0.1144	0.0656	6.40E-14
Sheep Mountain March 2022 T5	-0.216	0.1087	0.1096	0.8293
Sheep Mountain March 2022 T6	10.311	0.1230	0.0568	< 2.2e-16
Sheep Mountain March 2022 T7	22.015	0.3099	0.1976	< 2.2e-16
Sheep Mountain March 2022 T8	18.253	0.2625	0.1448	< 2.2e-16
Sheep Mountain March 2022 T9	21.849	0.2883	0.0940	< 2.2e-16

Table 22: Silver State One Sample t-test March 2022 evaluating UAV mean shrub cover of 100 transects versus AIM mean shrub cover across a single transect

Silver State One Sample t-test	t value	UAV Mean (100 transects) cm	AIM Mean (1 transect) cm	p-value
Silver State March 2022 T1	-5.019	0.1923	0.2500	2.30E-06
Silver State March 2022 T2	6.313	0.2535	0.2028	7.80E-09
Silver State March 2022 T3	11.337	0.2246	0.1252	< 2.2e-16
Silver State March 2022 T4	14.793	0.2196	0.1140	< 2.2e-16
Silver State March 2022 T5	21.419	0.2587	0.1044	< 2.2e-16
Silver State March 2022 T6	6.355	0.2500	0.1988	6.42E-09
Silver State March 2022 T7	-1.797	0.0987	0.1060	0.07536
Silver State March 2022 T8	-15.600	0.1485	0.2548	< 2.2e-16
Silver State March 2022 T9	1.115	0.1079	0.1020	0.2677
Silver State March 2022 T10	-1.713	0.1694	0.1836	0.08981
Silver State March 2022 T11	12.550	0.2046	0.1088	< 2.2e-16
Silver State March 2022 T12	-0.038	0.2013	0.2016	0.9701

Table 23: Coyote Springs One Sample t-test March 2022 evaluating UAV mean shrub cover of 100 transects versus AIM mean shrub cover across a single transect

Coyote North One Sample t-test	t value	UAV Mean (100 transects) cm	AIM Mean (1 transect) cm	p-value
Coyote North March 2022 T1	5.745	0.2904	0.2400	1.02E-07
Coyote North March 2022 T2	34.137	0.4366	0.1708	< 2.2e-16
Coyote North March 2022 T3	25.721	0.5046	0.2820	< 2.2e-16
Coyote North March 2022 T4	8.957	0.3354	0.2620	2.05E-14
Coyote North March 2022 T5	36.177	0.4181	0.1392	< 2.2e-16
Coyote North March 2022 T6	27.676	0.3260	0.1144	< 2.2e-16

Table 24: Stump Springs Zone 1 One Sample t-test March 2022 evaluating UAV mean shrub cover of 100 transects versus AIM mean shrub cover across a single transect

Stump Springs Zone 1 One Sample t-test	t value	UAV Mean (100 transects) cm	AIM Mean (1 transect) cm	p-value
Stump Springs Zone 1 March 2022 T1	-5.246	0.2334	0.2700	8.85E-07
Stump Springs Zone 1 March 2022 T2	21.599	0.2900	0.1620	< 2.2e-16
Stump Springs Zone 1 March 2022 T3	9.037	0.2447	0.1732	1.38E-14

Table 25: Stump Springs Zone 2 One Sample t-test March 2022 evaluating UAV mean shrub cover of 100 transects versus AIM mean shrub cover across a single transect

Stump Springs Zone 2 One Sample t-test	t value	UAV Mean (100 transects) cm	AIM Mean (1 transect) cm	p-value
Stump Springs Zone 2 March 2022 T1	15.882	0.2440	0.1000	< 2.2e-16
Stump Springs Zone 2 March 2022 T2	-7.356	0.2212	0.2696	5.60E-11
Stump Springs Zone 2 March 2022 T3	14.846	0.2196	0.1560	< 2.2e-16

Table 26: Stump Springs Zone 4 One Sample t-test March 2022 evaluating UAV mean shrub cover of 100 transects versus AIM mean shrub cover across a single transect

Stump Springs Zone 4 One Sample t-test	t value	UAV Mean (100 transects) cm	AIM Mean (1 transect) cm	p-value
Stump Springs Zone 4 March 2022 T1	14.020	0.2649	0.1696	< 2.2e-16
Stump Springs Zone 4 March 2022 T2	0.348	0.3339	0.3288	0.7288
Stump Springs Zone 4 March 2022 T3	18.298	0.2796	0.1820	< 2.2e-16

Table 27: McCullough Pass One Sample t-test April 2022 evaluating UAV mean shrub cover of 100 transects versus AIM mean shrub cover across a single transect

McCullough Pass One Sample t-test	t value	UAV Mean (100 transects) cm	AIM Mean (1 transect) cm	p-value
McCullough Pass April 2022 T1	-4.582	0.2077	0.2400	1.35E-05
McCullough Pass April 2022 T2	-24.949	0.1602	0.2992	< 2.2e-16
McCullough Pass April 2022 T3	-8.504	0.0888	0.1260	1.97E-13
McCullough Pass April 2022 T4	-1.881	0.1744	0.1876	0.06297
McCullough Pass April 2022 T5	-29.396	0.0851	0.1872	< 2.2e-16
McCullough Pass April 2022 T6	-8.872	0.0370	0.0568	7.52E-14
McCullough Pass April 2022 T7	-15.193	0.0526	0.1048	< 2.2e-16
McCullough Pass April 2022 T8	-62.191	0.0452	0.2252	< 2.2e-16
McCullough Pass April 2022 T9	-15.050	0.1791	0.2832	< 2.2e-16
McCullough Pass April 2022 T10	3.064	0.2325	0.2052	0.002814
McCullough Pass April 2022 T11	25.213	0.2686	0.1364	< 2.2e-16
McCullough Pass April 2022 T12	0.013	0.1677	0.1676	0.9894

Table 28: Sheep Mountain One Sample t-test April 2022 evaluating UAV mean shrub cover of 100 transects versus AIM mean shrub cover across a single transect

Sheep Mountain One Sample t-test	t value	UAV Mean (100 transects) cm	AIM Mean (1 transect) cm	p-value
Sheep Mountain April 2022 T1	2.038	0.2883	0.2696	0.04418
Sheep Mountain April 2022 T2	16.737	0.3746	0.2240	< 2.2e-16
Sheep Mountain April 2022 T3	19.483	0.2020	0.0292	< 2.2e-16
Sheep Mountain April 2022 T4	17.501	0.2451	0.1064	< 2.2e-16
Sheep Mountain April 2022 T5	8.922	0.1536	0.1000	2.45E-14
Sheep Mountain April 2022 T6	22.591	0.2198	0.0512	< 2.2e-16

TABLE 29: SILVER STATE ONE SAMPLE T-TEST APRIL 2022 EVALUATING UAV MEAN SHRUB COVER OF 100 TRANSECTS VERSUS AIM MEAN SHRUB COVER ACROSS A SINGLE TRANSECT

Silver State One Sample t-test	t value	UAV Mean (100 transects) cm	AIM Mean (1 transect) cm	p-value
Silver State April 2022 T1	4.577	0.2929	0.2320	1.37E-05
Silver State April 2022 T2	40.981	0.4548	0.1912	< 2.2e-16
Silver State April 2022 T3	19.001	0.4029	0.1804	< 2.2e-16
Silver State April 2022 T4	17.043	0.2250	0.1084	< 2.2e-16
Silver State April 2022 T5	7.939	0.2279	0.1672	3.24E-12
Silver State April 2022 T6	5.583	0.3596	0.2800	2.07E-07
Silver State April 2022 T7	-6.505	0.2016	0.2560	3.21E-09
Silver State April 2022 T8	6.208	0.1486	0.1156	1.26E-08
Silver State April 2022 T9	-1.778	0.1068	0.1144	0.07845
Silver State April 2022 T10	3.105	0.2473	0.2156	0.00248
Silver State April 2022 T11	6.135	0.2239	0.1732	1.76E-08
Silver State April 2022 T12	40.539	0.3668	0.1480	< 2.2e-16

TABLE 30: COYOTE SPRINGS ONE SAMPLE T-TEST APRIL 2022 EVALUATING UAV MEAN SHRUB COVER OF 100 TRANSECTS VERSUS AIM MEAN SHRUB COVER ACROSS A SINGLE TRANSECT

Coyote North One Sample t-test	t value	UAV Mean (100 transects) cm	AIM Mean (1 transect) cm	p-value
Coyote North April 2022 T1	-2.456	0.2349	0.2568	0.01579
Coyote North April 2022 T2	-6.148	0.2944	0.3388	1.66E-08
Coyote North April 2022 T3	2.291	0.2982	0.2780	0.02411
Coyote North April 2022 T4	2.677	0.2475	0.2228	0.0087
Coyote North April 2022 T5	7.367	0.2260	0.1780	5.31E-11
Coyote North April 2022 T6	14.250	0.2396	0.1220	< 2.2e-16

TABLE 31: STUMP SPRINGS ZONE 1 ONE SAMPLE T-TEST APRIL 2022 EVALUATING UAV MEAN SHRUB COVER OF 100 TRANSECTS VERSUS AIM MEAN SHRUB COVER ACROSS A SINGLE TRANSECT

Stump Springs Zone 1 One Sample t-test	t value	UAV Mean (100 transects) cm	AIM Mean (1 transect) cm	p-value
Stump Springs Zone 1 April 2022 T1	-2.094	0.2773	0.2956	0.03884
Stump Springs Zone 1 April 2022 T2	19.477	0.2773	0.1744	< 2.2e-16
Stump Springs Zone 1 April 2022 T3	4.348	0.2115	0.1840	3.34E-05

TABLE 32: STUMP SPRINGS ZONE 2 ONE SAMPLE T-TEST APRIL 2022 EVALUATING UAV MEAN SHRUB COVER OF 100 TRANSECTS VERSUS AIM MEAN SHRUB COVER ACROSS A SINGLE TRANSECT

Stump Springs Zone 2 One Sample t-test	t value	UAV Mean (100 transects) cm	AIM Mean (1 transect) cm	p-value
Stump Springs Zone 2 April 2022 T1	13.891	0.2673	0.1096	< 2.2e-16
Stump Springs Zone 2 April 2022 T2	-4.667	0.2407	0.2860	9.59E-06
Stump Springs Zone 2 April 2022 T3	1.192	0.2379	0.2320	0.2363

TABLE 33: STUMP SPRINGS ZONE 3 ONE SAMPLE T-TEST APRIL 2022 EVALUATING UAV MEAN SHRUB COVER OF 100 TRANSECTS VERSUS AIM MEAN SHRUB COVER ACROSS A SINGLE TRANSECT

Stump Springs Zone 3 One Sample t-test	t value	UAV Mean (100 transects) cm	AIM Mean (1 transect) cm	p-value
Stump Springs Zone 3 April 2022 T1	-0.604	0.1854	0.1888	0.5475
Stump Springs Zone 3 April 2022 T2	-1.626	0.1863	0.1964	0.1071
Stump Springs Zone 3 April 2022 T3	-2.539	0.1103	0.1208	0.01267

Table 34: Stump Springs Zone 4 One Sample t-test April 2022 evaluating UAV mean shrub cover of 100 transects versus AIM mean shrub cover across a single transect

Stump Springs Zone 4 One Sample t-test	t value	UAV Mean (100 transects) cm	AIM Mean (1 transect) cm	p-value
Stump Springs Zone 4 April 2022 T1	6.475	0.2718	0.2012	3.68E-09
Stump Springs Zone 4 April 2022 T2	-3.841	0.2986	0.3548	0.000217
Stump Springs Zone 4 April 2022 T3	-2.241	0.2441	0.2572	0.02723

Table 35: McCullough Pass One Sample t-test May 2022 evaluating UAV mean shrub cover of 100 transects versus AIM mean shrub cover across a single transect

McCullough Pass One Sample t-test	t value	UAV Mean (100 transects) cm	AIM Mean (1 transect) cm	p-value
McCullough Pass May 2022 T1	-5.308	0.2084	0.2312	6.80E-07
McCullough Pass May 2022 T2	-13.784	0.1729	0.2700	< 2.2e-16
McCullough Pass May 2022 T3	1.802	0.1377	0.1312	0.07465
McCullough Pass May 2022 T4	1.685	0.1989	0.1828	0.09512
McCullough Pass May 2022 T5	-9.883	0.1466	0.1968	< 2.2e-16
McCullough Pass May 2022 T6	-15.960	0.0354	0.0656	< 2.2e-16
McCullough Pass May 2022 T7	-18.688	0.0537	0.1140	< 2.2e-16
McCullough Pass May 2022 T8	-21.168	0.0614	0.1636	< 2.2e-16
McCullough Pass May 2022 T9	6.028	0.2783	0.2396	2.86E-08
McCullough Pass May 2022 T10	3.385	0.2719	0.2428	0.00102
McCullough Pass May 2022 T11	6.207	0.1710	0.1412	1.27E-08
McCullough Pass May 2022 T12	0.033	0.2170	0.2168	0.9739

Table 36: Sheep Mountain One Sample t-test May 2022 evaluating UAV mean shrub cover of 100 transects versus AIM mean shrub cover across a single transect

Sheep Mountain One Sample t-test	t value	UAV Mean (100 transects) cm	AIM Mean (1 transect) cm	p-value
Sheep Mountain May 2022 T1	-28.669	0.1253	0.3068	< 2.2e-16
Sheep Mountain May 2022 T2	0.970	0.1711	0.1624	0.3345
Sheep Mountain May 2022 T3	17.836	0.0785	0.0184	< 2.2e-16
Sheep Mountain May 2022 T4	11.419	0.1795	0.0948	< 2.2e-16
Sheep Mountain May 2022 T5	-8.453	0.1085	0.1400	2.54E-13
Sheep Mountain May 2022 T6	9.920	0.1010	0.0504	< 2.2e-16
Sheep Mountain May 2022 T7	-40.717	0.0857	0.2196	< 2.2e-16
Sheep Mountain May 2022 T8	-9.873	0.1165	0.1664	< 2.2e-16
Sheep Mountain May 2022 T9	-13.635	0.0929	0.1356	< 2.2e-16

Table 37: Silver State One Sample t-test May 2022 evaluating UAV mean shrub cover of 100 transects versus AIM mean shrub cover across a single transect

Silver State One Sample t-test	t value	UAV Mean (100 transects) cm	AIM Mean (1 transect) cm	p-value
Silver State May 2022 T1	-3.756	0.2331	0.2756	0.000292
Silver State May 2022 T2	17.958	0.3328	0.1896	< 2.2e-16
Silver State May 2022 T3	19.815	0.3239	0.0944	< 2.2e-16
Silver State May 2022 T4	20.823	0.2632	0.1228	< 2.2e-16
Silver State May 2022 T5	6.101	0.2579	0.2076	2.05E-08
Silver State May 2022 T6	14.917	0.3017	0.1740	< 2.2e-16
Silver State May 2022 T7	-1.543	0.2185	0.2304	0.1261
Silver State May 2022 T8	12.509	0.1883	0.1208	< 2.2e-16
Silver State May 2022 T9	5.713	0.1364	0.1084	1.17E-07
Silver State May 2022 T10	7.847	0.2792	0.2192	5.11E-12
Silver State May 2022 T11	-1.396	0.2124	0.2252	0.1659
Silver State May 2022 T12	17.193	0.2702	0.1528	< 2.2e-16

TABLE 38: COYOTE SPRINGS ONE SAMPLE T-TEST MAY 2022 EVALUATING UAV MEAN SHRUB COVER OF 100 TRANSECTS VERSUS AIM MEAN SHRUB COVER ACROSS A SINGLE TRANSECT

Coyote North One Sample t-test	t value	UAV Mean (100 transects) cm	AIM Mean (1 transect) cm	p-value
Coyote North May 2022 T1	-12.861	0.2127	0.3064	< 2.2e-16
Coyote North May 2022 T2	15.852	0.2530	0.1556	< 2.2e-16
Coyote North May 2022 T3	-2.090	0.2607	0.2760	0.03923
Coyote North May 2022 T4	7.298	0.2568	0.1920	7.40E-11
Coyote North May 2022 T5	6.800	0.1612	0.1196	8.00E-10
Coyote North May 2022 T6	14.762	0.1924	0.0876	< 2.2e-16

TABLE 39: STUMP SPRINGS ZONE 1 ONE SAMPLE T-TEST MAY 2022 EVALUATING UAV MEAN SHRUB COVER OF 100 TRANSECTS VERSUS AIM MEAN SHRUB COVER ACROSS A SINGLE TRANSECT

Stump Springs Zone 1 One Sample t-test	t value	UAV Mean (100 transects) cm	AIM Mean (1 transect) cm	p-value
Stump Springs Zone 1 May 2022 T1	-16.628	0.1856	0.2756	< 2.2e-16
Stump Springs Zone 1 May 2022 T2	24.948	0.2793	0.1488	< 2.2e-16
Stump Springs Zone 1 May 2022 T3	6.191	0.2201	0.1692	1.36E-08

TABLE 40: STUMP SPRINGS ZONE 2 ONE SAMPLE T-TEST MAY 2022 EVALUATING UAV MEAN SHRUB COVER OF 100 TRANSECTS VERSUS AIM MEAN SHRUB COVER ACROSS A SINGLE TRANSECT

Stump Springs Zone 2 One Sample t-test	t value	UAV Mean (100 transects) cm	AIM Mean (1 transect) cm	p-value
Stump Springs Zone 2 May 2022 T1	25.995	0.2203	0.0684	< 2.2e-16
Stump Springs Zone 2 May 2022 T2	-14.580	0.1783	0.2652	< 2.2e-16
Stump Springs Zone 2 May 2022 T3	-6.125	0.1451	0.1776	1.85E-08

TABLE 41: STUMP SPRINGS ZONE 3 ONE SAMPLE T-TEST MAY 2022 EVALUATING UAV MEAN SHRUB COVER OF 100 TRANSECTS VERSUS AIM MEAN SHRUB COVER ACROSS A SINGLE TRANSECT

Stump Springs Zone 3 One Sample t-test	t value	UAV Mean (100 transects) cm	AIM Mean (1 transect) cm	p-value
Stump Springs Zone 3 May 2022 T1	1.026	0.2290	0.2232	0.3076
Stump Springs Zone 3 May 2022 T2	9.283	0.3142	0.2232	4.01E-15
Stump Springs Zone 3 May 2022 T3	1.884	0.1456	0.1356	0.06249

TABLE 42: STUMP SPRINGS ZONE 4 ONE SAMPLE T-TEST MAY 2022 EVALUATING UAV MEAN SHRUB COVER OF 100 TRANSECTS VERSUS AIM MEAN SHRUB COVER ACROSS A SINGLE TRANSECT

Stump Springs Zone 4 One Sample t-test	t value	UAV Mean (100 transects) cm	AIM Mean (1 transect) cm	p-value
Stump Springs Zone 4 May 2022 T1	22.595	0.2916	0.1280	< 2.2e-16
Stump Springs Zone 4 May 2022 T2	-1.837	0.2715	0.2980	0.06929
Stump Springs Zone 4 May 2022 T3	13.911	0.2432	0.1584	< 2.2e-16

TABLE 43: MCCULLOUGH PASS ONE SAMPLE T-TEST SEPTEMBER 2022 EVALUATING UAV MEAN SHRUB COVER OF 100 TRANSECTS VERSUS AIM MEAN SHRUB COVER ACROSS A SINGLE TRANSECT

McCullough Pass One Sample t-test	t value	UAV Mean (100 transects) cm	AIM Mean (1 transect) cm	p-value
McCullough Pass September 2022 T1	0.231	0.2404	0.2388	0.8181
McCullough Pass September 2022 T2	-15.857	0.1871	0.2928	< 2.2e-16
McCullough Pass September 2022 T3	0.102	0.1345	0.1340	0.9186
McCullough Pass September 2022 T4	-11.281	0.1776	0.2620	< 2.2e-16
McCullough Pass September 2022 T5	-53.381	0.1183	0.3300	< 2.2e-16
McCullough Pass September 2022 T6	-22.307	0.0260	0.0648	< 2.2e-16
McCullough Pass September 2022 T7	3.208	0.1095	0.0948	0.0018
McCullough Pass September 2022 T8	-9.432	0.0864	0.1468	2.47E-15
McCullough Pass September 2022 T9	9.702	0.2639	0.2016	4.88E-16
McCullough Pass September 2022 T10	9.910	0.2993	0.1992	< 2.2e-16
McCullough Pass September 2022 T11	3.108	0.2375	0.2152	0.00246
McCullough Pass September 2022 T12	0.499	0.2361	0.2328	0.619

Table 44: Sheep Mountain One Sample t-test September 2022 evaluating UAV mean shrub cover of 100 transects versus AIM mean shrub cover across a single transect

Sheep Mountain One Sample t-test	t value	UAV Mean (100 transects) cm	AIM Mean (1 transect) cm	p-value
Sheep Mountain September 2022 T1	-2.182	0.3112	0.3312	4.02E-12
Sheep Mountain September 2022 T2	27.717	0.5179	0.2068	< 2.2e-16
Sheep Mountain September 2022 T3	20.416	0.2032	0.0400	< 2.2e-16
Sheep Mountain September 2022 T4	26.070	0.3039	0.0624	< 2.2e-16
Sheep Mountain September 2022 T5	17.679	0.1911	0.0772	< 2.2e-16
Sheep Mountain September 2022 T6	16.424	0.1983	0.0396	< 2.2e-16
Sheep Mountain September 2022 T7	4.053	0.1886	0.1684	0.0001006
Sheep Mountain September 2022 T8	5.637	0.1894	0.1512	1.64E-07
Sheep Mountain September 2022 T9	10.784	0.1923	0.1252	< 2.2e-16

Table 45: Silver State One Sample t-test September 2022 evaluating UAV mean shrub cover of 100 transects versus AIM mean shrub cover across a single transect

Silver State One Sample t-test	t value	UAV Mean (100 transects) cm	AIM Mean (1 transect) cm	p-value
Silver State September 2022 T1	6.207	0.2879	0.2312	1.27E-08
Silver State September 2022 T2	13.054	0.4078	0.2504	< 2.2e-16
Silver State September 2022 T3	21.681	0.3891	0.1472	< 2.2e-16
Silver State September 2022 T4	28.202	0.3614	0.1180	< 2.2e-16
Silver State September 2022 T5	10.324	0.3111	0.2008	< 2.2e-16
Silver State September 2022 T6	13.291	0.3942	0.2384	< 2.2e-16
Silver State September 2022 T7	1.971	0.1910	0.1752	0.05151
Silver State September 2022 T8	6.382	0.2017	0.1540	5.67E-09
Silver State September 2022 T9	-0.834	0.1124	0.1160	0.4061
Silver State September 2022 T10	5.265	0.2862	0.2532	8.17E-07
Silver State September 2022 T11	0.085	0.2333	0.2324	0.9327
Silver State September 2022 T12	7.839	0.2500	0.1980	5.30E-12

Table 46: Coyote Springs One Sample t-test September 2022 evaluating UAV mean shrub cover of 100 transects versus AIM mean shrub cover across a single transect

Coyote North One Sample t-test	t value	UAV Mean (100 transects) cm	AIM Mean (1 transect) cm	p-value
Coyote North September 2022 T1	4.762	0.2879	0.2444	6.56E-06
Coyote North September 2022 T2	19.127	0.2634	0.1288	< 2.2e-16
Coyote North September 2022 T3	11.383	0.3075	0.2332	< 2.2e-16
Coyote North September 2022 T4	13.321	0.2996	0.1960	< 2.2e-16
Coyote North September 2022 T5	13.421	0.2425	0.1380	< 2.2e-16
Coyote North September 2022 T6	17.785	0.1935	0.0912	< 2.2e-16

Table 47: Stump Springs Zone 1 One Sample t-test September 2022 evaluating UAV mean shrub cover of 100 transects versus AIM mean shrub cover across a single transect

Stump Springs Zone 1 One Sample t-test	t value	UAV Mean (100 transects) cm	AIM Mean (1 transect) cm	p-value
Stump Springs Zone 1 September 2022 T1	15.675	0.4878	0.2280	< 2.2e-16
Stump Springs Zone 1 September 2022 T2	36.811	0.3825	0.1616	< 2.2e-16
Stump Springs Zone 1 September 2022 T3	20.462	0.3614	0.1908	< 2.2e-16

Table 48: Stump Springs Zone 2 One Sample t-test September 2022 evaluating UAV mean shrub cover of 100 transects versus AIM mean shrub cover across a single transect

Stump Springs Zone 2 One Sample t-test	t value	UAV Mean (100 transects) cm	AIM Mean (1 transect) cm	p-value
Stump Springs Zone 2 September 2022 T1	18.251	0.3173	0.1136	< 2.2e-16
Stump Springs Zone 2 September 2022 T2	6.116	0.2545	0.2072	1.92E-08
Stump Springs Zone 2 September 2022 T3	6.407	0.2190	0.1732	5.05E-09

TABLE 49: STUMP SPRINGS ZONE 3 ONE SAMPLE T-TEST SEPTEMBER 2022 EVALUATING UAV MEAN SHRUB COVER OF 100 TRANSECTS VERSUS AIM MEAN SHRUB COVER ACROSS A SINGLE TRANSECT

Stump Springs Zone 3 One Sample t-test	t value	UAV Mean (100 transects) cm	AIM Mean (1 transect) cm	p-value
Stump Springs Zone 3 September 2022 T1	20.036	0.2911	0.1776	< 2.2e-16
Stump Springs Zone 3 September 2022 T2	19.874	0.3108	0.1368	< 2.2e-16
Stump Springs Zone 3 September 2022 T3	19.342	0.2641	0.1272	< 2.2e-16

TABLE 50: STUMP SPRINGS ZONE 4 ONE SAMPLE T-TEST SEPTEMBER 2022 EVALUATING UAV MEAN SHRUB COVER OF 100 TRANSECTS VERSUS AIM MEAN SHRUB COVER ACROSS A SINGLE TRANSECT

Stump Springs Zone 4 One Sample t-test	t value	UAV Mean (100 transects) cm	AIM Mean (1 transect) cm	p-value
Stump Springs Zone 4 September 2022 T1	16.793	0.4047	0.2060	< 2.2e-16
Stump Springs Zone 4 September 2022 T2	2.053	0.3329	0.3028	0.04267
Stump Springs Zone 4 September 2022 T3	28.187	0.3272	0.1588	< 2.2e-16